

Aus der Klinik für  
Hämatologie, Onkologie und Tumorummunologie  
der Medizinischen Fakultät Charité – Universitätsmedizin Berlin

DISSERTATION

Epstein-Barr Virus-spezifische T-Zell-Rezeptoren für den  
adoptiven Transfer transduzierter T-Zellen im Rahmen der  
allogenen Stammzelltransplantation

Epstein-Barr virus-specific T cell receptors for adoptive transfer  
of transduced T cells in allogeneic stem cell transplantation

zur Erlangung des akademischen Grades

Doctor of Philosophy (PhD)

vorgelegt der Medizinischen Fakultät  
Charité – Universitätsmedizin Berlin

von

María Fernanda Lammoglia Cobo

Datum der Promotion: 30.11.2023



## Table of contents

Table of contents .....	iii
List of tables .....	iv
List of figures .....	v
List of abbreviations.....	vi
Abstract .....	1
Zusammenfassung .....	2
1. Introduction.....	3
2. Methods.....	6
2.1 Article 1 .....	6
2.2 Article 2 .....	7
2.3 Article 3 .....	9
3. Results.....	11
3.1 Article 1 .....	11
3.2 Article 2 .....	13
3.3 Article 3 .....	17
4. Discussion .....	21
4.1 Short summary of results .....	21
4.2 Interpretation of results.....	21
4.3 Embedding the results into the current state of research .....	22
4.4 Strengths and weaknesses of the studies .....	23
4.5 Implications for practice and/or future research .....	24
5. Conclusions .....	26
Reference list.....	27
Statutory Declaration .....	35
Declaration of your own contribution to the publications.....	36
Excerpt from Journal Summary List.....	38
Printed copies of the publications .....	43
Curriculum Vitae .....	89
Publication list.....	90
Acknowledgments .....	91

---

**List of tables**

Table 1: Peptides used for graft stimulation.....	7
Table 2: EBV-derived peptides for T cell product .....	9
Table 3: Follow-up of EBV-specific T cells after adoptive transfer.....	19

## List of figures

Figure 1: Allogeneic stem cell transplantation (alloSCT) and the window susceptibility to EBV infection .....	4
Figure 2: Distinct phenotype compartments of TILs and TUMs .....	11
Figure 3: Clonal overlap among TIL, TUM, and peripheral blood T cells .....	12
Figure 4: Presence of TCR target antigen in tumor and unaffected mucosa tissue .....	13
Figure 5: Peptide-specific expansion of CD8 <sup>+</sup> T cells .....	14
Figure 6: Clonal expansion after peptide stimulation .....	14
Figure 7: Selected TCRs are target-peptide specific .....	15
Figure 8: TCR-recombinant PBLs recognize EBV-infected cell lines .....	16
Figure 9: T cell activation by EBV <sup>+</sup> LCLs is peptide- and HLA-dependent .....	16
Figure 10: T cell expansion after peptide stimulation in the cellular product .....	17
Figure 11: Identification of peptide-specific TCR clonotypes in the cellular product .....	18
Figure 12: Patient EBV viremia and CD8 <sup>+</sup> T cell levels post-engraftment .....	19
Figure 13: Frequency of peptide-specific T cells before and after adoptive transfer .....	20

## List of abbreviations

- alloSCT: Allogeneic stem cell transplantation
- AITL: Angioimmunoblastic T-cell lymphoma
- APC: Antigen presenting cells
- ATG: Anti-thymocyte globulin
- ATMP: Advanced Therapeutic Medicinal Product
- BL: Burkitt lymphoma
- CsA: Cyclosporine A
- CTL: Cytotoxic T cell lymphocytes
- DLI: Donor lymphocyte infusion
- EBV: Epstein-Barr Virus
- EDTA: Ethylenediaminetetraacetic acid
- EMA: European Medicines Agency
- ELISA: Enzyme-linked immunosorbent assay
- FACS: Fluorescence activated cell sorting
- FBS: Fetal bovine serum
- GC: Gastric cancer
- G-CSF: Granulocyte colony stimulating factor
- GvHD: Graft-versus-Host Disease
- HL: Hodgkin lymphoma
- HHV-4: Human Herpesvirus 4
- HHV-6: Human Herpesvirus 6
- HTS: High-throughput sequencing
- IFN- $\gamma$ : Interferon  $\gamma$
- ngs: Next-generation sequencing
- LCL: Lymphoblastoid cell line
- NFAT: Nuclear factor of activated T cells
- NPC: Nasopharyngeal carcinoma
- PB: Peripheral blood
- PBMC: Peripheral blood mononuclear cells
- PBS: Phosphate-buffered saline
- PCR: Polymerase chain reaction

- pMHC: Peptide-MHC
- PTLD: Post-Transplant Lymphoproliferative Disorder
- TAA: Tumor-associated antigens
- TCR: T cell receptor
- TIL: Tumor-infiltrating T cells
- TSA: Tumor-specific antigens
- TUM: T cell from unaffected mucosa
- Tx: Transplantation

## Abstract

More than one third of patients experience Epstein-Barr Virus (EBV) reactivation after allogeneic stem cell transplantation (alloSCT) and up to 3% of transplanted patients develop post-transplant lymphoproliferative disorders (PTLD). In healthy individuals, virus epitope-specific T cells are critical for EBV control; however, post-transplant cytopenia and immunosuppression leaves patients vulnerable to virus reactivation and associated malignancies. Antibody-mediated depletion of B cells, which are natural targets and reservoirs for EBV, delays the reconstitution of cellular immunity and comes with considerable short- and long-term side effects.

The goal of this work is to identify EBV-specific T cell receptors (TCR) and transduce them into T cells for adoptive transfer. Stimulation of stem cell grafts or peripheral blood cells with EBV plasmid-recombinant antigen-presenting cells (APC) or EBV-derived peptides leads to a substantial expansion of EBV-specific T cells; however, the degree of expansion is dependent on an antigen-experienced memory compartment non-existing in EBV seronegative donors. I present three articles that, combined, describe the identification and characterization of 16 different EBV-specific TCRs for TCR-based immunotherapy.

In the first article, we established efficient single cell immune phenotyping and TCR sequencing using rectal cancer infiltrating T cells as an example. In the second article, we applied this technology to identify EBV peptide-specific TCRs which can be transduced into peripheral blood T cells and recognize EBV-infected B cells. In the third article, we tracked adoptively transferred virus-specific T cells in an alloSCT patient during EBV reactivation.

We were able to establish a robust, GMP-compliant pipeline for the discovery of EBV-specific TCRs with prophylactic and therapeutic potential. The use of single EBV-peptides for stimulation facilitated targeting of different antigens, HLA-restrictions, and potentially other viruses. Identified TCRs for selected HLA restrictions can be stored as TCR libraries to prepare readily available off-the-shelf products.

Reconstitution of cellular immunity against EBV can offer protection against associated complications and potentially contributes to a better outcome post-transplant. We propose adoptive transfer of virus-specific T cells transduced with carefully selected TCRs as a prophylactic and therapeutic approach to prevent EBV-infection, reactivation, and associated complications.



## Zusammenfassung

Bei mehr als einem Drittel der Patienten kommt es nach allogener Stammzelltransplantation (AlloSZT) zur Reaktivierung des Epstein-Barr-Virus (EBV) und bis zu 3% der Patienten entwickeln eine lymphoproliferative Erkrankung nach Transplantation (PTLD). EBV-spezifische T-Zellen spielen eine entscheidende Rolle bei der Virus-Kontrolle, jedoch erhöht die Zytopenie und immunsuppressive Therapie nach AlloSZT das Risiko für eine EBV-Reaktivierung. Die Depletion von B-Zellen, den primären Wirtszellen von EBV, durch monoklonale Antikörper verzögert die Wiederherstellung der zellulären Immunität und ist von schwerwiegenden Nebenwirkungen begleitet.

Ziel dieser Arbeit ist die Identifizierung EBV-spezifischer T-Zell-Rezeptoren (TCR) und ihre Transduktion in T-Zellen für den adoptiven Transfer. EBV-spezifische T-Zellen können ausgehend von unterschiedlichen Spenderzellen, mit rekombinanten antigen-präsentierenden Zellen oder EBV-Peptiden *in vitro* expandiert werden. Das Ausmaß der Expansion ist spenderabhängig und insbesondere bei seronegativen Spendern ohne EBV-spezifische Gedächtniszellen nicht erfolgreich. In drei Publikationen wird die Identifizierung und Charakterisierung von insgesamt 16 verschiedenen EBV-spezifischen TCR beschrieben, die sich für TCR-basierte Immuntherapien eignen.

In der ersten Veröffentlichung wird eine Einzelzell-Technik zur Immunphänotypisierung und TCR-Sequenzierung am Beispiel Tumor-infiltrierender T-Zellen beim Rektumkarzinom entwickelt. In der zweiten Veröffentlichung nutzen wir diese Technik zur Identifizierung EBV-peptid-spezifischer TCRs, die, transduziert in T-Zellen, EBV-infizierte Zellen erkennen. In der dritten Veröffentlichung verfolgen wir adoptiv-transferierte T-Zellen in einem Patienten mit EBV-Reaktivierung nach AlloSZT.

Wir haben eine effiziente Methodik zur Identifizierung EBV-spezifischer TCRs mit prophylaktischem und therapeutischem Potenzial etabliert. Die Verwendung einzelner Peptide zur Stimulation erlaubt die Auswahl definierter Zielantigene bei bekannter HLA-Restriktion und kann perspektivisch auch für die Identifizierung von TCRs gegen andere Viren genutzt werden. Die Arbeiten ermöglichen potentiell den Aufbau von TCR Bibliotheken mit exakt definierten Spezifitäten zur Herstellung gezielter Zelltherapeutika.

Die Wiederherstellung der zellulären Immunität gegen EBV schützt Patienten vor EBV-assoziierten Komplikationen. Wir schlagen den adoptiven Transfer TCR-rekombinanter Zellen mit sorgfältig ausgewählten Spezifitäten als prophylaktischen und therapeutischen Ansatz gegen EBV-Infektion, Reaktivierung und assoziierte Komplikationen vor.

## 1. Introduction

Allogeneic stem cell transplantation (alloSCT) is a treatment option for several malignant and non-malignant hematological disorders, in which patients receive stem cells from an HLA-matched or mismatched donor after chemo-, radiotherapy, and/or antithymocyte globulin (ATG) conditioning. Along with increasing numbers of alloSCT procedures per year [1], transplant-related mortality has significantly decreased over time [2].

Nevertheless, malignant relapse, Graft-versus-Host Disease (GvHD), and viral infections severely compromise alloSCT success rates and the patients' quality of life. Post-transplant immunosuppression and lymphopenia also leave patients vulnerable to virus reactivation and associated malignancies [3]. More than one third of immunocompromised patients experience an Epstein-Barr Virus (EBV) infection and 3% (range 1-11%) of transplanted patients develop a post-transplant lymphoproliferative disorder (PTLD) in the first year post-transplant [4–6].

EBV is an oncogenic, DNA double-stranded gamma-herpesvirus (HHV-4) with a prevalence above 90% in adults [7]. After initial infection, EBV remains in an asymptomatic latent state in memory B cells. Disruption of latency, if not controlled by T cells, is associated with lymphoid and epithelial malignancies such as Burkitt lymphoma (BL), Hodgkin lymphoma (HL), nasopharyngeal carcinoma (NPC), and gastric cancer (GC). 17% of deaths in these four cancer types were caused by the EBV-attributed fraction [8].

Transition between EBV lytic and latent phases is controlled by humoral and cellular immunity [9,10]. In the cellular response, EBV-specific T cells mediate killing of virus-producing B cells and control EBV at its latent, less immunogenic stages [11]. *In vitro* studies contributed to the isolation of CD8<sup>+</sup> T cells that recognize EBV-infected lymphoblastoid cell lines (LCL) [12] and led to the identification of EBV-derived immunodominant epitopes [13–19].

T cell depletion of donor grafts and conditioning regimes with ATG, while aimed to prevent graft rejection and GvHD, hinders T cell-mediated responses against EBV and increase the risk of EBV infection, reactivation, and development of EBV-associated lymphomas [20,21]. Most cases of post-transplant EBV reactivation and EBV-associated PTLD take place in the early post-engraftment period, when T cell immunity has not been reconstituted [22] (Fig. 1). Antibody-mediated depletion of B cells, which are natural targets and reservoirs for EBV, further delays the reconstitution of cellular immunity and comes with considerable short- and long-term side effects, such as opportunistic infections [23].

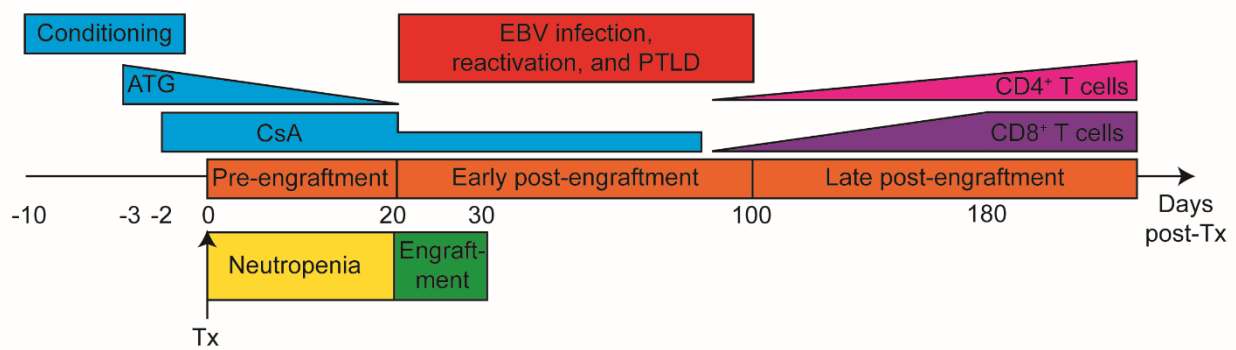


**Figure 1: Allogeneic stem cell transplantation (alloSCT) and the window susceptibility to EBV infection**

A typical regimen for alloSCT is shown. Starting with chemo- and/or radiotherapy conditioning regimens, anti-thymocyte globulin (ATG) and cyclosporine A (CsA) as T cell-targeting immunosuppressants are used to avoid graft rejection and Graft versus Host Disease (GvHD) [24,25]. During early post-engraftment (day 20-100), lymphopenia leaves patients vulnerable to EBV infection, reactivation, or PTLD development. CD8<sup>+</sup> and CD4<sup>+</sup> T cell immunity, critical for EBV control, is typically reconstituted from 6 months to one year (CD8<sup>+</sup>) and up to two years post-transplant (CD4<sup>+</sup>) [26]. Tx= transplantation. Own representation: Lammoglia Cobo

Adoptive transfer of EBV-specific T cells offers a curative treatment option for EBV-associated complications and reinstalls T cell immunity. Since the first successful use of EBV-specific T cell therapy to treat PTLD in 1995 [27], several strategies to produce virus-specific T cells have been established. Repeated stimulation of donor cells with EBV-infected lymphoblastoid cells [27,28] or recombinant antigen-presenting cells (APC) [29] lead to cytotoxic T cell expansion; however, serial stimulations are time consuming and additional product safety testing is required when working with virus-infected cells. As an alternative, stimulation of donor cells with EBV-derived peptides leads to rapid epitope-specific T cell expansion without additional APCs [19,30]. These strategies can be adapted to target multiple epitopes from either a single or several viruses (such as Cytomegalovirus (CMV)) for adoptive transfer of virus-specific T cells [31,32].

These strategies to produce EBV-specific T cells have one limitation in common: The degree of expansion is dependent on the antigen-experienced memory compartment non-existing in EBV seronegative donors. EBV seropositivity varies across age and geographical locations, with younger populations in North America and Europe developing 90% of seropositivity until early adulthood [33,34]. Delayed seroconversion in Western

countries and the use of stem cell grafts from children or younger adults in haploidentical transplantation increase the likelihood of donor EBV seronegativity and, therefore, the risk of EBV infection and PTLD [35].

T cell receptor (TCR)-based immunotherapies circumvent this constrain, as re-expression of carefully selected, peptide-specific TCRs in donor T cells can direct T cell immunity against clinically-relevant targets [36]. Methodologies to identify EBV-specific TCRs [37–40] face the challenge to optimize times and workload to simultaneously characterize TCRs with different HLA restrictions and epitope specificities.

The goal of this work is the efficient identification and transduction of EBV-specific TCRs for adoptive transfer in the context of two different HLA types. My hypothesis was that the re-expression of carefully selected TCRs (from *in vitro* expanded CD8<sup>+</sup> T cell clones) in third-party T cells leads to recognition of EBV-infected LCLs. Throughout the work, I describe the identification and characterization of 16 EBV-specific TCRs with prophylactic and therapeutic potential for TCR-based immunotherapy.

In the first article, “Localization-associated immune phenotypes of clonally expanded tumor-infiltrating T cells and distribution of their target antigens in rectal cancer” (Article 1) [41], we established efficient single cell immune phenotyping and TCR sequencing using rectal cancer infiltrating T cells as an example. We then applied this technology to identify EBV peptide-specific TCRs which can be transduced into peripheral blood T cells and recognize EBV-infected B cells. These results were published in the second article, “Rapid single cell identification of Epstein-Barr virus-specific T cell receptors for cellular therapy” (Article 2) [42]. In parallel to my main project, we tracked adoptively transferred virus-specific T cells in an alloSCT patient after EBV reactivation and published the results in the article “Reconstitution of EBV-directed T cell immunity by adoptive transfer of peptide-stimulated T cells in a patient after allogeneic stem cell transplantation for AITL” (Article 3) [43].

## 2. Methods

### 2.1 Article 1 [41]

#### ❖ Patient samples

Use of patient material was approved by the Charité University Hospital ethics committee (Num. EA1/007/16). Samples of colorectal tumors, unaffected mucosa, and peripheral blood (PB) were obtained from five patients during surgery and PB was additionally obtained at one follow-up visit. To collect tumor infiltrating T cells (TIL) and T cells from unaffected mucosa (TUM), the tissue was cut into 2-4 mm<sup>3</sup> pieces and incubated 30 min in PBS with 10mM ethylenediaminetetraacetic acid (EDTA). While cells in suspension were passed through a 100 µm cell strainer, the tissue was incubated 30 min in RPMI1640 with 5% fetal bovine serum (FBS) and 0.5 mg/ml collagenase NB 4. Tissue cells were then recovered through Percoll gradient centrifugation; peripheral blood mononuclear cells (PBMC), through Ficoll density gradient centrifugation [44]. All cells were cryopreserved in RPMI 1640 with 50% FBS and 10% DMSO.

#### ❖ Single cell sequencing

Barcoding, PCR amplification, library preparation, MiSeq Illumina sequencing, and index sorting were carried out as previously described [45]. Clones were defined when two or more cells shared the same TCR $\alpha$  and TCR $\beta$  amino acid sequences and a 10-reads cutoff was set for cytokine and transcription factors expression. For each clone, markers were considered either positive or negative based on the expression of more than half of the clone's single cells.

#### ❖ TCR $\beta$ sequencing

Bulk TCR $\beta$  sequencing was carried out as previously described with a frequency cutoff of 10<sup>-4</sup> reads [46].

#### ❖ TCR re-expression in 58 $\alpha\beta$ <sup>-</sup> cell line

TCRs were manually selected, reconstructed, and synthesized for transfection in a 58 $\alpha\beta$ <sup>-</sup> hybridoma T cell line with recombinant human CD8 expression and a GFP reporter controlled by the nuclear factor of activated T cells (NFAT) [47]. TCR re-expression was confirmed with CD3 (clone UCHT1) staining and flow cytometry.

#### ❖ Coculture of TCR-recombinant 58 $\alpha\beta$ <sup>-</sup> cell lines with target cells

Co-culture of TCR-recombinant 58 $\alpha\beta$ <sup>-</sup> cell lines and target cells (tumor, unaffected mucosa, or HLA-mismatched tissue) were carried out for 16h. Target cell numbers

varied due to available patient material. NFAT-driven GFP expression was measured with flow cytometry and fluorescence microscopy; supernatant IL-2 concentrations were assessed using enzyme-linked immunosorbent assay (ELISA).

## 2.2 Article 2 [42]

### ❖ Recovery of mononuclear cells from stem cell grafts

After transplantation of granulocyte colony stimulating factor (G-CSF)-mobilized peripheral blood stem cell grafts, remaining cells from five HLA-B\*35:01<sup>+</sup> and one HLA-A\*02:01<sup>+</sup> EBV-seropositive adult donors were washed out of the stem cell bags with 0.9% sodium chloride solution. Mononuclear cells were recovered through Ficoll density gradient separation and frozen at 1-10<sup>7</sup> cells per vial. Use of patient material was approved by the Charité University Hospital ethics committee (Num. EA2/197/18).

### ❖ Peptide stimulation

Thawed mononuclear cells from stem cell grafts were cultured overnight and incubated the next day with EBV-derived synthetic peptides (Table 1, final concentration: 1µg/ml) for 2 hours. Cells were washed twice and cultured for 9 days in CellGro DC Medium with 50 IU/ml IL-2, 1% GlutaMAX, and 1% donor serum before freezing. Additional medium (50 IU/ml IL-2, 1% GlutaMAX, and 1% donor serum) was supplemented on day 5. To measure peptide-specific T cell expansion, cells before and after peptide stimulation were analyzed with flow cytometry using CD3 (clone UCHT1) and CD8 (clone RPA-T8) antibodies and EBV peptide-MHC (pMHC) tetramers.

**Table 1: Peptides used for graft stimulation**

Label	Sequence	Antigen	Latent / Lytic	HLA-restriction
HPV	HPVGEADYFEY	EBNA1	Latent	B*35:01
YPL	YPLHEQHGM	EBNA3A	Latent	B*35:01
EPL	EPLPQGQLTAY	BZLF1	Lytic	B*35:01
GLC	GLCTLVAML	BMLF1	Lytic	A*02:01
CLG	CLGGLLTMV	LMP2A	Latent	A*02:01
FLY	FLYALALLL	LMP2A	Latent	A*02:01
YVL	YVLDHLIVV	BRLF1	Lytic	A*02:01

Modified from Table 1, Lammoglia Cobo *et al.* 2022

### ❖ **Flow cytometric single cell sort and TCR sequencing**

Single pMHC<sup>+</sup>CD3<sup>+</sup>CD8<sup>+</sup> T cells were index-sorted into 96 well plates. Barcoding, PCR amplification, and TCR $\alpha\beta$  sequencing was carried out as previously described [41,45]. Clones were defined as two or more cells with identical TCR $\alpha$  and  $\beta$  amino acid sequences.

### ❖ **TCR transfection in 58 $\alpha\beta$ <sup>-</sup> hybridoma cell line**

Transfection of plasmids encoding selected TCR $\alpha\beta$  chains in CD8<sup>+</sup> 58 $\alpha\beta$ <sup>-</sup> hybridoma cells was carried out as previously described [41,47].

### ❖ **Coculture of TCR-recombinant 58 $\alpha\beta$ <sup>-</sup> hybridoma cell line with target cell lines**

To test TCRs for their (assumed) target peptide specificity, miniLCLs [48] were artificially loaded with target or non-target peptides and co-cultured with TCR-recombinant 58 $\alpha\beta$ <sup>-</sup> cells at a 10:6 ratio for 16h. For recognition of EBV-infected lymphoblastoid (LCL) and lymphoma cell lines, target cell lines were co-cultured with the TCR-recombinant 58 $\alpha\beta$ <sup>-</sup> cells at a 10:6 ratio for 16h.

NFAT-driven GFP was detected by flow cytometry and fluorescence microscopy; IL-2 was measured from culture supernatant using ELISA. 58 $\alpha\beta$ <sup>-</sup> cells were stained with anti-human CD8 (clone RPA-T8), anti-mouse CD3 (clone 17A2), and Zombie Red live/dead staining for flow cytometry analysis.

### ❖ **TCR transduction in human lymphocytes**

Part of the TCR $\beta$  constant region was exchanged with its murine counterpart to reduce probability of TCR mispairing with endogenous TCR. Furthermore, the murine constant region expressed on transduced T cells allowed to measure TCR transduction efficiency with an anti-mouse TCR $\beta$  (clone H57-597) antibody [49].

293Vec-RD114 packaging cells were transfected with 18  $\mu$ g of MP71-TCR vector. For transduction, 1.5 million peripheral blood lymphocytes (PBL) from a third-party, HLA-A\*02:01<sup>+</sup> and HLA-B\*35:01<sup>+</sup> donor were stimulated with 300 IU/ml IL-2 on anti-CD3- and anti-CD28-coated plates for 2 days. PBLs were transduced with 1 ml of viral supernatant, 400 IU/ml IL-2, and 8  $\mu$ g/ml protamine sulfate and spinoculated on two consecutive days. Cells were then kept 10 days in culture in fresh medium with 10% FBS and 400 IU/ml IL-2 and rested 2 days with 40 IU/ml IL-2 before freezing. Before freezing, TCR expression was confirmed with flow cytometry using anti-mouse TCR $\beta$  (clone H57-597) and anti-human CD8 (clone RPA-T8) antibodies.

### ❖ **Co-culture of TCR-recombinant T cells with EBV<sup>+</sup> LCLs**

TCR-recombinant human T cells were cocultured at a ratio of 50,000 T cells (average transduction efficiency: 34%) with 10,000 EBV<sup>+</sup> LCLs for 16-20 h; exact effector-to-target ratio depended on the respective TCR transduction efficiency. CD137 expression and IFN- $\gamma$  in the supernatant were measured as readouts with flow cytometry and ELISA, respectively. As an additional control to estimate the cytotoxic potential for one specific TCR-recombinant T cell and target coculture, CD107a expression and TNF- $\alpha$  and Granzyme B in the supernatant were also measured with flow cytometry and ELISA, respectively.

### 2.3 Article 3 [43]

#### ❖ Patient clinical information

A patient with chemotherapy-refractory angioimmunoblastic T cell lymphoma (AITL) received a G-CSF-mobilized stem cell graft from an HLA 10/10 match donor. 42 days after transplantation (day 42), the patient relapsed for AITL and eventually developed an EBV infection on day 66, which reached a peak in DNA copy levels in PB on day 89. For this reason, he received a donor lymphocyte infusion (day 76) and 4 weekly Rituximab doses (starting on day 68). As major symptoms persisted, he received an adoptive transfer of *in vitro* expanded, EBV-specific T cells (day 105). No EBV reactivation was detectable after day 111. The patient died from treatment resistant HSV-1 reactivation on day 352.

#### ❖ Production of EBV-specific T cells

EBV-specific T cells were expanded by peptide stimulation from donor lymphocytes [19]. Approximately 600 million PBMC were stimulated with synthetic, EBV-derived peptides (Table 2) for 2 hours, washed, and cultured for 9 days before freezing. Additional medium was supplied on day 5. Use of patient PBMC was approved by the University of Erlangen ethics committee (Ref. 4388).

**Table 2: EBV-derived peptides for T cell product**

Abb.	Sequence	Antigen	Abb.	Sequence	Antigen
CLG	CLGGLLTMV	LMP2	YPL	YPLHEQHGM	EBNA3A
GLC	GLCTLVAML	BMLF1	HPV	HPVGEADYFEY	EBNA1
YVL	YVLDHLIVV	BRLF1	EPL	EPLPQGQLTAY	BZLF1
FLY	FLYALALLL	LMP2	PYY	PYYVVDLSVRGM	BHRF1
RLR	RLRAEAQVK	EBNA3A	VVRM	VVRMFMRRERQLPQS	EBNA3C



RPP	RPPIFIRRL	EBNA3A	FGQL	FGQLTPHTKAVYQPR	BLLF1
QAK	QAKWRLQTL	EBNA3A	IPQC	IPQCRLTPLSRLPFG	EBNA1
RAK	RAKFKQLL	BZLF1	TDAW	TDAWRFAMNYPRNPT	BNRF1

Abb.= abbreviation. Modified from Table 1, Lammoglia Cobo & Ritter *et al.* 2022

### ❖ Flow cytometry and cell sort

50µl of patient's PB were stained in Trucount tubes with a CD8 (clone SK1), CD25 (clone 2A3), CD14 (clone MφP9), CD56 (clone B159), CD19 (clone SJ25C1), CD4 (clone RPA-T4), CD3 (clone UCHT1), and CD45 (clone HI30) antibody panel and measured with flow cytometry to obtain an absolute cell count of leukocytes (CD45<sup>+</sup>), lymphocytes (CD45<sup>high</sup>CD14<sup>-</sup>), and lymphocyte-gated T cells (CD3<sup>+</sup>), B cells (CD19<sup>+</sup>), and NK cells (CD56<sup>+</sup>). T cells were further subdivided into CD4<sup>+</sup> and CD8<sup>+</sup> T cells.

For multimer staining, one million cells from the cellular product were stained with pMHC pentamers; PE-Fluorotag; and CCR7 (clone 150503), CD8 (clone SK1), CD62 (clone DREG-56), CD45RA (clone HI100), CD4 (clone RPA-T4), and CD3 (clone UCHT1) antibodies and measured with flow cytometry.

### ❖ TCRβ bulk sequencing

DNA isolation was carried with the Qiagen AllPrep DNA/RNA Mini Kit. The TCR β-chains (TCRβ) from 100 ng of cellular DNA, equivalent to approximately 14,500 T cells, were amplified through multiplex PCR and sequenced with an Illumina HiSeq2000 system [46].

### ❖ Definition of clones and peptide-specific T cells

We defined clones as cells with TCRβ rearrangements above a 0.01% percentage-of-reads cutoff. To classify T cell clones as peptide-specific, we used (i) a frequency cutoff of 0.1% before and after multimer sort to reduce noise and (ii) a ternary exclusion criterion with an enrichment ratio (frequency after / frequency before multimer sort): Clones with an enrichment ratio 10 times stronger in EPL-, RAK-, or HPV-multimer-sorted populations as compared to the other two were designated as peptide-specific.

### 3. Results

#### 3.1 Article 1 [41]

##### ❖ Tumor-infiltrating T cells (TILs) and T cells from unaffected mucosa (TUMs) show distinct immune phenotypes

Our first question in this project was whether there is a phenotypic difference between TILs in the rectal tumor and TUMs. Multi-parameter flow cytometry with 13 different differentiation and checkpoint molecule antibodies showed that phenotypes could be compartmentalized as TIL, TUM, or overlapping (Fig. 2).

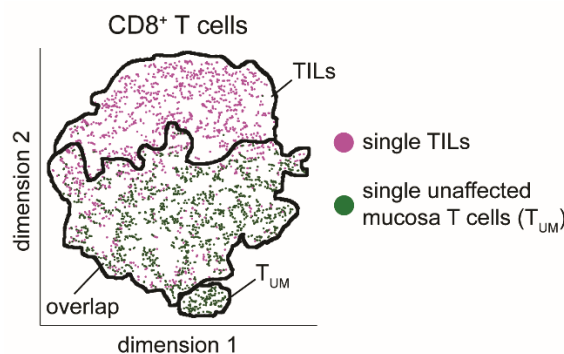


**Figure 2: Distinct phenotype compartments of TILs and TUMs**

t-Distributed Stochastic Neighbor Embedding (t-SNE) visualization. Modified from Fig. 2, Pen-ter *et al.* 2019

##### ❖ Differential T cell presence in tumor, adjacent tissue, and PB

Using single cell index sorting, single TILs and TUMs were analyzed for clonality (based on TCR $\alpha\beta$  sequencing), immune phenotypes, and cytokine expression. Clonally expanded TILs could be phenotypically distinguished from clonally expanded TUMs by characteristic TIM3 and PD1 expression.

While single cell sequencing is useful for the identification of clone-associated immune phenotypes, TCR $\beta$  bulk sequencing allows the search of TCR sequences in a larger cellular cohort. We performed TCR $\beta$  bulk sequencing of CD8+ peripheral blood T cells to search for TIL clonotypes previously identified by single cell sequencing.

From 149 expanded TIL clones, 61.7% were exclusively found in the tumor, 19.5% were also detectable in unaffected mucosa, and 32.9% could be found circulating in peripheral blood (Fig.3). Clones with the previously characterized TIM3+ PD1+ phenotype rarely appeared in PB and unaffected mucosa but were enriched in the tumor. No TCR clonotype was found shared among patients.

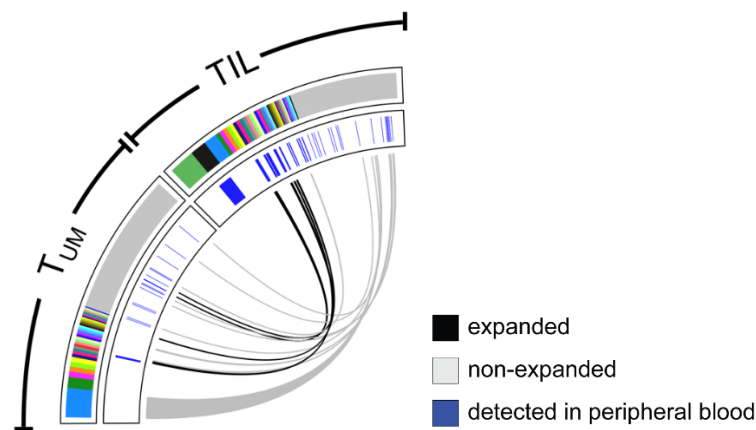


**Figure 3: Clonal overlap among TIL, TUM, and peripheral blood T cells**

Data from patient no. 3 are shown as an example. Single vertical and colored lines on the outer ring represent expanded T cell clones. Gray area corresponds to non-expanded T cells. Blue lines in the inner circle indicate clones that appeared in PB. Black connectors show overlap of expanded TIL clones with TUM; gray connectors, of expanded TUM clones with TIL. Modified from Fig. 4, Penter *et al.* 2019

#### ❖ Clonally expanded TILs recognize antigens on tumor and unaffected mucosa cells

Four tumor-exclusive and three overlapping TCRs were chosen to determine whether their target antigens were expressed solely on tumor tissue. Selected TCRs were expressed on 58 $\alpha$  $\beta$ <sup>-</sup> hybridoma cell lines carrying an NFAT-GFP reporter and were then co-cultured with tumor and unaffected mucosa cells.

Rare cell aggregates with GFP expression were visible with fluorescent microscopy indicating T cell antigen recognition. From four TIL-exclusive TCRs, one recognized an antigen solely from the tumor, one solely from unaffected mucosa, and two from both (one example of a TIL-exclusive TCR recognizing both tumor and unaffected mucosa cells is shown in Fig. 4). From the three overlapping TCRs, two were activated by both tumor and unaffected mucosa cells; one, only by unaffected mucosa. Therefore, TIL target-antigens were not found exclusively on tumor cells.

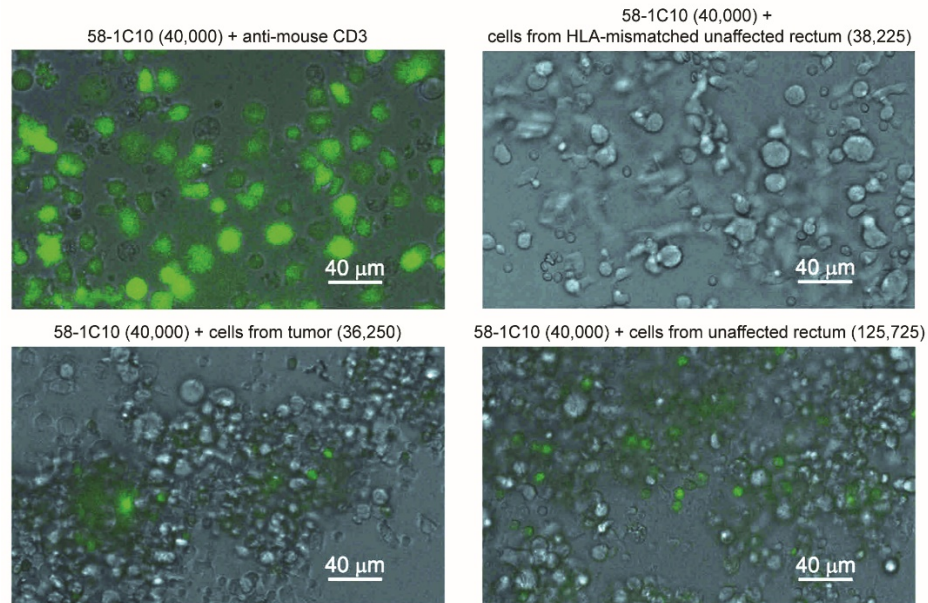


**Figure 4: Presence of TCR target antigen in tumor and unaffected mucosa tissue**

Fluorescence microscopy of 1C10-recombinant  $58\alpha\beta^-$  hybridoma reporter cells (58-1C10) stimulated with plate-bound anti-mouse CD3 antibody (as positive control) or co-cultured with tumor, unaffected mucosa, or HLA-mismatched unaffected mucosa (as negative control). GFP was measured as a readout of TCR-driven activation. 1C10 TCR is shown as an example of two TIL-restricted TCRs that were tested. Numbers in parenthesis indicate number of cells in each co-culture. Modified from Fig. 5, Penter *et al.* 2019

### 3.2 Article 2 [42]

#### ❖ Epitope-specific CD8<sup>+</sup> T cells expand after peptide stimulation

We stimulated mononuclear cells from 5 allogeneic stem cell grafts with three synthetic peptides presented on HLA-B\*35:01 (HPV, YPL, and EPL) and one graft with four peptides presented on HLA-A\*02:01 (GLC, CLG, FLY, and YVL) (Table 1). While absolute leukocyte counts decreased, CD8<sup>+</sup> T cells expanded. Peptide-specific T cell frequencies increased on average 42-fold (range: 1-228, median: 27) (Fig. 5) and expansion degree varied among donors and peptides.

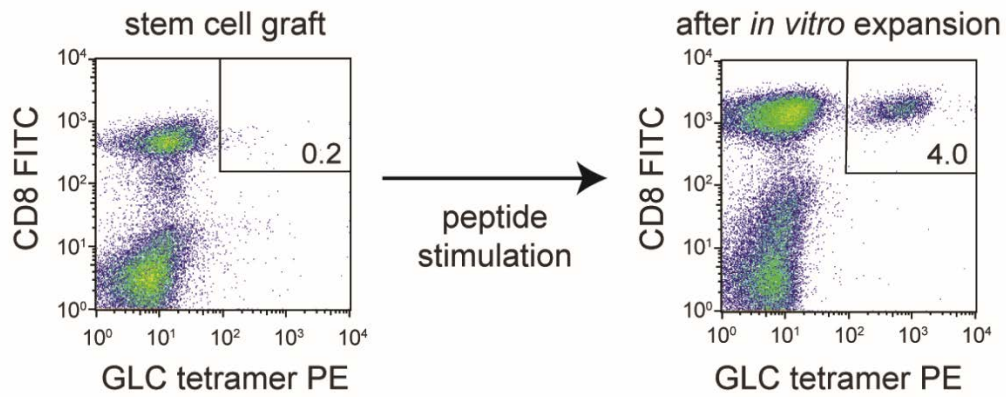


**Figure 5: Peptide-specific expansion of CD8<sup>+</sup> T cells**

Data from one stem cell graft expansion driven by GLC peptide presented on HLA-A\*02:01 are shown as an example. Plots were pre-gated on live, CD45<sup>+</sup>, CD3<sup>+</sup> lymphocytes. Modified from Fig. 1, Lammoglia Cobo *et al.* 2022

❖ **Clonal T cell expansion patterns are donor- and peptide-dependent**

We single cell index-sorted tetramer-binding CD8<sup>+</sup> T cells from *in vitro* stimulated cells and sequenced their TCR $\alpha$ - and  $\beta$  chains. We observed two different patterns regarding the number and frequency of expanded T cell clones: i) expansions with a single dominant clone of frequency above 40% in clonally expanded cells (example from 5 of 13 expansions in Fig. 6A, left pie chart) and ii) oligoclonal expansion (example from 8 of 13 expansions in Fig. 6A, right pie chart). Numbers and sizes of expanded T cell clones varied among donors and peptides used for stimulation (Fig. 6B).

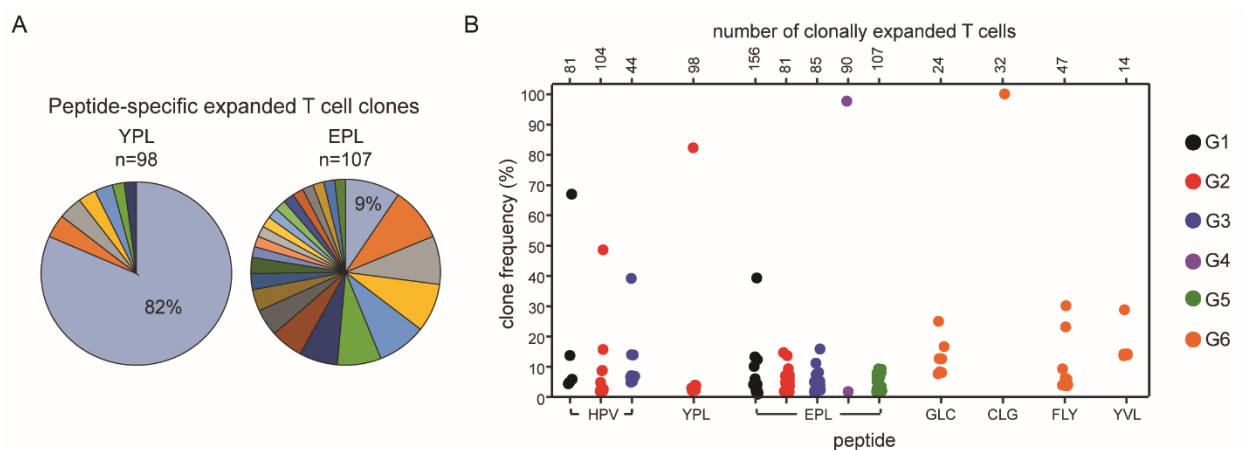


**Figure 6: Clonal expansion after peptide stimulation**

(A) Example of an expansion with a single dominant clone (YPL) and an oligoclonal expansion with a variety of less dominant clones (EPL). n= number of clones per graft after peptide stimulation. Percentage indicates frequency of the most dominant clone. (B) Frequencies of

individual clones among total identified clones per expansion per sample. G= graft number. Modified from Fig. 2, Lammoglia Cobo *et al.* 2022

### ❖ Dominant T cell clones are target peptide-specific

To test TCR peptide specificity, we re-expressed TCRs of 17 dominant T cells covering specificities for EBV latent and lytic antigens on 58 $\alpha\beta$ - hybridoma cells with NFAT-driven GFP. Sixteen out of seventeen TCR-recombinant cell lines were activated when co-incubated with target peptide-loaded miniLCLs expressing the required HLA-molecule (Fig. 7). No signal was detected with non-target peptides or when HLA-mismatched miniLCLs were used as antigen-presenting cells.

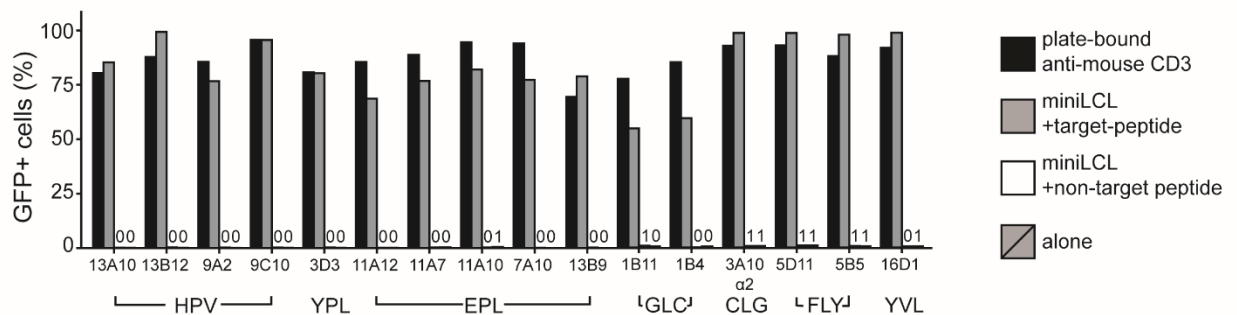


**Figure 7: Selected TCRs are target-peptide specific**

TCR-recombinant 58 $\alpha\beta$  hybridoma cells were co-cultured with miniLCLs loaded with target or non-target peptide. Plate-bound anti-mouse CD3 stimulation was used as positive control. GFP expression indicated TCR-dependent T cell activation. Modified from Fig. 3, Lammoglia Cobo *et al.* 2022

### ❖ TCR-recombinant lymphocytes recognize EBV<sup>+</sup> LCLs

Once we confirmed target peptide specificity, we tested whether TCR-recombinant T cells recognized EBV-infected cell lines. To strengthen the translational approach, we selected 7 TCRs for re-expression in third-party human PBLs.

Three HLA-B\*35:01- and four HLA-A\*02:01-restricted TCRs were transduced in human PBLs with an average 34% (range 17.9% - 55.6%) of recombinant TCR expression in CD8<sup>+</sup> T cells. TCR-recombinant T cells were activated by HLA-B\*35:01<sup>+</sup> (B01-LCL and DJS-LCL) or HLA-A\*02:01<sup>+</sup> (B03-LCL, DJS-LCL, and JY-LCL) LCLs, as measured by CD137 expression and IFN- $\gamma$  production. Non-transduced T cells were used as a negative control (Fig. 8). One recombinant TCR was used to characterize T cell activation in more detail by using HLA-mismatched LCLs, target peptide-loaded

LCLs, and additional readouts (CD107a expression and TNF- $\alpha$  and Granzyme B secretion in cell culture supernatant). This analysis confirmed specific activation of T cells transduced with EBV peptide-specific TCRs by LCLs (Fig. 9).

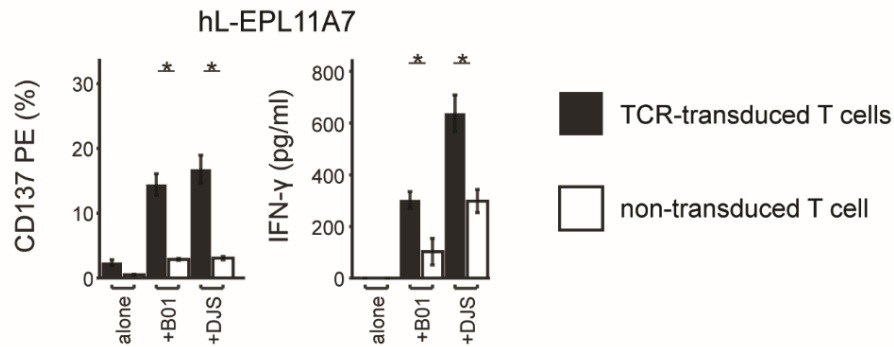


**Figure 8: TCR-recombinant PBLs recognize EBV-infected cell lines**

PBLs were transduced with three HLA-B\*35:01- and four HLA-A\*02:01-restricted TCRs and co-cultured with LCLs. CD137 expression and IFN- $\gamma$  production were measured as readouts of T cell activation. Co-incubation of HLA-B\*35:01-restricted, EPL-specific TCR is shown as an example for 3 independent experiments. Bars show mean  $\pm$  standard error. \*  $p < 0.05$  by Welch two sample t-test. Modified from Fig. 4, Lammoglia Cobo *et al.* 2022

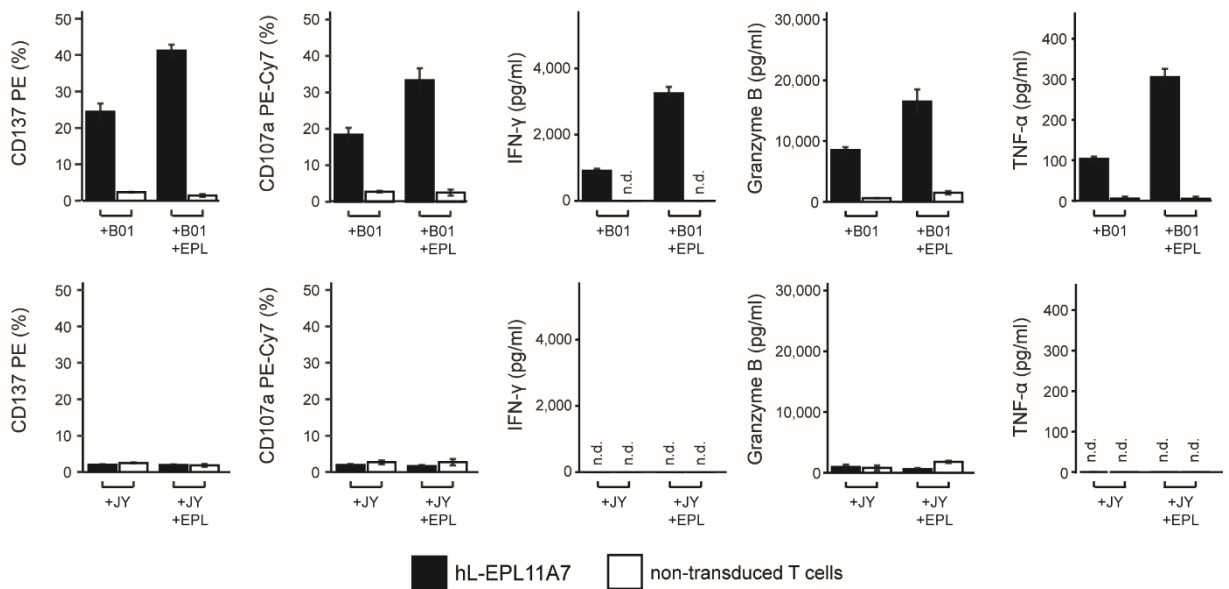


**Figure 9: T cell activation by EBV+ LCLs is peptide- and HLA-dependent**

hL-EPL11A7 and non-transduced T cells were co-cultured with HLA\*35:01+ B01-LCLs or HLA-mismatched JY-LCLs alone or loaded with 5 $\mu$ M EPL (target peptide). CD137 and CD107a expression and IFN- $\gamma$ , Granzyme B, and TNF- $\alpha$  secretion in cell culture supernatant

were measured as readouts. Bars show mean  $\pm$  standard error of triplicates. Modified from Supp. Fig. 7, Lammoglia Cobo *et al.* 2022

### 3.3 Article 3 [43]

#### ❖ Multimer-binding CD8<sup>+</sup> T cells expand after peptide-stimulation

After stimulation of 600 million PBMCs with immunogenic EBV-derived peptides, absolute T cell numbers doubled from 315 million to 631 million with a relative frequency increase from 53% to 83% of all leukocytes. Of note, CD8<sup>+</sup> T cells increased 5.7-fold, from 87.6 to 500 million cells (Fig. 10A).

Within the CD3<sup>+</sup>CD8<sup>+</sup> T cell compartment, cells that bound multimers loaded with EBV-derived peptides RAK, EPL, and HPV increased 37.8-, 21.9-, and 17.3-fold, respectively (Fig. 10B). After peptide stimulation, CD8<sup>+</sup> T cells shifted towards an effector memory phenotype (CCR7<sup>-</sup>CD45RA<sup>-</sup>).

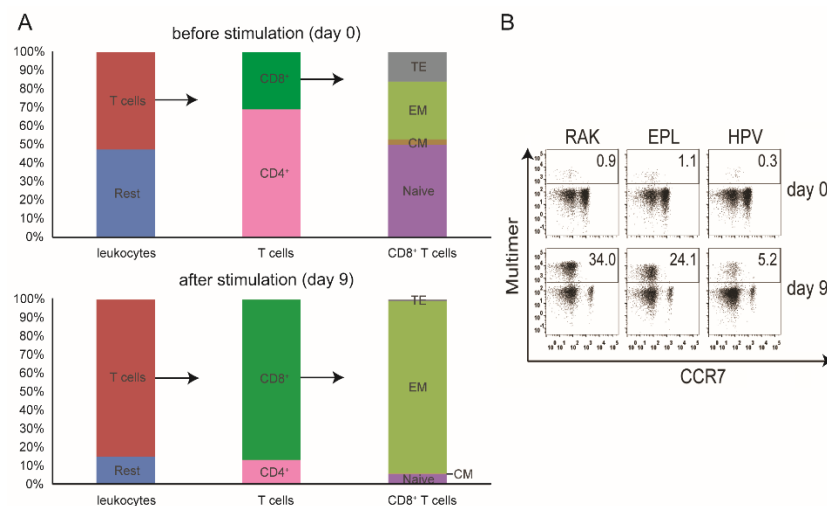


**Figure 10: T cell expansion after peptide stimulation in the cellular product**

(A) Relative frequency of subpopulations in Leukocytes, T cells, and CD8<sup>+</sup> T cells. (B) RAK, EPL, and HPV multimer staining before (day 0) and after (day 9) peptide stimulation. Modified from Fig. 1, Lammoglia Cobo & Ritter *et al.* 2022

#### ❖ EBV peptide-specific clones dominate the TCR repertoire

Sequencing of 100 ng DNA (approximately 14,500 T cells) from the T cell product before (day 0) and after peptide stimulation (day 9) revealed a strong expansion of V $\beta$  segments V $\beta$ 6 and V $\beta$ 7 after peptide stimulation. V $\beta$ 6 was the most dominant rearrangement in EPL and HPV multimer-sorted populations, while V $\beta$ 4 and V $\beta$ 7 were the most frequent ones in RAK-sorted cells. While the most dominant clonotype on day 0



had a relative frequency of 1.4%, the most dominant one on day 9 had 14.5%, indicating a strong selection process in the T cell product.

We found 327 EPL, 341 RAK, and 313 HPV multimer-binding clonotypes in the cellular product on day 9. Gating for multimer sort was stringent enough to achieve a purity above 98%; however, contaminant and overlapping clonotypes with minor frequencies still appeared. To remove unspecific multimer binding and characterize clones as peptide-specific, we used additional frequency and ternary exclusion criteria of the enrichment ratio for all three multimers. From 471 TCRs identified in the cellular product, these criteria led to the identification and characterization of 40 EPL-, 28 RAK-, and 9 HPV-specific T cell clonotypes, which covered 15.1%, 30.3%, and 29.5% of total reads, respectively (Fig. 11).

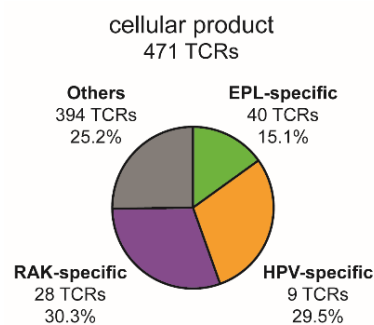


**Figure 11: Identification of peptide-specific TCR clonotypes in the cellular product**

Modified from Fig.2, Lammoglia Cobo & Ritter *et al.* 2022

#### ❖ EBV-specific T cell clones survive long-term *in vivo* after adoptive transfer

Before adoptive transfer, the patient had an EBV infection that reached a peak of 140,000 DNA copies/ $\mu$ l in blood on day 89 post-transplant. As major symptoms persisted despite treatment of EBV viremia with DLI and Rituximab, the patient received the adoptive transfer of EBV-specific cells on day 105 post-transplant. Along with an initial peak of CD8<sup>+</sup> T cells on day 113, there was no further EBV reactivation after transfer (Fig. 12).

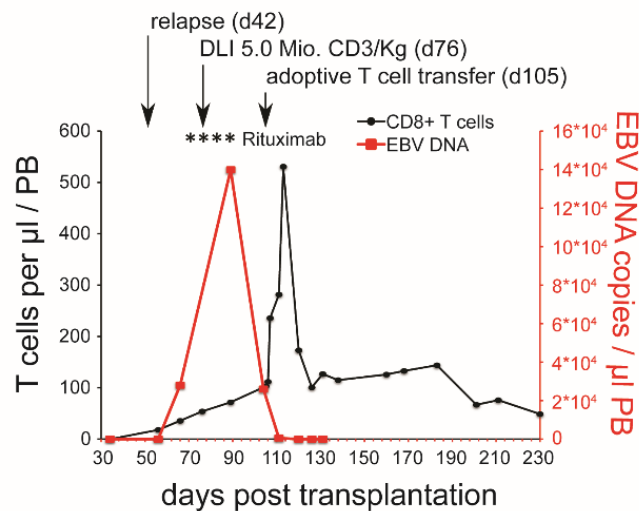


**Figure 12: Patient EBV viremia and CD8<sup>+</sup> T cell levels post-engraftment**

Modified from Fig. 3, Lammoglia Cobo & Ritter *et al.* 2022

TCR $\beta$  bulk sequencing of PB on days 60, 120, 180, and 232 post-transplant were used to monitor the fate of adoptively transferred, EBV-specific T cells. On day 60, prior to T cell transfer, number of EBV-specific T cells remained low. After adoptive transfer on day 105, we observed a substantial expansion of EBV-specific T cells on day 120. The frequency of EBV-specific cells slowly decreased after this point (Table 3, Fig. 13). As no further EBV reactivation was detected after day 110, we conclude only few T cell specificities survive long term and contribute to EBV control.

**Table 3: Follow-up of EBV-specific T cells after adoptive transfer**

days post-Tx	EPL-specific T cells		RAK-specific T cells		HPV-specific T cells	
	No. TCR clonotypes	frequency of reads (%)	No. TCR clonotypes	frequency of reads (%)	No. TCR clonotypes	frequency of reads (%)
60	2	3.67	4	4.78	0	0.00
120	34	15.43	21	5.06	6	2.37
180	33	11.05	21	3.92	5	2.45
232	34	7.09	18	1.21	3	0.19

Number of peptide-specific clonotypes and percentage of reads from CD8<sup>+</sup> T cell samples. Adoptive transfer of EBV-specific T cells took place on day 105 post-transplantation (post-Tx). Modified from Supp. Table 5, Lammoglia Cobo & Ritter *et al.* 2022

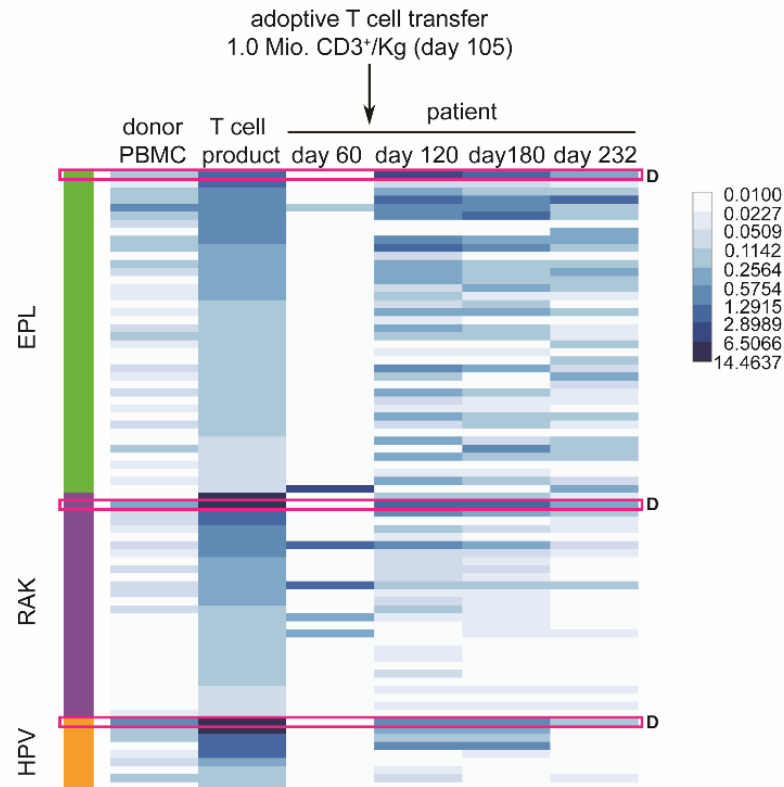


**Figure 13: Frequency of peptide-specific T cells before and after adoptive transfer**

Heatmap shows the frequency of reads from single peptide-specific T cell clonotypes in total CD8<sup>+</sup> T cells. Each horizontal line represents a single clone. Clones identified as D indicate the peptide-specific clone with the highest frequency in the cellular product. Modified from Fig. 4, Lammoglia Cobo & Ritter *et al.* 2022

## 4. Discussion

### 4.1 Short summary of results

In this work, my goal was to identify EBV peptide-specific TCRs for adoptive transfer of TCR-transduced T cells after alloSCT. It was therefore necessary to i) establish a methodology to determine TCR $\alpha$ - and  $\beta$  sequences at single cell resolution, ii) identify and test re-expressed EBV-specific TCRs for clinical potential, and iii) understand long-term survival and associated viral control of adoptively transferred, EBV-specific T cells.

In Article 1 [41], I learned a methodology previously established in our lab to determine immune phenotype and TCR sequences at the single cell level [44]. In Article 2 [42], single cell TCR sequencing and TCR re-expression were used to identify 16 EBV peptide-specific TCRs. Seven of these TCRs were transduced in third-party T cells and TCR-recombinant T cells recognized EBV-infected LCL. In Article 3 [43], we tracked *in vitro* expanded, EBV-specific T cells in an alloSCT patient after EBV reactivation. Long-term survival of few EBV peptide-specific T cell clonotypes was associated with reconstitution of EBV-specific immunity and protection against the virus. The patient died of systemic HSV-1 reactivation (an EBV-unrelated cause), thus emphasizing the importance of prophylactic strategies for viral control in a post-transplant context.

### 4.2 Interpretation of results

We had two starting materials available for EBV peptide-specific T cell expansion: G-CSF-mobilized stem cell grafts (Article 2 [42]) and non-mobilized PBMC (Article 3 [43]). Stem cell grafts had several advantages: There are plenty of CD8<sup>+</sup> T cells; no further collection of donor samples is required (especially to avoid a second apheresis); and HLA haplotyping and EBV serostatus are readily available. However, when unavailable, PBMC proved to be an equally good source of EBV-specific CD8<sup>+</sup> T cells [30].

Peptide stimulation of donor material led to a strong expansion of pMHC multimer-binding, CD8<sup>+</sup> T cells (up to 74.8% of all TCR reads in the cellular product of Article 3 [43]) without the need of antigen-recombinant APC. These peptide-stimulated cells served as either cellular product for adoptive transfer (Article 3 [43] and clinical study EudraCT 2012-004240-30) or as a source to identify EBV-specific TCRs (Article 2 [42]).

Despite the high level of purity in pMHC multimer<sup>+</sup> cell sorting, non-target clones appear probably either due to unspecific multimer binding or contamination. To exclude them, we used two different approaches: In Article 3 [43], we applied (i) stringent gating for a pMHC multimer sort purity above 98%, (ii) a higher frequency cutoff before and after multimer

sort, and (iii) a ternary exclusion criterion with an enrichment ratio at least 10 times higher for one of the multimers to exclude multimer unspecific bindings. While this approach removed most contaminants and cells with unspecific pMHC binding, an additional method was required to test selected TCRs for functionality and peptide specificity. Hence, in Articles 1 [41] and 2 [42], we sorted and sequenced T cells at the single cell level and then re-expressed selected TCRs in the CD8<sup>+</sup> 58αβ<sup>-</sup> reporter cell line. Single cell sequencing has the advantage of yielding naturally occurring paired TCRα- and β sequences for clonal characterization and TCR re-expression. Using this method, we identified EBV peptide-specific TCRs for adoptive transfer.

We developed two strategies to monitor EBV-specific T cells: In Article 3 [43], bulk sequencing of TCRβ variable and joining segments from 14,500 T cells was used to track expanded clonotypes from the cellular product in patient's PB samples. In Article 2 [42], the TCR constructs contained a chimeric mouse constant to monitor TCR-recombinant T cells using an anti-mouse TCRβ antibody. These two methodologies give us the possibility to track adoptively transferred, EBV-specific T cells in patient's PB samples.

### 4.3 Embedding the results into the current state of research

There is a strong correlation between the presence of adoptively-transferred EBV-specific T cells and the absence of EBV-associated lymphomas [50], EBV reactivation [51], and the control of active infections [52,53]. For this reason, survival of either *in vitro* expanded or TCR-recombinant, EBV-specific T cells and absence or control of EBV-associated complications indicate prophylactic or therapeutic success after adoptive transfer.

To identify EBV-specific TCRs, sequencing methodologies can use donor T cell samples without prior *in vitro* stimulation [54,55] or stimulated with either EBV-antigen-recombinant APC [29,40] or EBV-infected cell lines [28] as starting material. We decided to stimulate T cells *in vitro* with synthetic peptides to specifically expand low frequency EBV-specific T cell clones and to increase single cell sort and sequencing efficiency with an enriched target population. Despite using peptide-loaded target cells, TCR-recombinant T cells were able to recognize EBV-infected LCLs and, therefore, naturally processed and presented peptides.

In our articles, pMHC multimer usage was restricted for analytic purposes and pMHC tetramers were used as part of the TCR discovery platform. Previous studies used a multimer-based approach to generate virus-specific T cell products [56–59]; however, our

cellular product in Article 3 [43] was adoptively transferred without preselection of multimer-binding cells [30] on two premises: 1) It is currently debated whether multimer-binding requires a higher affinity than T cell activation [60] and would therefore introduce a bias and 2) multimer-binding may lead to prolonged T cell activation or altered functionality [56,61]. Still, pMHC multimers were essential to characterize epitope-specific compartments in detail in Article 3 [43] and to sort epitope-specific T cells for TCR identification in Article 2 [42].

#### 4.4 Strengths and weaknesses of the studies

To select TCRs for potential clinical application, we focused on TCRs targeting immunodominant EBV-derived epitopes presented on selected HLAs. However, we were surprised by the large TCR diversity and minimal TCR overlap among different donors for TCRs with the same peptide specificity and HLA restriction. In Article 2 [42], we observed T cell clonotype selection and clonal expansion patterns after peptide stimulation to be donor specific, with only a few shared TCRs among donors. Due to this high diversity of EBV-specific T cell clones, readily available TCRs with known specificity and which have been tested for EBV<sup>+</sup> cell line recognition may offer a more consistent therapeutic approach for TCR re-expression and adoptive T cell transfer. This potentially curative approach is of particular importance in the case of EBV-seronegative donors with no EBV-specific memory compartment available.

The main strengths of our strategies are:

- ❖ Identification of EBV-specific TCRs with clinical potential
  - Epitope specificity is demonstrated by activation of recombinant reporter cell lines in co-culture with target peptide-loaded cells.
  - Selected TCRs are not alloreactive.
  - TCR-transduced PBLs recognize EBV<sup>+</sup> LCLs.
- ❖ TCR clonotype identification through:
  - molecular characterization of the cellular product and TCR $\beta$  bulk sequencing (Article 3 [43]),
  - single cell index sorting and sequencing (Articles 1 [41] and 2 [42]), and
  - mTCR $\beta$  FACS staining (Article 2 [42]).
- ❖ Flexibility of the manufacturing protocol to incorporate peptides from different antigens, viruses, or presented on different HLA-types

- ❖ Clinical translation of TCR-recombinant T cells available for patients with EBV infection, EBV-reactivation, or EBV-associated malignancies, not restricted to a post-alloSCT context

The main limitation of our approach is dependency on available data concerning immunodominant epitopes. For example, information on HLA restrictions is mostly derived from studies on populations of European descent. Despite this, EBV is a well-characterized virus for which several immunodominant peptides have been identified and for which we expect scientific knowledge, including from less-well represented population cohorts, to keep expanding in the future.

While stimulation with high peptide concentrations may result in the expansion of irrelevant TCR clonotypes, we incorporated TCR re-expression in reporter cell lines and co-culture of TCR-recombinant T cells with LCLs to validate peptide specificity and possible clinical relevance. Our methodology proved to be highly selective, as 16 of 17 tested TCRs were peptide-specific and T cells transduced with seven selected TCR were activated when co-cultured with EBV-infected cell lines.

#### **4.5 Implications for practice and/or future research**

The question remains as to which is the optimal TCR candidate for re-expression and adoptive transfer. A combination rather than a single TCR will be the best approach for clinical translation and, for improved survival, T cell transfers may even have to include CD4<sup>+</sup> helper T cells. The complex pathogenesis of EBV-associated diseases involves progression through several latency and lytic phases, with different antigen expression patterns appearing in EBV-associated malignancies [62–64]. Considering EBV has co-evolved with humans over thousands of years and produces a life-long infection in humans, a combination of T cell clones with different avidities, specificities, and phenotypes remains in the T cell memory compartment and controls EBV in its different stages [65]. Polyclonal T cell expansion specific for a single epitope indicates *in vivo* selection of TCRs with different affinities for one single specificity. Therefore, future studies can help clarify the role of single EBV-specific T cells and their combined dynamics during EBV latency, EBV lytic infection, and development of EBV-associated malignancies.

As we tracked adoptively transferred cells in the patient from Article 3 [43], we noticed that only few peptide-specific T cell clonotypes survived long-term and mediated EBV control. This points to the importance of carefully selecting several TCRs for re-expression and possible need for repeated adoptive T cell transfer.

GMP-compliant protocols for a retroviral TCR transduction into human T cells have already been established [66,67] and will facilitate clinical translation as a gene therapy according to the Advanced Therapeutic Medicinal Products (ATMP) of the European Medicines Agency (EMA). Identified TCRs can therefore be compiled into an HLA-restricted TCR library for transduction into third-party donor cells to produce readily available, off-the-shelf products with a manufacturing and clinical license.

In this project, we selected four HLA-A\*02:01 and three HLA-B\*35:01-presented EBV-derived peptides to establish an efficient platform for the identification of EBV-specific T cells. Our methodology proved to be very robust, as 16 out of 17 reconstructed TCRs were target peptide-specific. With this information, the flexibility of the manufacturing pipeline easily allows us to expand our peptide library for additional EBV antigens, HLA-restrictions, and transplant-relevant viruses such as CMV, Adenovirus, and Human Herpesvirus 6 (HHV-6). Finally, as PTLD is not limited to alloSCT but also present in adult solid organ transplantation [68], our cellular products can be used in different post-transplantation or immunocompromised scenarios as required.



## 5. Conclusions

Adoptive transfer of EBV-specific T cells offers the possibility to reconstitute cellular immunity against EBV, protect patients against EBV-related complications without comprising B cell immunity, and therefore contribute to a better outcome post-transplant. In this project, we were able to establish a robust pipeline for the discovery of EBV-specific TCRs of clinical potential. The ability to easily exchange peptides in the process allows targeting of different antigens, HLA-restrictions, and potentially other viruses. TCRs of defined peptide specificity and HLA restriction can then be stored in TCR libraries to prepare readily available off-the-shelf products.

Using single cell sorting and sequencing of *in vitro* peptide-stimulated cells, we identified EBV peptide-specific TCRs which, transduced in third party T cells, recognize EBV-infected cell lines. Simultaneously, we observed the long-term *in vivo* survival of adoptively transferred EBV-specific T cells and the associated immune control of EBV in a case study. Based on these findings, we propose adoptive transfer of virus-specific T cells transduced with carefully selected TCRs as a prophylactic and therapeutic approach to prevent EBV-associated complications.

## Reference list

1. Passweg JR, Baldomero H, Chabannon C, Basak GW, Corbacioglu S, Duarte R, Dolstra H, Lankester AC, Mohty M, Montoto S, Peffault de Latour R, Snowden JA, Styczynski J, Yakoub-Agha I, Kröger N. The EBMT activity survey on hematopoietic-cell transplantation and cellular therapy 2018: CAR-T's come into focus. *Bone Marrow Transplant* 2020; 55(8): 1604–13.
2. Penack O, Peczynski C, Mohty M, Yakoub-Agha I, Styczynski J, Montoto S, Duarte RF, Kröger N, Schoemans H, Koenecke C, Peric Z, Basak GW. How much has allogeneic stem cell transplant-related mortality improved since the 1980s? A retrospective analysis from the EBMT. *Blood Adv* 2020; 4(24): 6283–90.
3. Ogonek J, Kralj Juric M, Ghimire S, Varanasi PR, Holler E, Greinix H, Weissinger E. Immune Reconstitution after Allogeneic Hematopoietic Stem Cell Transplantation. *Front Immunol* 2016; 7: 507.
4. Liu L, Zhang X, Feng S. Epstein-Barr Virus-Related Post-Transplantation Lymphoproliferative Disorders After Allogeneic Hematopoietic Stem Cell Transplantation. *Biol Blood Marrow Transplant* 2018; 24(7): 1341–9.
5. Compagno F, Basso S, Panigari A, Bagnarino J, Stoppini L, Maiello A, Mina T, Zelini P, Perotti C, Baldanti F, Zecca M, Comoli P. Management of PTLN After Hematopoietic Stem Cell Transplantation: Immunological Perspectives. *Front Immunol* 2020; 11: 567020.
6. Styczynski J, Gil L, Tridello G, Ljungman P, Donnelly JP, van der Velden W, Omar H, Martino R, Halkes C, Faraci M, Theunissen K, Kalwak K, Hubacek P, Sica S, Nozzoli C, Fagioli F, Matthes S, Diaz MA, Migliavacca M, Balduzzi A, Tomaszewska A, La Camara R de, van Biezen A, Hoek J, Iacobelli S, Einsele H, Cesaro S. Response to rituximab-based therapy and risk factor analysis in Epstein Barr Virus-related lymphoproliferative disorder after hematopoietic stem cell transplant in children and adults: a study from the Infectious Diseases Working Party of the European Group for Blood and Marrow Transplantation. *Clin Infect Dis* 2013; 57(6): 794–802.
7. Young LS, Yap LF, Murray PG. Epstein-Barr virus: more than 50 years old and still providing surprises. *Nat Rev Cancer* 2016; 16(12): 789–802.
8. Khan G, Fitzmaurice C, Naghavi M, Ahmed LA. Global and regional incidence, mortality and disability-adjusted life-years for Epstein-Barr virus-attributable malignancies, 1990-2017. *BMJ Open* 2020; 10(8): e037505.

9. Middeldorp JM. Epstein-Barr Virus-Specific Humoral Immune Responses in Health and Disease. *Curr Top Microbiol Immunol* 2015; 391: 289–323.
10. Tangye SG, Palendira U, Edwards ESJ. Human immunity against EBV-lessons from the clinic. *J Exp Med* 2017; 214(2): 269–83.
11. Moss DJ, Rickinson AB, Pope JH. Long-term T-cell-mediated immunity to Epstein-Barr virus in man. I. Complete regression of virus-induced transformation in cultures of seropositive donor leukocytes. *Int J Cancer* 1978; 22(6): 662–8.
12. Moss DJ, Misko IS, Burrows SR, Burman K, McCarthy R, Sculley TB. Cytotoxic T-cell clones discriminate between A- and B-type Epstein-Barr virus transformants. *Nature* 1988; 331(6158): 719–21.
13. Lee SP, Thomas WA, Murray RJ, Khanim F, Kaur S, Young LS, Rowe M, Kurilla M, Rickinson AB. HLA A2.1-restricted cytotoxic T cells recognizing a range of Epstein-Barr virus isolates through a defined epitope in latent membrane protein LMP2. *J Virol* 1993; 67(12): 7428–35.
14. Burrows SR, Gardner J, Khanna R, Steward T, Moss DJ, Rodda S, Suhrbier A. Five new cytotoxic T cell epitopes identified within Epstein-Barr virus nuclear antigen 3. *J Gen Virol* 1994; 75 (Pt 9): 2489–93.
15. Steven NM, Annels NE, Kumar A, Leese AM, Kurilla MG, Rickinson AB. Immediate early and early lytic cycle proteins are frequent targets of the Epstein-Barr virus-induced cytotoxic T cell response. *J Exp Med* 1997; 185(9): 1605–17.
16. Rickinson AB, Moss DJ. Human cytotoxic T lymphocyte responses to Epstein-Barr virus infection. *Annu Rev Immunol* 1997; 15: 405–31.
17. Saulquin X, Ibisch C, Peyrat M-A, Scotet E, Hourmant M, Vie H, Bonneville M, Houssaint E. A global appraisal of immunodominant CD8 T cell responses to Epstein-Barr virus and cytomegalovirus by bulk screening. *Eur J Immunol* 2000; 30(9): 2531–9.
18. Meij P, Leen A, Rickinson AB, Verkoeijen S, Vervoort MBHJ, Bloemena E, Middeldorp JM. Identification and prevalence of CD8(+) T-cell responses directed against Epstein-Barr virus-encoded latent membrane protein 1 and latent membrane protein 2. *Int J Cancer* 2002; 99(1): 93–9.
19. Moosmann A, Bigalke I, Tischer J, Schirrmann L, Kasten J, Tippmer S, Leeping M, Prevalsek D, Jaeger G, Ledderose G, Mautner J, Hammerschmidt W, Schendel DJ, Kolb H-J. Effective and long-term control of EBV PTLD after transfer of peptide-selected T cells. *Blood* 2010; 115(14): 2960–70.

20. Rouce RH, Louis CU, Heslop HE. Epstein-Barr virus lymphoproliferative disease after hematopoietic stem cell transplant. *Curr Opin Hematol* 2014; 21(6): 476–81.
21. Gyurkocza B, Sandmaier BM. Conditioning regimens for hematopoietic cell transplantation: one size does not fit all. *Blood* 2014; 124(3): 344–53.
22. Pereira MR, Pouch SM, Scully B. Infections in Allogeneic Stem Cell Transplantation. In: Safdar A, editor. *Principles and Practice of Transplant Infectious Diseases*. New York, NY: Springer New York 2019; 209–26
23. Janeczko M, Mielcarek M, Rybka B, Ryczan-Krawczyk R, Noworolska-Sauren D, Kałwak K. Immune recovery and the risk of CMV/ EBV reactivation in children post allogeneic haematopoietic stem cell transplantation. *Cent Eur J Immunol* 2016; 41(3): 287–96.
24. Nishihori T, Al-Kadhimi Z, Hamadani M, Kharfan-Dabaja MA. Antithymocyte globulin in allogeneic hematopoietic cell transplantation: benefits and limitations. *Immunotherapy* 2016; 8(4): 435–47.
25. Jenkins MK, Schwartz RH, Pardoll DM. Effects of cyclosporine A on T cell development and clonal deletion. *Science* 1988; 241(4873): 1655–8.
26. Alho AC, Kim HT, Chammas MJ, Reynolds CG, Matos TR, Forcade E, Whangbo J, Nikiforow S, Cutler CS, Koreth J, Ho VT, Armand P, Antin JH, Alyea EP, Lacerda JF, Soiffer RJ, Ritz J. Unbalanced recovery of regulatory and effector T cells after allogeneic stem cell transplantation contributes to chronic GVHD. *Blood* 2016; 127(5): 646–57.
27. Rooney C, Ng C, Loftin S, Smith C, Li C, Krance R, Brenner M, Heslop H. Use of gene-modified virus-specific T lymphocytes to control Epstein-Barr-virus-related lymphoproliferation. *The Lancet* 1995; 345(8941): 9–13.
28. Hammer MH, Brestrich G, Mittenzweig A, Roemhild A, Zwinger S, Subklewe M, Beier C, Kurtz A, Babel N, Volk H-D, Reinke P. Generation of EBV-specific T cells for adoptive immunotherapy: a novel protocol using formalin-fixed stimulator cells to increase biosafety. *J Immunother* 2007; 30(8): 817–24.
29. Gerdemann U, Katari UL, Papadopoulou A, Keirnan JM, Craddock JA, Liu H, Martinez CA, Kennedy-Nasser A, Leung KS, Gottschalk SM, Krance RA, Brenner MK, Rooney CM, Heslop HE, Leen AM. Safety and clinical efficacy of rapidly-generated trivirus-directed T cells as treatment for adenovirus, EBV, and CMV infections after allogeneic hematopoietic stem cell transplant. *Mol Ther* 2013; 21(11): 2113–21.

30. Gary R, Aigner M, Moi S, Schaffer S, Gottmann A, Maas S, Zimmermann R, Zingsem J, Strobel J, Mackensen A, Mautner J, Moosmann A, Gerbitz A. Clinical-grade generation of peptide-stimulated CMV/EBV-specific T cells from G-CSF mobilized stem cell grafts. *J Transl Med* 2018; 16(1): 124.
31. Heslop HE, Slobod KS, Pule MA, Hale GA, Rousseau A, Smith CA, Bollard CM, Liu H, Wu M-F, Rochester RJ, Amrolia PJ, Hurwitz JL, Brenner MK, Rooney CM. Long-term outcome of EBV-specific T-cell infusions to prevent or treat EBV-related lymphoproliferative disease in transplant recipients. *Blood* 2010; 115(5): 925–35.
32. Gary R, Aigner M, Moosmann A, Ritter J, Seitz V, Moi S, Schaffer S, Balzer H, Maas S, Strobel J, Zimmermann R, Zingsem J, Kremer A, Hennig S, Hummel M, Mackensen A, Gerbitz A. Adoptive Transfer of CMV- and EBV- Specific Peptide-Stimulated T Cells after Allogeneic Stem Cell Transplantation: First Results of a Phase I/IIa Clinical Trial [Multivir-01] *Blood* 2016; 128(22): 2179.
33. Winter JR, Jackson C, Lewis JE, Taylor GS, Thomas OG, Stagg HR. Predictors of Epstein-Barr virus serostatus and implications for vaccine policy: A systematic review of the literature. *J Glob Health* 2020; 10(1): 10404.
34. Choi A, Marcus K, Pohl D, Eyck PT, Balfour H, Jackson JB. Epstein-Barr virus infection status among first year undergraduate university students. *J Am Coll Health* 2020: 1–4.
35. Kołodziejczak M, Gil L, La Camara R de, Styczyński J. Impact of donor and recipient Epstein-Barr Virus serostatus on outcomes of allogeneic hematopoietic cell transplantation: a systematic review and meta-analysis. *Ann Hematol* 2021; 100(3): 763–77.
36. Chandran SS, Klebanoff CA. T cell receptor-based cancer immunotherapy: Emerging efficacy and pathways of resistance. *Immunol Rev* 2019; 290(1): 127–47.
37. Klarenbeek PL, Remmerswaal EBM, Berge IJM ten, Doorenspleet ME, van Schaik BDC, Esveldt REE, Koch SD, Brinke A ten, van Kampen AHC, Bemelman FJ, Tak PP, Baas F, Vries N de, van Lier RAW. Deep sequencing of antiviral T-cell responses to HCMV and EBV in humans reveals a stable repertoire that is maintained for many years. *PLoS Pathog* 2012; 8(9): e1002889.
38. Soares MVD, Plunkett FJ, Verbeke CS, Cook JE, Faint JM, Belaramani LL, Fletcher JM, Hammerschmitt N, Rustin M, Bergler W, Beverley PCL, Salmon M, Akbar AN. Integration of apoptosis and telomere erosion in virus-specific CD8+ T cells from blood and tonsils during primary infection. *Blood* 2004; 103(1): 162–7.

39. Cho H-I, Kim U-H, Shin A-R, Won J-N, Lee H-J, Sohn H-J, Kim T-G. A novel Epstein-Barr virus-latent membrane protein-1-specific T-cell receptor for TCR gene therapy. *Br J Cancer* 2018; 118(4): 534–45.
40. Dudaniec K, Westendorf K, Nössner E, Uckert W. Generation of Epstein-Barr Virus Antigen-Specific T Cell Receptors Recognizing Immunodominant Epitopes of LMP1, LMP2A, and EBNA3C for Immunotherapy. *Hum Gene Ther* 2021
41. Penter L, Dietze K, Ritter J, Lammoglia Cobo MF, Garmshausen J, Aigner F, Bullinger L, Hackstein H, Wienzek-Lischka S, Blankenstein T, Hummel M, Dornmair K, Hansmann L. Localization-associated immune phenotypes of clonally expanded tumor-infiltrating T cells and distribution of their target antigens in rectal cancer. *Oncoimmunology* 2019; 8(6): e1586409.
42. Lammoglia Cobo MF, Welters C, Rosenberger L, Leisegang M, Dietze K, Pircher C, Penter L, Gary R, Bullinger L, Takvorian A, Moosmann A, Dornmair K, Blankenstein T, Kammertöns T, Gerbitz A, Hansmann L. Rapid single-cell identification of Epstein-Barr virus-specific T-cell receptors for cellular therapy. *Cytotherapy* 2022
43. Lammoglia Cobo MF, Ritter J, Gary R, Seitz V, Mautner J, Aigner M, Völkl S, Schaffer S, Moi S, Seegebarth A, Bruns H, Rösler W, Amann K, Büttner-Herold M, Hennig S, Mackensen A, Hummel M, Moosmann A, Gerbitz A. Reconstitution of EBV-directed T cell immunity by adoptive transfer of peptide-stimulated T cells in a patient after allogeneic stem cell transplantation for AITL. *PLoS Pathog* 2022; 18(4): e1010206.
44. Han A, Glanville J, Hansmann L, Davis MM. Linking T-cell receptor sequence to functional phenotype at the single-cell level. *Nat Biotechnol* 2014; 32(7): 684–92.
45. Penter L, Dietze K, Bullinger L, Westermann J, Rahn H-P, Hansmann L. FACS single cell index sorting is highly reliable and determines immune phenotypes of clonally expanded T cells. *Eur J Immunol* 2018; 48(7): 1248–50.
46. Ritter J, Seitz V, Balzer H, Gary R, Lenze D, Moi S, Pasemann S, Seegebarth A, Wurdack M, Hennig S, Gerbitz A, Hummel M. Donor CD4 T Cell Diversity Determines Virus Reactivation in Patients After HLA-Matched Allogeneic Stem Cell Transplantation. *Am J Transplant* 2015; 15(8): 2170–9.
47. Siewert K, Malotka J, Kawakami N, Wekerle H, Hohlfeld R, Dornmair K. Unbiased identification of target antigens of CD8+ T cells with combinatorial libraries coding for short peptides. *Nat Med* 2012; 18(5): 824–8.

48. Kempkes B, Pich D, Zeidler R, Sugden B, Hammerschmidt W. Immortalization of human B lymphocytes by a plasmid containing 71 kilobase pairs of Epstein-Barr virus DNA. *J Virol* 1995; 69(1): 231–8.
49. Sommermeyer D, Neudorfer J, Weinhold M, Leisegang M, Engels B, Noessner E, Heemskerk MHM, Charo J, Schendel DJ, Blankenstein T, Bernhard H, Uckert W. Designer T cells by T cell receptor replacement. *Eur J Immunol* 2006; 36(11): 3052–9.
50. Long HM, Meckiff BJ, Taylor GS. The T-cell Response to Epstein-Barr Virus-New Tricks From an Old Dog. *Front Immunol* 2019; 10: 2193.
51. Meij P, van Esser JWJ, Niesters HGM, van Baarle D, Miedema F, Blake N, Rickinson AB, Leiner I, Pamer E, Lowenberg B, Cornelissen JJ, Gratama JW. Impaired recovery of Epstein-Barr virus (EBV)--specific CD8+ T lymphocytes after partially T-depleted allogeneic stem cell transplantation may identify patients at very high risk for progressive EBV reactivation and lymphoproliferative disease. *Blood* 2003; 101(11): 4290–7.
52. Bollard CM, Kuehnle I, Leen A, Rooney CM, Heslop HE. Adoptive immunotherapy for posttransplantation viral infections. *Biology of Blood and Marrow Transplantation* 2004; 10(3): 143–55.
53. Kaeuferle T, Krauss R, Blaeschke F, Willier S, Feuchtinger T. Strategies of adoptive T-cell transfer to treat refractory viral infections post allogeneic stem cell transplantation. *J Hematol Oncol* 2019; 12(1): 13.
54. Ma K-Y, Schonnesen AA, He C, Xia AY, Sun E, Chen E, Sebastian KR, Guo Y-W, Balderas R, Kulkarni-Date M, Jiang N. High-throughput and high-dimensional single-cell analysis of antigen-specific CD8+ T cells. *Nat Immunol* 2021; 22(12): 1590–8.
55. Kobayashi E, Mizukoshi E, Kishi H, Ozawa T, Hamana H, Nagai T, Nakagawa H, Jin A, Kaneko S, Muraguchi A. A new cloning and expression system yields and validates TCRs from blood lymphocytes of patients with cancer within 10 days. *Nat Med* 2013; 19(11): 1542–6.
56. Neudorfer J, Schmidt B, Huster KM, Anderl F, Schiemann M, Holzapfel G, Schmidt T, Germeroth L, Wagner H, Peschel C, Busch DH, Bernhard H. Reversible HLA multimers (Streptamers) for the isolation of human cytotoxic T lymphocytes functionally active against tumor- and virus-derived antigens. *J Immunol Methods* 2007; 320(1-2): 119–31.

57. Cobbold M, Khan N, Pourgheysari B, Tauro S, McDonald D, Osman H, Assenmacher M, Billingham L, Steward C, Crawley C, Olavarria E, Goldman J, Chakraverty R, Mahendra P, Craddock C, Moss PAH. Adoptive transfer of cytomegalovirus-specific CTL to stem cell transplant patients after selection by HLA-peptide tetramers. *J Exp Med* 2005; 202(3): 379–86.
58. Schmitt A, Tonn T, Busch DH, Grigoleit GU, Einsele H, Odendahl M, Germeroth L, Ringhoffer M, Ringhoffer S, Wiesneth M, Greiner J, Michel D, Mertens T, Rojewski M, Marx M, Harsdorf S von, Döhner H, Seifried E, Bunjes D, Schmitt M. Adoptive transfer and selective reconstitution of streptamer-selected cytomegalovirus-specific CD8+ T cells leads to virus clearance in patients after allogeneic peripheral blood stem cell transplantation. *Transfusion* 2011; 51(3): 591–9.
59. Uhlin M, Gertow J, Uzunel M, Okas M, Berglund S, Watz E, Brune M, Ljungman P, Maeurer M, Mattsson J. Rapid salvage treatment with virus-specific T cells for therapy-resistant disease. *Clin Infect Dis* 2012; 55(8): 1064–73.
60. Laugel B, van den Berg HA, Gostick E, Cole DK, Wooldridge L, Boulter J, Milicic A, Price DA, Sewell AK. Different T cell receptor affinity thresholds and CD8 coreceptor dependence govern cytotoxic T lymphocyte activation and tetramer binding properties. *J Biol Chem* 2007; 282(33): 23799–810.
61. Chen DS, Soen Y, Stuge TB, Lee PP, Weber JS, Brown PO, Davis MM. Marked differences in human melanoma antigen-specific T cell responsiveness after vaccination using a functional microarray. *PLoS Med* 2005; 2(10): e265.
62. Smith C, Khanna R. Generation of cytotoxic T lymphocytes for immunotherapy of EBV-associated malignancies. *Methods Mol Biol* 2010; 651: 49–59.
63. Price AM, Luftig MA. To be or not IIb: a multi-step process for Epstein-Barr virus latency establishment and consequences for B cell tumorigenesis. *PLoS Pathog* 2015; 11(3): e1004656.
64. NovaliA Z, van Rossen TM. Agents and Approaches for Lytic Induction Therapy of Epstein-Barr Virus Associated Malignancies. *Med chem (Los Angeles)* 2016; 6(7)
65. Hislop AD, Gudgeon NH, Callan MF, Fazou C, Hasegawa H, Salmon M, Rickinson AB. EBV-specific CD8+ T cell memory: relationships between epitope specificity, cell phenotype, and immediate effector function. *J Immunol* 2001; 167(4): 2019–29.



66. Straetemans T, Kierkels GJJ, Doorn R, Jansen K, Heijhuurs S, Dos Santos JM, van Muyden ADD, Vie H, Clemenceau B, Raymakers R, Witte M de, Sebestyén Z, Kullball J. GMP-Grade Manufacturing of T Cells Engineered to Express a Defined  $\gamma\delta$ TCR. *Front Immunol* 2018; 9: 1062.
67. Jin J, Gkitsas N, Fellowes VS, Ren J, Feldman SA, Hinrichs CS, Stroncek DF, Highfill SL. Enhanced clinical-scale manufacturing of TCR transduced T-cells using closed culture system modules. *J Transl Med* 2018; 16(1): 13.
68. Feuchtinger T, Matthes-Martin S, Richard C, Lion T, Fuhrer M, Hamprecht K, Handgretinger R, Peters C, Schuster FR, Beck R, Schumm M, Lotfi R, Jahn G, Lang P. Safe adoptive transfer of virus-specific T-cell immunity for the treatment of systemic adenovirus infection after allogeneic stem cell transplantation. *Br J Haematol* 2006; 134(1): 64–76.

## Statutory Declaration

"I, María Fernanda Lammoglia Cobo, by personally signing this document in lieu of an oath, hereby affirm that I prepared the submitted dissertation on the topic "Epstein-Barr virus-specific T cell receptors for adoptive transfer of transduced T cells in allogeneic stem cell transplantation / Epstein-Barr Virus-spezifische T-Zell-Rezeptoren für den adoptiven Transfer transduzierter T-Zellen im Rahmen der allogenen Stammzelltransplantation", independently and without the support of third parties, and that I used no other sources and aids than those stated.

All parts which are based on the publications or presentations of other authors, either in letter or in spirit, are specified as such in accordance with the citing guidelines. The sections on methodology (in particular regarding practical work, laboratory regulations, statistical processing) and results (in particular regarding figures, charts and tables) are exclusively my responsibility.

Furthermore, I declare that I have correctly marked all of the data, the analyses, and the conclusions generated from data obtained in collaboration with other persons, and that I have correctly marked my own contribution and the contributions of other persons (cf. declaration of contribution). I have correctly marked all texts or parts of texts that were generated in collaboration with other persons.

My contributions to any publications to this dissertation correspond to those stated in the below joint declaration made together with the supervisor. All publications created within the scope of the dissertation comply with the guidelines of the ICMJE (International Committee of Medical Journal Editors; [www.icmje.org](http://www.icmje.org)) on authorship. In addition, I declare that I shall comply with the regulations of Charité – Universitätsmedizin Berlin on ensuring good scientific practice.

I declare that I have not yet submitted this dissertation in identical or similar form to another Faculty.

The significance of this statutory declaration and the consequences of a false statutory declaration under criminal law (Sections 156, 161 of the German Criminal Code) are known to me."

Date

Signature

## Declaration of your own contribution to the publications

Maria Fernanda Lammoglia Cobo contributed the following to the below listed publications:

Publication 1: Penter L, Dietze K, Ritter J, Lammoglia Cobo MF, Garmshausen J, Aigner F, Bullinger L, Hackstein H, Wienzek-Lischka S, Blankenstein T, Hummel M, Dornmair K, Hansmann L. Localization-associated immune phenotypes of clonally expanded tumor-infiltrating T cells and distribution of their target antigens in rectal cancer. *Oncoimmunology* 2019; 8(6): e1586409.

Contribution:

- Critical revision of the draft
- Discussions on data interpretation and visual representation
- Manuscript- review and editing

Publication 2: Lammoglia Cobo MF, Welters C, Rosenberger L, Leisegang M, Dietze K, Pircher C, Penter L, Gary R, Bullinger L, Takvorian A, Moosmann A, Dornmair K, Blankenstein T, Kammertöns T, Gerbitz A, Hansmann L. Rapid single-cell identification of Epstein-Barr virus-specific T-cell receptors for cellular therapy. *Cytotherapy* 2022; 1(Pt 9): 156.

Contribution:

- Project and experiment design
- Carry out experiments: peptide stimulation of grafts, flow cytometry, single cell FACS sorting, T cell receptor (TCR) re-expression in 58 $\alpha$ - $\beta$ - reporter cell line, TCR transduction in human lymphocytes, co-culture of effector and target cells, fluorescence microscopy, and mouse IL-2 and human IFN- $\gamma$  ELISAs
- Data and statistical analysis
- Design of Tables 1-2, Supplementary Tables 1-5, Figures 1-4, and Supplementary Figures 1-5
- Manuscript- writing, review, editing, and preparation for publishing

Publication 3: Lammoglia Cobo MF<sup>†</sup>, Ritter J<sup>†</sup>, Gary R, Seitz V, Mautner J, Aigner M, Völkl S, Schaffer S, Moi S, Seegebarth A, Bruns H, Rösler W, Amann K, Büttner-Herold M, Hennig S, Mackensen A, Hummel M, Moosmann A<sup>§</sup>, Gerbitz A<sup>§</sup>. Reconstitution of EBV-directed T cell immunity by adoptive transfer of peptide-stimulated T cells in a patient after allogeneic stem cell transplantation for AITL. *PLoS Pathog* 2022; 18(4): e1010206.

<sup>†</sup> Both authors contributed equally to this work.

<sup>§</sup> Both authors contributed equally to this work.

Contribution:

- Design of bioinformatic analysis
- Wet lab and clinical data analysis and interpretation

- Improvement of content and design of Figures 1-4, Supplementary Figures 1 and 4, Tables 1-2, and Supplementary Tables 1 and 5
- Creation of Supplementary Figures 2-3 and 5-9 and Supplementary Tables 2-4
- Incorporation of viral clinical data on Figure 3
- Major contribution in Results and Discussion sections
- Writing, review, editing, and preparation for publishing and peer review

## Excerpt from Journal Summary List

### *Oncoimmunology*

Journal Data Filtered By: **Selected JCR Year: 2017** Selected Editions: SCIE,SSCI  
 Selected Categories: "Immunology" Selected Category Scheme: WoS  
**Gesamtanzahl: 155 Journale**

Rank	Full Journal Title	Total Cites	Journal Impact Factor	Eigenfactor Score
1	NATURE REVIEWS IMMUNOLOGY	39,215	41.982	0.085360
2	Annual Review of Immunology	17,086	22.714	0.028800
3	NATURE IMMUNOLOGY	41,410	21.809	0.102290
4	IMMUNITY	46,541	19.734	0.136360
5	TRENDS IN IMMUNOLOGY	11,204	14.188	0.026850
6	JOURNAL OF ALLERGY AND CLINICAL IMMUNOLOGY	49,229	13.258	0.083800
7	Lancet HIV	1,476	11.355	0.007950
8	JOURNAL OF EXPERIMENTAL MEDICINE	62,537	10.790	0.078310
9	IMMUNOLOGICAL REVIEWS	14,555	9.217	0.028540
10	Cancer Immunology Research	4,361	9.188	0.021180
11	CLINICAL INFECTIOUS DISEASES	61,618	9.117	0.120010
12	AUTOIMMUNITY REVIEWS	8,956	8.745	0.020990
13	Journal for ImmunoTherapy of Cancer	1,675	8.374	0.007130
14	CURRENT OPINION IN IMMUNOLOGY	9,275	7.932	0.020120
15	JOURNAL OF AUTOIMMUNITY	6,410	7.607	0.015490
16	Cellular & Molecular Immunology	3,633	7.551	0.008300
17	EMERGING INFECTIOUS DISEASES	29,657	7.422	0.057980
18	Mucosal Immunology	6,105	7.360	0.021860
19	SEMINARS IN IMMUNOLOGY	4,552	7.206	0.010950
20	EXERCISE IMMUNOLOGY REVIEW	740	7.105	0.001110
21	Journal of Allergy and Clinical Immunology-In Practice	2,802	6.966	0.009670
22	CLINICAL REVIEWS IN ALLERGY & IMMUNOLOGY	2,741	6.442	0.005880
23	Seminars in Immunopathology	2,967	6.437	0.009290
24	BRAIN BEHAVIOR AND IMMUNITY	12,583	6.306	0.026850
25	ALLERGY	16,476	6.048	0.025790
26	Emerging Microbes & Infections	1,318	6.032	0.005910
27	Advances in Immunology	2,423	5.935	0.004250
28	Current Topics in Microbiology and Immunology	5,633	5.829	0.011740
29	World Allergy Organization Journal	1,352	5.676	0.003800
30	Frontiers in Immunology	16,999	5.511	0.067470

Rank	Full Journal Title	Total Citese	Journal Impact Factor	Eigenfactor Score
31	Oncolmmunology	5,963	5.503	0.020500
32	INFECTIOUS DISEASE CLINICS OF NORTH AMERICA	2,503	5.449	0.005170
33	Journal of Neuroinflammation	9,761	5.193	0.024860
34	INTERNATIONAL IMMUNOLOGY	5,989	5.189	0.005930
35	JOURNAL OF INFECTIOUS DISEASES	45,662	5.186	0.075270
36	CLINICAL AND EXPERIMENTAL ALLERGY	10,784	5.158	0.014370
37	Journal of the International AIDS Society	3,638	5.131	0.013920
38	AIDS	20,578	4.914	0.038030
39	JOURNAL OF IMMUNOLOGY	128,250	4.539	0.148890
40	BONE MARROW TRANSPLANTATION	12,506	4.497	0.020610
41	BIOLOGY OF BLOOD AND MARROW TRANSPLANTATION	10,583	4.484	0.026940
42	Current Opinion in HIV and AIDS	2,266	4.409	0.008060
43	Expert Review of Vaccines	3,869	4.271	0.009750
44	EUROPEAN JOURNAL OF IMMUNOLOGY	21,417	4.248	0.029960
45	JOURNAL OF CLINICAL IMMUNOLOGY	4,641	4.227	0.009100
46	CANCER IMMUNOLOGY IMMUNOTHERAPY	7,509	4.225	0.012830
47	JOURNAL OF LEUKOCYTE BIOLOGY	17,244	4.224	0.021200
48	PEDIATRIC ALLERGY AND IMMUNOLOGY	4,341	4.137	0.006970
49	JAIDS-JOURNAL OF ACQUIRED IMMUNE DEFICIENCY SYNDROMES	14,668	4.116	0.033010
50	ALLERGOLOGY INTERNATIONAL	1,696	4.036	0.003460
51	Immunity & Ageing	749	4.019	0.001580
52	TRANSPLANTATION	24,731	3.960	0.030960
53	Virulence	2,944	3.947	0.008450
54	Journal of Innate Immunity	1,922	3.837	0.005060
55	JOURNAL OF IMMUNOTHERAPY	3,093	3.826	0.004590
56	BIODRUGS	1,435	3.825	0.002460
57	Allergy Asthma & Immunology Research	1,385	3.809	0.003430
58	IMMUNOLOGY AND CELL BIOLOGY	5,385	3.795	0.009610
59	IMMUNOLOGY AND ALLERGY CLINICS OF NORTH AMERICA	1,569	3.694	0.002730

*Cytotherapy*

Journal Data Filtered By: **Selected JCR Year: 2020** Selected Editions: SCIE,SSCI  
 Selected Categories: **"BIOTECHNOLOGY and APPLIED MICROBIOLOGY"**  
 Selected Category Scheme: WoS  
**Gesamtanzahl: 159 Journale**

Rank	Full Journal Title	Total Cites	Journal Impact Factor	Eigenfactor Score
1	NATURE REVIEWS DRUG DISCOVERY	41,989	84.694	0.048220
2	NATURE BIOTECHNOLOGY	78,786	54.908	0.145670
3	TRENDS IN BIOTECHNOLOGY	20,693	19.536	0.018170
4	BIOTECHNOLOGY ADVANCES	23,792	14.227	0.017000
5	GENOME BIOLOGY	54,758	13.583	0.098990
6	MOLECULAR THERAPY	24,333	11.454	0.030250
7	BIOSENSORS & BIOELECTRONICS	69,561	10.618	0.075140
8	JOURNAL OF NANOBIO TECHNOLOGY	6,775	10.435	0.007010
9	PLANT BIOTECHNOLOGY JOURNAL	13,143	9.803	0.018400
10	METABOLIC ENGINEERING	10,661	9.783	0.015260
11	CURRENT OPINION IN BIOTECHNOLOGY	18,835	9.740	0.019700
12	BIORESOURCE TECHNOLOGY	166,941	9.642	0.102960
13	GENOME RESEARCH	47,141	9.043	0.064690
14	Annual Review of Animal Biosciences	1,470	8.923	0.003280
15	CRITICAL REVIEWS IN BIOTECHNOLOGY	5,631	8.429	0.006090
16	REVIEWS IN ENVIRONMENTAL SCIENCE AND BIOTECHNOLOGY	3,762	8.044	0.002800
17	npj Biofilms and Microbiomes	1,282	7.290	0.003180
18	BIOINFORMATICS	149,362	6.937	0.155170
19	STEM CELLS	23,967	6.277	0.017860

Rank	Full Journal Title	Total Citese	Journal Impact Factor	Eigenfactor Score
20	Biotechnology for Biofuels	14,171	6.040	0.018670
21	CANCER GENE THERAPY	3,768	5.987	0.002720
22	Microbial Biotechnology	6,007	5.813	0.006990
23	GENOMICS	11,771	5.736	0.006800
24	HUMAN GENE THERAPY	7,074	5.695	0.006860
25	Artificial Cells Nanomedicine and Biotechnology	8,530	5.678	0.011380
26	MUTATION RESEARCH-REVIEWS IN MUTATION RESEARCH	4,185	5.657	0.003170
27	FOOD MICROBIOLOGY	15,020	5.516	0.011100
28	CYTOTHERAPY	7,694	5.414	0.006940
29	Microbial Cell Factories	10,869	5.328	0.012460
30	Nanomedicine	10,613	5.307	0.009140
31	Environmental Technology & Innovation	2,657	5.263	0.002660
32	GENE THERAPY	8,112	5.250	0.004130
33	Current Opinion in Chemical Engineering	2,795	5.163	0.003980
34	Advances in Applied Microbiology	2,246	5.086	0.001390
35	New Biotechnology	4,198	5.079	0.004590
36	BIOMASS & BIOENERGY	24,521	5.061	0.012580
37	APPLIED MICROBIOLOGY AND BIOTECHNOLOGY	54,507	4.813	0.036130
38	APPLIED AND ENVIRONMENTAL MICROBIOLOGY	118,391	4.792	0.042550
39	Synthetic and Systems Biotechnology	725	4.708	0.001650
40	Biotechnology Journal	7,684	4.677	0.009140
41	Probiotics and Antimicrobial Proteins	2,370	4.609	0.002340



*PLoS Pathogens*

Journal Data Filtered By: Selected JCR Year: 2020 Selected Editions: SCIE,SSCI  
 Selected Categories: "PARASITOLOGY" Selected Category Scheme: WoS  
 Gesamtanzahl: 38 Journale

Rank	Full Journal Title	Total Cites	Journal Impact Factor	Eigenfactor Score
1	Cell Host & Microbe	28,716	21.023	0.062110
2	TRENDS IN PARASITOLOGY	8,666	9.014	0.011080
3	<b>PLoS Pathogens</b>	<b>55,666</b>	<b>6.823</b>	<b>0.085520</b>
4	Infectious Diseases of Poverty	3,434	4.520	0.006920
5	PLoS Neglected Tropical Diseases	35,321	4.411	0.060440
6	International Journal for Parasitology-Drugs and Drug Resistance	1,428	4.077	0.002310
7	INTERNATIONAL JOURNAL FOR PARASITOLOGY	11,815	3.981	0.005940
8	Parasites & Vectors	19,634	3.876	0.031090
9	Advances in Parasitology	2,809	3.870	0.002860
10	Ticks and Tick-Borne Diseases	4,726	3.744	0.006820
11	PARASITOLOGY	12,276	3.234	0.007930
12	ACTA TROPICA	11,474	3.112	0.012720
13	Parasite	2,306	3.000	0.003030
14	MALARIA JOURNAL	15,906	2.979	0.023870
15	Pathogens and Global Health	1,504	2.894	0.002530
16	MEMORIAS DO INSTITUTO OSWALDO CRUZ	7,753	2.743	0.004530
17	VETERINARY PARASITOLOGY	19,576	2.738	0.009130
18	International Journal for Parasitology-Parasites and Wildlife	1,434	2.674	0.002680
19	PARASITOLOGY RESEARCH	15,341	2.289	0.011870
20	PARASITE IMMUNOLOGY	3,484	2.280	0.002700

# Printed copies of the publications

ONCOIMMUNOLOGY  
2019, VOL. 8, NO. 6, e1586409 (12 pages)  
<https://doi.org/10.1080/2162402X.2019.1586409>



ORIGINAL RESEARCH

OPEN ACCESS

## Localization-associated immune phenotypes of clonally expanded tumor-infiltrating T cells and distribution of their target antigens in rectal cancer

Livius Penter<sup>a,b</sup>, Kerstin Dietze<sup>a</sup>, Julia Ritter<sup>c</sup>, Maria Fernanda Lammoglia Cobo<sup>b</sup>, Josefin Garmshausen<sup>a,d</sup>, Felix Aigner<sup>e</sup>, Lars Bullinger<sup>a,d</sup>, Holger Hackstein<sup>f</sup>, Sandra Wienzek-Lischka<sup>g</sup>, Thomas Blankenstein<sup>b,d,h,i</sup>, Michael Hummel<sup>c,d</sup>, Klaus Dornmair<sup>j</sup>, and Leo Hansmann<sup>a,b,d</sup>

<sup>a</sup>Department of Hematology, Oncology, and Tumor Immunology, Charité – Universitätsmedizin Berlin (CVK), Berlin, Germany; <sup>b</sup>Berlin Institute of Health (BIH), Berlin, Germany; <sup>c</sup>Institute for Pathology, Charité – Universitätsmedizin Berlin, Berlin, Germany; <sup>d</sup>German Cancer Consortium (DKTK), Partner site Berlin, Berlin, Germany; <sup>e</sup>Department of Surgery, Charité – Universitätsmedizin Berlin (CCM and CVK), Berlin, Germany; <sup>f</sup>Transfusion Medicine, University Hospital Erlangen, Erlangen, Germany; <sup>g</sup>Institute for Clinical Immunology and Transfusion Medicine, Justus-Liebig-University Giessen, Giessen, Germany; <sup>h</sup>Institute for Immunology Charité – Universitätsmedizin Berlin, Berlin, Germany; <sup>i</sup>Molecular Immunology and Gene Therapy, Max-Delbrück-Center for Molecular Medicine (MDC) Berlin, Berlin, Germany; <sup>j</sup>Institute of Clinical Neuroimmunology, Biomedical Center and Hospital of the LMU, Munich, Germany

### ABSTRACT

The degree and type of T cell infiltration influence rectal cancer prognosis regardless of classical tumor staging. We asked whether clonal expansion and tumor infiltration are restricted to selected-phenotype T cells; which clones are accessible in peripheral blood; and what the spatial distribution of their target antigens is.

From five rectal cancer patients, we isolated paired tumor-infiltrating T cells (TILs) and T cells from unaffected rectum mucosa ( $T_{UM}$ ) using 13-parameter FACS single cell index sorting. TCR $\alpha\beta$  sequences, cytokine, and transcription factor expression were determined with single cell sequencing. TILs and  $T_{UM}$  occupied distinct phenotype compartments and clonal expansion predominantly occurred within CD8<sup>+</sup> T cells. Expanded TIL clones identified by paired TCR $\alpha\beta$  sequencing and exclusively detectable in the tumor showed characteristic PD-1 and TIM-3 expression. TCR $\beta$  repertoire sequencing identified 49 out of 149 expanded TIL clones circulating in peripheral blood and 41 (84%) of these were PD-1<sup>+</sup> TIM-3<sup>+</sup>. To determine whether clonal expansion of predominantly tumor-infiltrating T cell clones was driven by antigens uniquely presented in tumor tissue, selected TCRs were reconstructed and incubated with cells isolated from corresponding tumor or unaffected mucosa. The majority of clones exclusively detected in the tumor recognized antigen at both sites.

In summary, rectal cancer is infiltrated with expanded distinct-phenotype T cell clones that either i) predominantly infiltrate the tumor, ii) predominantly infiltrate the unaffected mucosa, or iii) overlap between tumor, unaffected mucosa, and peripheral blood. However, the target antigens of predominantly tumor-infiltrating TIL clones do not appear to be restricted to tumor tissue.

### ARTICLE HISTORY

Received 3 January 2019  
Revised 5 February 2019  
Accepted 6 February 2019

### KEYWORDS

Rectal cancer; tumor-infiltrating lymphocytes; single cell technologies; T cell receptor sequencing; single cell immune phenotyping; clonal T cell expansion; T cell antigen specificity; human immunology; cancer immunology

### Introduction

The incidence of colorectal cancer ranks fourth in men and third in women among all cancer entities and the five year survival rate is approximately 64% for all stages combined.<sup>1</sup> Among a variety of prognostic parameters, the type and density of tumor-infiltrating T cells (TILs) have been shown to affect clinical outcomes and overall survival independent of classical tumor-node-metastasis (TNM) staging.<sup>2–7</sup>

T cell function is determined by T cell receptor (TCR) specificity and the expression patterns of characteristic transcription factors and cytokines.<sup>8–12</sup> Depending on their differentiation state, T cells can contribute to recognition and elimination of (foreign) antigens, autoimmunity, induction of tolerance, and effective B cell responses. T cell-mediated tumor control relies on the integration of antigen-dependent mechanisms (T cell specificity) and mechanisms that are not directly antigen-dependent (immune checkpoints, microenvironment).

According to current understanding, the role of TILs includes the recognition and killing of tumor cells based on their presentation of mutation-derived neo-antigens. In fact, subsets of T cells from colorectal cancer patients have been shown to recognize neo-antigens. Patients with microsatellite instability, who can be expected to harbor high mutational loads, have increased numbers of TILs and better clinical outcomes.<sup>13,14</sup> Furthermore, the therapeutic success of adoptively transferred *in vitro*-expanded neo-antigen-specific T cells highlights their outstanding role in cancer control.<sup>15</sup> In addition to neo-antigens, certain unmutated self-antigens have been shown to induce tumor-directed T cell responses even across different patients.<sup>16</sup>

T cell function is critically dependent on co-stimulatory and co-inhibitory signals. Expression of immune checkpoint molecules (PD-1 and TIM-3 among others) on colorectal cancer-infiltrating T cells suggests an exhausted immune

**CONTACT** Leo Hansmann [leo.hansmann@charite.de](mailto:leo.hansmann@charite.de) Department of Hematology, Oncology, and Tumor Immunology, Charité – Universitätsmedizin Berlin (CVK), Augustenburger Platz 1, Berlin 13353, Germany

Supplemental data for this article can be accessed on the publisher's website

© 2019 The Author(s). Published with license by Taylor & Francis Group, LLC.

This is an Open Access article distributed under the terms of the Creative Commons Attribution-NonCommercial-NoDerivatives License (<http://creativecommons.org/licenses/by-nc-nd/4.0/>), which permits non-commercial re-use, distribution, and reproduction in any medium, provided the original work is properly cited, and is not altered, transformed, or built upon in any way.

e1586409-2  L. PENTER ET AL.

phenotype interfering with anti-tumor T cell function.<sup>17</sup> However, treatment of colorectal cancer with antibodies against PD-1 or its ligand PD-L1 has not been effective to date except in patients with a high mutational burden.<sup>13,14,18,19</sup>

Defining the functions of different phenotype TILs and the spatial distribution of their target antigens is critical for understanding the composition of immune cells in the cancer-associated microenvironment and for the design of novel immunotherapies. We asked whether clonal expansion and tumor infiltration are restricted to selected phenotype and specificity T cells, and which clones are accessible in the peripheral blood of rectal cancer patients. To minimize phenotype diversity due to location-dependent molecular and clinical features in colorectal cancer,<sup>20,21</sup> we restricted the study to rectal cancer patients. Our technologies for single cell phenotyping and TCR sequencing<sup>22-24</sup> comparatively defined clonal expansion-associated immune phenotypes of T cells from cancer tissue and adjacent unaffected mucosa from five treatment-naïve patients at the single cell level. The identified clones were tracked in the peripheral blood of the same patients at the time of surgical tumor removal and one follow-up visit using multi-parameter flow cytometry, TCR $\beta$  repertoire and single cell sequencing.<sup>25</sup> Selected T cell clones were recombinantly expressed<sup>26</sup> and incubated with cells isolated from tumor and unaffected mucosa of the same patients to determine the spatial distribution of the corresponding target antigens (Figure 1 for study specimens and workflow).

## Results

### Tumor infiltration is associated with characteristic T cell immune phenotypes

Rectal cancer shapes its microenvironment by attracting and re-programming selected types of (immune) cells, supporting tolerance and immune evasion. We hypothesized that immune phenotypes of tumor-infiltrating T cells (TILs) would be substantially different from T cells infiltrating the adjacent unaffected mucosa ( $T_{UM}$ ).

Multi-parameter flow cytometry (FACS) was used to define T cell immune phenotypes from TILs and  $T_{UM}$  isolated in parallel from surgical specimens of five treatment-naïve rectal cancer patients (Figure 1, Table 1). The FACS panel included 13 markers for the identification of major states of T cell differentiation and selected immune checkpoint molecules (Suppl. Table 1). Using t-stochastic neighbor embedding (t-SNE), we could identify phenotype compartments occupied by i) TILs, ii)  $T_{UM}$  and iii) T cells with phenotype characteristics overlapping between both sites (Figure 2(a)). Although the degree of phenotype overlap varied between individual patients, these three compartments were consistently identified in all patients (Suppl. Figure 1).  $CD8^+$  T cell phenotypes were especially distinct between TILs and  $T_{UM}$  (Figure 2). While CD38 and PD-1 were expressed on significantly more  $CD8^+$  TILs when compared to  $T_{UM}$ , B- and T-lymphocyte attenuator (BTLA) was expressed at higher frequencies on  $CD8^+$   $T_{UM}$  (Figure 2(b,c)). The immune checkpoint molecule TIM-3, and CD57, a marker associated with exhausted-phenotype T cells, were also enriched on TILs compared to  $T_{UM}$ , although this finding did not reach statistical significance.

### Clonal expansion predominantly occurs in T cells with distinct immune phenotypes

Previous studies have reported clonal expansion of  $CD4^+$  and  $CD8^+$  TILs in colorectal cancer.<sup>16,22,27</sup> We asked whether clonal T cell expansion was associated with particular immune phenotypes and applied our technology for single cell paired TCR $\alpha\beta$  and phenotype sequencing in combination with 13-parameter FACS index sorting<sup>24</sup> to four selected rectal cancer patients. Randomly selected single TCR $\alpha\beta^+$  TILs and  $T_{UM}$  were index-sorted for single cell phenotyping and sequencing (Figure 3(a), Suppl. Figures 2 and 3). Clonal expansion was defined as the detection of at least two T cells with identical TCR $\alpha\beta$  complementarity-determining region (CDR)-3 amino acid sequences. Numbers of expanded clones were not significantly different between TILs and  $T_{UM}$  (Figure 3(b)). Independent of tissue location, expanded T cell clones were predominantly  $CD8^+$  (134 of 149 TIL clones and 85 of 105

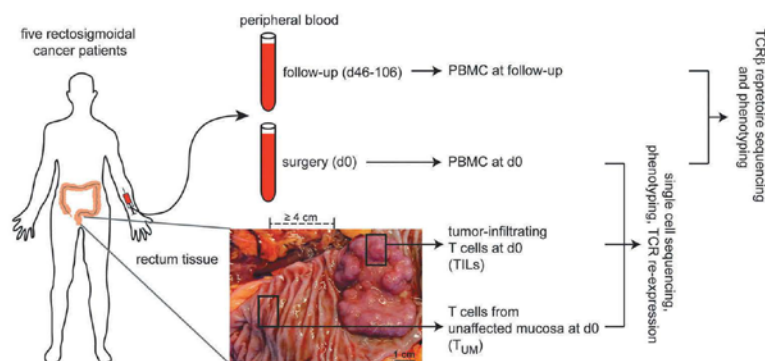


**Figure 1.** Study specimens and workflow. The distance between the tumor margin and the specimen of unaffected mucosa tissue was  $> 4$  cm for all cases but varied between patients. PBMC: peripheral blood mononuclear cells, TILs: tumor-infiltrating T cells,  $T_{UM}$ : T cells from unaffected mucosa, TCR: T cell receptor, d: day after surgery.

**Table 1.** Patient characteristics.

Pt	Sex	Age (years)	Histology	Tumor stage	MSI	HLA class 1	Clinical follow-up
1	f	80	Moderately differentiated adenocarcinoma	pT3 pN2a (4/12) M0 G2 R0 L0 V0	No	A* 02:01, 11:01 B* 08:01, 15:01 C* 03:04, 07:01	no follow-up data available
2	m	76	Mucinous adenocarcinoma	pT3(m) pN0 (0/14) M0 R0 L0 V0	No	A* 01:01, 68:01 B* 51:01, 52:01 C* 04:01, 12:02	alive +20 months, relapse-free
3	m	57	Moderately differentiated adenocarcinoma	pT3 pN0 (0/13) M0 G2 R0 L0 V0	No	A* 32:01, 33:01 B* 07:05, 40:06 C* 15:02, 15:05	alive +20 months, relapse-free
4	m	62	Moderately differentiated partially mucinous (< 30%) adenocarcinoma	pT2 pN0 (0/16) M0 G2 R0 L0 V0	No	A* 24:02, 26:01 B* 13:02, 18:01 C* 06:02, 07:01	no follow-up data available
5	m	77	Moderately differentiated adenocarcinoma	pT2 pN0 (0/14) M0 G2 R0 L0 V0	No	n.d.	death +1 month due to complication

Pt: patient, f: female, m: male, MSI: microsatellite instability, L0: no lymphatic vessel invasion, V0: no venous invasion, (m): multiple primary tumors in a single site, n.d.: not determined

$T_{UM}$  clones) (Figure 3(c)). Clonally expanded TILs could be distinguished by phenotype from clonally expanded  $T_{UM}$  (Figure 3(d), Suppl. Figure 4), as clonally expanded TILs were significantly more frequently CD38<sup>+</sup>, PD-1<sup>+</sup>, and TIM-3<sup>+</sup> (Figure 3(e)). *IFNG*, *PRFI*, and *GZMB* expression was significantly different between clonally expanded and non-expanded T cells (Suppl. Figure 5) and followed the same patterns in TILs and  $T_{UM}$ . Notably, the transcription factor *FOXP3* was predominantly expressed in non-expanded TILs (Figure 3(a,f)).

#### Selectively tumor-infiltrating T cell clones express the checkpoint molecules TIM-3 and PD-1 and rarely circulate in peripheral blood

We asked whether subsets of clonally expanded TILs were preferentially detectable in the tumor, whether they overlapped with adjacent unaffected mucosa or peripheral blood, and to what extent circulation in peripheral blood was affected by complete tumor removal. Peripheral blood mononuclear cells (PBMCs) were isolated from each patient at the day of surgery and at one follow-up visit (day 46–106 after surgery, Figure 1). Bulk CD8<sup>+</sup> and CD8<sup>-</sup> T cells were FACS-sorted (on average  $5.8 \times 10^5$  and  $1.2 \times 10^6$  cells per patient respectively, Suppl. Table 2, Suppl. Fig. 6) and their TCR $\beta$  repertoires were sequenced using deep sequencing. As prior experiments had shown that clonal T cell expansion in TILs and  $T_{UM}$  predominantly occurred in the CD8<sup>+</sup> compartment (Figure 3(c)), we focused on CD8<sup>+</sup> peripheral blood T cells for repertoire sequencing.

We detected on average 962 (range 343–2,244) individual CD8<sup>+</sup> T cell clones per time point and patient by peripheral blood TCR $\beta$  repertoire sequencing (Suppl. Table 2). TCR sequences from single TILs,  $T_{UM}$ , and the corresponding peripheral blood showed substantial clonal overlap within individual patients but not a single TCR overlapped between different patients (Figure 4(a)). From a total of 149 expanded TIL clones, 29 (19.5%) were detectable in the unaffected mucosa and 49 (32.9%) in the peripheral blood, whereas 92 (61.7%) were exclusively detectable among TILs (Figure 4(a,b)). Predominantly tumor-infiltrating clones expressed PD-1 and TIM-3 (42.6% and 21.2% of the clones respectively), whereas TIL clones that overlapped with unaffected mucosa and/or peripheral blood were PD-1<sup>-</sup> TIM-3<sup>-</sup> (Figure 4(c)). When focusing on the TIL clones

detectable in the peripheral blood, PD-1 and TIM-3 expression was mostly absent (84% of the clones, Figure 4(d)).

The accurate determination of clonal overlap between TILs and  $T_{UM}$  relies on the stability of immune phenotypes over time and the detection limit of our sequencing assays.

The immune phenotypes of peripheral blood CD8<sup>+</sup> T cells, in particular CD38, integrin beta-7, and CD45RA expression, were substantially different from TILs (Figure 4(e)), albeit stable over time as shown for CD4 and CD45RA as examples (Figure 4(f)). PD-1 and TIM-3 expression was enriched on clones selectively infiltrating the tumor (Figure 4(c)) and rare in peripheral blood (<1.4% and <6.6% of CD8<sup>+</sup> T cells for PD-1 and TIM-3, respectively, Figure 4(e)). To focus on these rare populations, we specifically sorted single peripheral blood T cells with increased PD-1 or TIM-3 expression (184 cells per population and patient, Suppl. Fig. 7) and sequenced their TCRs using single cell sequencing (Suppl. Tab. 3). Clones were determined to be absent in the peripheral blood if they could not be detected by TCR $\beta$  repertoire or single cell sequencing (Figure 4(a,b)). The dominantly expanded CD8<sup>+</sup> T cell clones in the peripheral blood were stable across different time points and clones with a frequency of >0.2% in peripheral blood at the day of surgery (day 0) were consistently detectable in the follow-up samples (Figure 4(g)) regardless of surgical tumor removal. This suggests that cues other than tumor neo-antigens are likely to be the drivers of their expansion.

#### Expanded T cell clones, irrespective of their origins, recognize antigens present in corresponding tumor and unaffected mucosa tissues

PD-1<sup>+</sup> TIM-3<sup>+</sup> expanded T cell clones predominantly infiltrated the tumor. We asked whether the presentation of antigens driving clonal expansion of predominantly tumor-infiltrating T cells was restricted to tumor tissue.

Based on their frequencies, we chose four T cell clones exclusively detected in the tumor and three clones overlapping between tumor, unaffected mucosa, and peripheral blood (Figure 5(a), Table 2). Their TCRs were reconstructed and functionally expressed on 58a $\beta$ - T hybridoma cells that had previously been transfected with GFP under the control of nuclear factor of activated T cells (NFAT)<sup>26</sup> and human CD8a $\beta$  chains.<sup>28</sup> GFP expression and mouse IL-2

e1586409-4 L. PENTER ET AL.

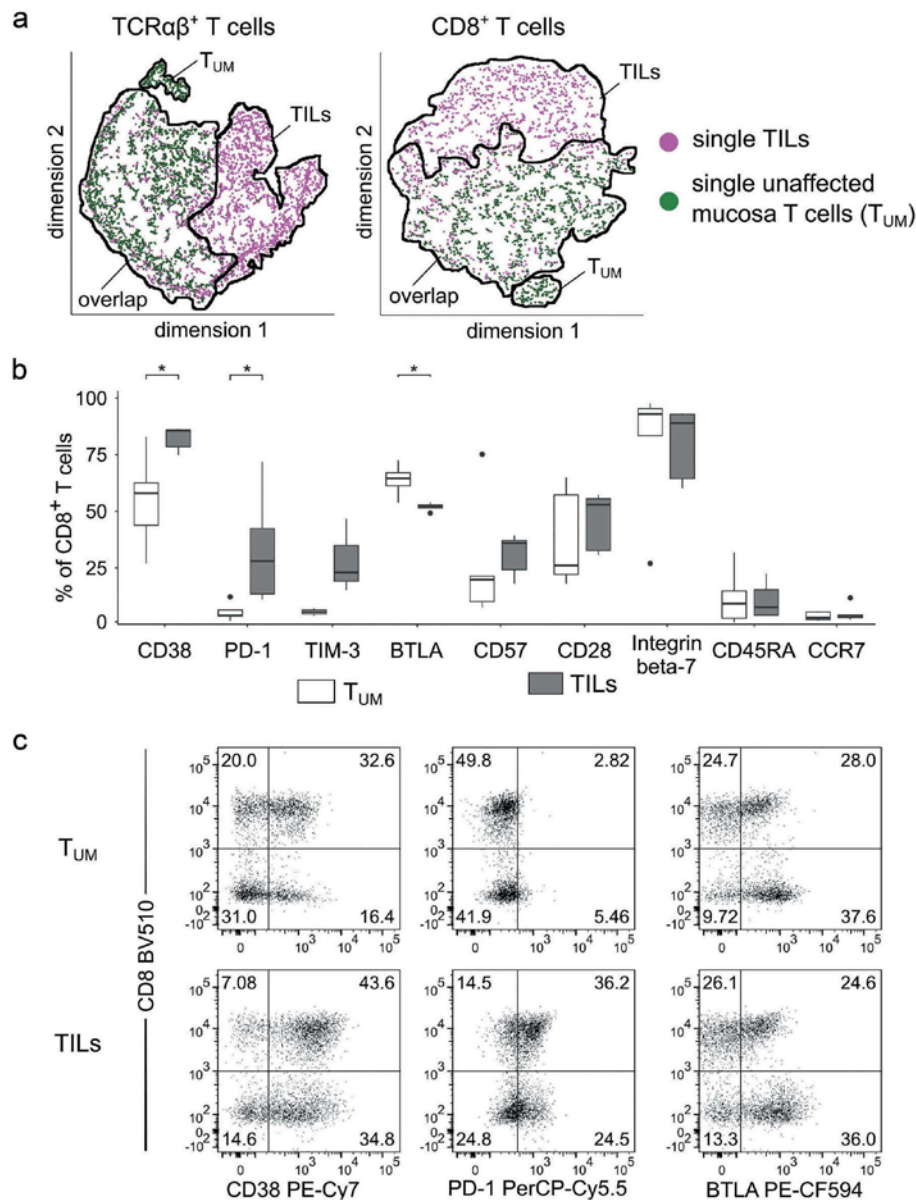


**Figure 2.** Subsets of TILs and  $T_{UM}$  show distinct immune phenotypes. TILs and  $T_{UM}$  pairs from five patients were stained in parallel with a multi-parameter FACS panel. (a) t-SNE visualization distinguished TILs from  $T_{UM}$  and identified immune phenotype compartments i) predominantly occupied by TILs, ii) predominantly occupied by  $T_{UM}$ , or iii) occupied by T cells from both locations. Each data point represents one single cell from patient 3 as an example. (b) Detailed immune phenotypes of CD8 $^+$  TILs and CD8 $^+$   $T_{UM}$  from all  $n = 5$  patients ( $n = 3$  for TIM-3,  $n = 4$  for CD28 and BTLA) determined by FACS were visualized as box plots. \*  $p < 0.05$ , Student's t-test (c) shows detailed FACS plots for the parameters significantly differently expressed between TILs and  $T_{UM}$  from patient 3 as an example. Gates for CD38 and BTLA were set based on expression of the respective markers on TCR $\alpha\beta^+$  cells. PD-1 gates were adjusted to the 98<sup>th</sup> expression percentile on TCR $\alpha\beta^+$  cells. All FACS plots were pre-gated on single live TCR $\alpha\beta^+$  lymphocytes.

production were detected as readouts for antigen-dependent T cell activation. After stimulation with plate-bound anti-mouse CD3 (positive control), the seven 58 $\alpha^- \beta^-$  cell lines expressing recombinant TCRs were on average 77% GFP $^+$

and produced on average 8,613 pg/ml murine IL-2 (Suppl. Fig. 8). To test whether target antigens were presented, TCR-recombinant 58 $\alpha^- \beta^-$  cells were co-incubated with leftover cells isolated from tumor and unaffected mucosa

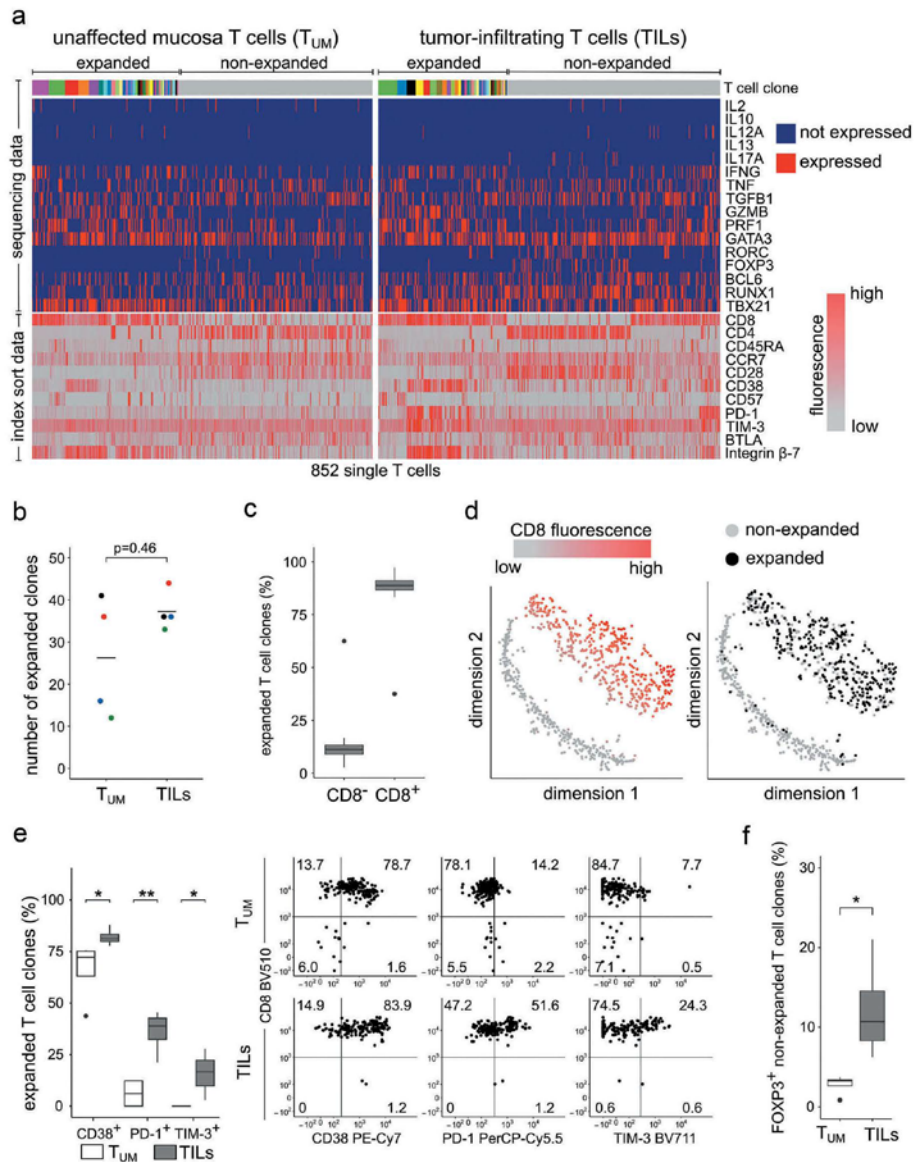


**Figure 3.** Clonal expansion-associated phenotype patterns of TILs and  $T_{UM}$ . (a) Parallel next generation sequencing of TCR $\beta$ , transcription factor, and cytokine genes from amplified cDNA of single TILs and  $T_{UM}$  (Suppl. Figure 2 for sorting gates). The sequencing and FACS data of single cells are arranged in columns with each column representing one single cell. The top bar indicates TCR sequences; adjacent columns with the same color in the top bar indicate single cells with identical CDR3 amino acid sequences of their TCR $\beta$  genes. Clonal expansion was defined as the detection of at least two cells with identical TCR $\beta$  sequences. The lower part of the heatmap is derived from the corresponding FACS index sort data and fluorescence intensities are color-coded from grey (lowest expression) to red (highest expression) for the indicated parameters. The heatmap shows data from patient 1 as an example (see Suppl. Figure 3 for detailed data of all patients in the study). (b) Shows numbers of expanded T cell clones per patient. Each data point represents one patient (black, blue, red, green for patients 1, 2, 3, 4, respectively). (c) Shows CD8 expression on expanded T cell clones. (d) Single TCR-sequenced TILs and  $T_{UM}$  from patient 1 as an example are visualized with t-SNE. Clonal expansion was enriched in CD8<sup>+</sup> compartments. (e) Shows selected markers significantly differentially expressed between clonally expanded TILs and  $T_{UM}$ . The left panel shows data from all patients summarized as box plots. Each data point in the FACS plots (data from patient 1 as an example) represents one single cell belonging to an expanded T cell clone. An individual clone was considered positive for a particular marker based on the majority of cells of the respective clone. Gates for CD38 were set based on expression on TCR $\beta$ <sup>-</sup> cells. TIM-3 and PD-1 gates were adjusted to the 98<sup>th</sup> expression percentile on TCR $\beta$ <sup>-</sup> cells. Clonal expansion determined by sequencing in non-expanded T cell clones. Box plots: The lower and upper hinges correspond to the 25<sup>th</sup> and 75<sup>th</sup> percentiles. The upper and lower whiskers extend from the hinge to the largest or lowest values respectively, no further than 1.5 x inter-quartile range. Data beyond the end of the whiskers are plotted individually. \* $p < 0.05$ , \*\* $p < 0.01$ , Student's t-test

e1586409-6 L. PENTER ET AL.

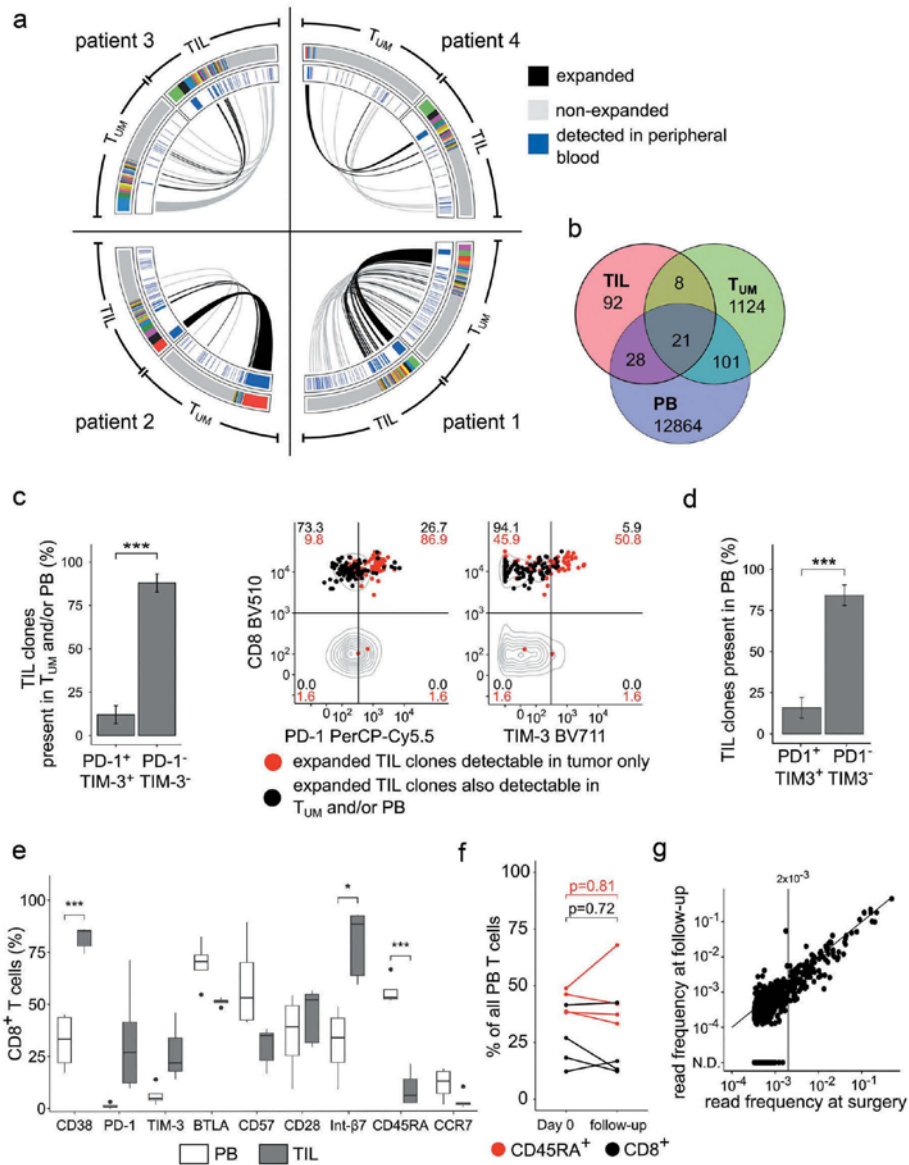


**Figure 4.** Clonal overlap between TILs and T<sub>UM</sub> is associated with characteristic immune phenotypes. The outer circle shows single cell TCR $\beta$  CDR3 sequencing data of TILs and T<sub>UM</sub> from patients 1–4. Cells with the same TCR $\beta$  CDR3 sequences are represented with the same color and cells are ordered by clone size. Grey represents single non-expanded T cells. The inner circle indicates whether a particular T cell clone was detected in peripheral blood by TCR $\beta$  repertoire or single cell sequencing at any time point. Connectors indicate clonal overlap between TILs and T<sub>UM</sub> (black if the clone was expanded within TILs, otherwise grey). (b) Absolute numbers of overlapping clones between clonally expanded TILs, T<sub>UM</sub> (clonally expanded and non-expanded), and peripheral blood are shown in a Venn diagram for patients 1–4 combined. (c) The left panel shows the frequency of PD-1 and/or TIM-3 expression on expanded TIL clones also detectable in peripheral blood and/or unaffected mucosa for all patients combined. PD-1<sup>+</sup> TIM-3<sup>-</sup> summarizes cells that were PD-1<sup>+</sup> and/or TIM-3<sup>-</sup>. PD-1<sup>-</sup> TIM-3<sup>-</sup> cells were negative for both markers. FACS plots show data from patient 1 as an example. Each data point represents one single cell of an expanded T cell clone. An individual clone was considered positive for a particular marker based on the majority of cells of the respective clone. PD-1 and TIM-3 gates were adjusted to the 98<sup>th</sup> expression percentile on TCR $\beta$ <sup>+</sup> cells. (d) shows the frequencies of PD-1 and/or TIM-3 expression on expanded TIL clones detectable in peripheral blood for all patients combined. PD-1<sup>+</sup> TIM-3<sup>-</sup> summarizes cells that were PD-1<sup>+</sup> and/or TIM-3<sup>-</sup>. PD-1<sup>-</sup> TIM-3<sup>-</sup> cells were negative for both markers. (e) Paired TIL and peripheral blood FACS phenotype data are visualized as box plots. The lower and upper hinges correspond to the 25<sup>th</sup> and 75<sup>th</sup> percentiles. The upper and lower whiskers extend from the hinge to the largest or lowest values respectively, no further than 1.5  $\times$  inter-quartile range. Data beyond the end of the whiskers are plotted individually. TIL data are derived from all  $n = 5$  patients ( $n = 3$  for TIM-3,  $n = 4$  for CD28 and BTLA) including  $n = 4$  patients for peripheral blood phenotypes. (f) illustrates the consistency of peripheral blood immune phenotypes over time. (g) shows frequencies of CD8<sup>+</sup> peripheral blood T cell clones determined with TCR $\beta$  repertoire sequencing at the day of surgery (d0) and follow-up. The figure shows the most expanded clones covering 80% of all sequencing reads per patient and time point. Each data point represents one out of 519 clones from all patients combined. PB: peripheral blood; \*  $p < 0.05$ , \*\*  $p < 0.01$ , \*\*\*  $p < 0.005$ , Student's t-test

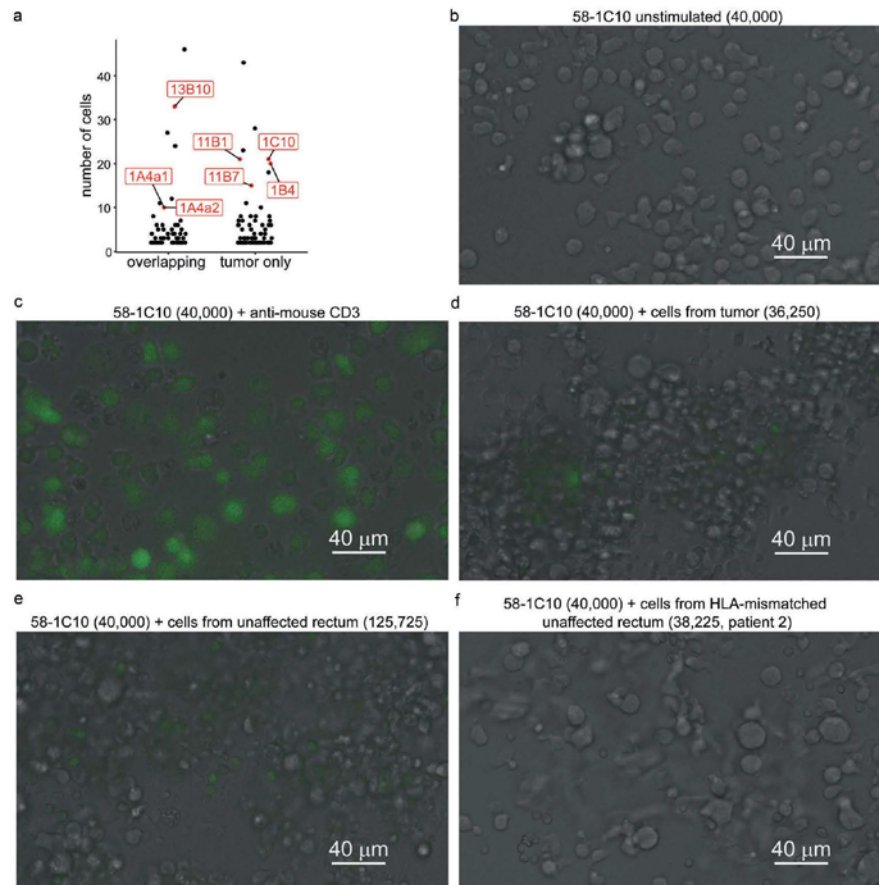


**Figure 5.** Spatial presentation of target antigens of predominantly tumor-infiltrating expanded T cells. (a) shows the expansion of individual T cell clones only detectable in the tumor or overlapping between tumor, unaffected mucosa, and peripheral blood. The figure shows data from all four patients combined and each data point represents one clone. Clones selected for reconstruction and expression in 58 $\alpha$ <sup>-</sup>β<sup>-</sup> cell lines were highlighted in red. CDR3 sequences and corresponding patients for each reconstructed clone can be found in Table 2. (b–f) shows fluorescence microscopy of 58-1C10 (as an example for an expanded TCR only detectable in TILs) unstimulated, stimulated with plate-bound anti-mouse CD3 (positive control), or after co-incubation with cells from the corresponding tumor, unaffected mucosa tissue, or HLA-mismatched unaffected mucosa (negative control). Numbers in parentheses indicate absolute cell numbers for co-incubation. Fluorescence microscopy was used to screen the entire co-incubation wells for GFP<sup>+</sup> cells. (d–f) represent images of single GFP<sup>+</sup> cells if any were detectable in the entire well. See Supplementary Figure 10 for data from all re-expressed TCRs. For detailed cell numbers and culture conditions, see Supplementary Table 4.

**Table 2.** Spatial distribution and CDR3 amino acid sequences of T cell clones for re-expression on 58 $\alpha$ <sup>-</sup>β<sup>-</sup> cells.

TCR label	Pt	TRAV	CDR3 alpha amino acid sequence	TRAJ	TRBV	CDR3 beta amino acid sequence	TRBJ	Detected in		
								TIL	T <sub>UM</sub>	PB
13B10	2	27*01	CAGGVNINAGNMLTF	39*01	20-1*01	CSARDLRSTDTQYF	2-3*01	Yes	Yes	Yes
11B1	2	8-2*01	CAVSDVSGGYQKVTF	13*02	2*01	CASSGGRASGSGEQFF	2-1*01	Yes	No	No
11B7	2	39*01	CAAPIMEYGNKLVF	47*01	10-2*01	CASAPGLREKLEFF	1-4*01	Yes	No	No
1C10	3	21*01	CAVTFPNAGNMLTF	39*01	6-6*01	CASSYGARLNTAFAF	1-1*01	Yes	No	No
1B4	4	13-1*01	CAVTGTASKLTF	44*01	29-1*01	CSVVGQDYEQYF	2-7*01	Yes	No	No
1A4-1	4	19*01	CALSEYGGSGNLIFF	42*01	6-1*01	CASSEASGSWTGELFF	2-2*01	Yes	Yes	Yes
1A4-2	4	1-2*01	CAVTDSNYQLIW	33*01	6-1*01	CASSEASGSWTGELFF	2-2*01	Yes	Yes	Yes

Pt: patient. PB: peripheral blood. TRAV: TCR $\alpha$  V-gene and allele. TRAJ: TCR $\alpha$  J-gene and allele. TRBV: TCR $\beta$  V-gene and allele. TRBJ: TCR $\beta$  J-gene and allele. TCR-recombinant 58 $\alpha$ <sup>-</sup>β<sup>-</sup> cell lines were named "58-TCR label", e.g. "58-1C10".

tissues (Suppl. Tab. 4 for cell numbers). We detected neither IL-2 production with ELISA nor GFP expression with FACS significantly above background for any TCR-recombinant

cell line (Suppl. Fig. 9 as an example). However, by screening with fluorescence microscopy, we could observe single cell aggregates containing GFP<sup>+</sup> cells that could not be



e1586409-8  L. PENTER ET AL.

detected with FACS due to their low frequencies (Figure 5 (b–f)). Of the four expanded TCRs exclusively detected in tumor tissue (Figure 5(a)), one recognized antigen only within cells isolated from the tumor (11B7), one recognized antigen only within cells isolated from unaffected mucosa (1B4), and two got activated by cells from both tumor and unaffected mucosa (1C10 and 11B1, Figure 5(d,e) as an example, Suppl. Fig. 10A for all re-expressed TCRs). From the three expanded TCRs detectable in tumor, unaffected mucosa, and peripheral blood, two were activated by cells isolated from both tumor and unaffected mucosa (13B10, 1A4-1), and one got activated only by cells isolated from unaffected mucosa (1A4-2, Suppl. Fig. 10B).

In conclusion, rectal cancer is infiltrated by expanded T cell clones that either i) selectively infiltrate the tumor but are functionally inhibited by the expression of immune checkpoint molecules or ii) overlap between tumor, unaffected mucosa, and peripheral blood, show distinct immune phenotypes, and, at least the dominant clones, persist after surgical tumor removal. The antigens underlying selective TIL expansion do not appear to be exclusively presented in tumor tissue.

## Discussion

A variety of cellular cancer treatment approaches including adoptive T cell transfer, chimeric antigen receptor (CAR) T cells, immune checkpoint blockade, and bispecific antibodies depend on efficient, targeted T cell functions. We addressed the following questions at the single cell level: i) Which are the phenotypes and presumed functional capacities of rectal cancer-infiltrating T cells, ii) are particular immune phenotypes associated with predominant tumor infiltration, iii) which TIL clones are accessible in peripheral blood, and iv) what is the spatial distribution of target antigens of expanded TIL clones?

Data on detailed immune phenotypes of paired TILs and  $T_{UM}$  from the same patients are limited<sup>5</sup> and often disregard the exact location of the tumor (different parts of the colon vs. rectum). Studies addressing clonal T cell interrelatedness at the single cell level are limited to single cases.<sup>16,22,29</sup>

Irrespective of clonal expansion, we identified tumor infiltration-associated T cell immune phenotypes.  $CD38^+$  and  $PD-1^+$  T cells were significantly enriched among TILs and we observed similar trends for  $TIM-3$  and  $CD57$ , though they did not reach statistical significance.  $PD-1$  and  $TIM-3$  have previously been shown to be expressed on colorectal cancer-infiltrating T cells,<sup>17,30</sup> however,  $PD-1$ -targeting therapies were particularly effective in tumors with DNA mismatch-repair deficiencies.<sup>31</sup> Notably, none of the patients in our study showed features of microsatellite instability (Table 1). The role of  $BTLA$ , a receptor involved in regulation of T cell function, has been under debate. Depending on downstream signaling pathways,  $BTLA$  may transmit stimulatory or inhibitory signals possibly accounting for its controversial roles in malignant melanoma, gastric, and gall bladder cancer.<sup>32–37</sup> We show that  $BTLA$  was expressed on more than 50% of  $CD8^+$  T cells isolated from peripheral blood, tumor, and unaffected mucosa although expression was less on TILs compared to  $T_{UM}$ . The functional and clinical significance of  $BTLA$  expression on TILs and  $T_{UM}$  in rectal cancer has to be determined in future studies. Data on  $CD38$  and  $CD57$  expression on TILs in

comparison with  $T_{UM}$  are limited but  $CD38$  expression has been shown to be induced by the tumor microenvironment and can inhibit  $CD8^+$  T cell function via adenosine receptor signaling.<sup>38</sup> Elevated numbers of  $CD57^+$  T and NK cells have been reported at the invasive margins of colorectal cancer.<sup>3</sup>

Independent from the particular set of markers, which will be subject to change depending on the selection of parameters and sample size in future studies, we conclude that immune phenotypes of TILs and  $T_{UM}$  are substantially different.

Immune phenotypes and functions associated with clonal T cell expansion can only be reliably studied at the single cell level. To complement single cell paired  $TCR\alpha\beta$  sequencing, additional  $TCR\beta$  repertoire sequencing was chosen for selected research questions. Tissue samples, especially from tumors and unaffected mucosa, were limited and we were particularly interested in clonal expansion-associated immune phenotypes. Therefore, we applied single cell sequencing, which is superior in terms of efficiency and the parallel determination of single cell immune phenotypes. Surprisingly, numbers of expanded clones were not significantly different between TILs and  $T_{UM}$ . While clonal TIL expansion could be tumor-specific/associated, we assume the cues driving clonal  $T_{UM}$  expansion not to be directly tumor-related. This assumption is based on the majority of expanded  $T_{UM}$  clones not being detectable among TILs, but a substantial amount overlapping with peripheral blood and showing phenotype characteristics of functional, non-exhausted T cells ( $PD-1^- TIM-3^-$ ).

In sequencing several hundred single T cells per patient and tissue type, there remains a chance of falsely determining clones to be non-overlapping or non-expanded. However, the identified immune phenotypes were significantly associated with the assigned status (overlapping vs. non-overlapping). In summary, combined single cell flow cytometry and sequencing data suggest the functional differentiation of clonally expanded TILs towards tolerance in an antigen-specific fashion by the expression of immune checkpoint and inhibitory molecules ( $PD-1$ ,  $CD57$ ,  $CD38$ ).  $FOXP3$  expression in non-expanded TILs can be assumed to support the tolerogenic microenvironment. Albeit not clonally expanded, a substantial proportion of  $CD4^+$  TILs were  $CD45RA^- CCR7^+ CD28^+$  (Figure 3) characterizing them as central memory T cells.<sup>39,40</sup> Their partial expression of  $TGFB$  and  $FOXP3$  mostly in the absence of  $PREF1$ ,  $GZMB$ , and  $IFNG$  suggests tolerogenic differentiation. The clinical significance and underlying differentiation mechanisms of these cells have to be determined in future studies.

It is important to accurately identify TIL clones circulating in the peripheral blood, as a variety of therapeutic approaches rely on the accessibility of tumor-specific T cells in the peripheral blood. Consistent with previous studies,<sup>41</sup> expanded T cell clones in peripheral blood remained mostly stable over time and unchanged months after tumor resection, suggesting that their expansion was not driven by resected tumor-associated neo-antigens. Dominant T cell clones in the peripheral blood of healthy individuals have been considered specific for antigens of chronic infections such as cytomegalovirus (CMV) or Epstein-Barr virus (EBV), among others. In fact, one of the most expanded peripheral blood TCRs in patient 1 ( $TCR\beta$  CDR3 amino acid sequence: CASSANYGYTF), which was also expanded among this patient's TILs and  $T_{UM}$ , has already been reported CMV-specific.<sup>42</sup>

As previously reported,<sup>17</sup> particular phenotypes enriched in TILs (PD-1<sup>+</sup>, TIM-3<sup>+</sup>) were rare in peripheral blood (Figure 4(d)), however, especially PD-1<sup>+</sup> peripheral blood T cells have previously been considered tumor-specific.<sup>15</sup> To increase the chance of detection, we extended our bulk sequencing data with high-efficiency single cell TCR $\alpha\beta$  sequencing of specifically sorted T cell populations with increased PD-1 and TIM-3 expression.

A recent study suggests the distinction of exhausted-phenotype, presumably tumor-specific, T cells and bystander T cells in colorectal and lung cancer based on the expression of the ecto-ATP/ADPase CD39.<sup>43</sup> Selectively rectal cancer-infiltrating T cells were exhausted and functionally inhibited, as represented by PD-1, TIM-3, CD38, and CD57 expression. By re-expressing selected TCRs in 58 $\alpha\beta^-$  T hybridoma cell lines and incubating them with cells isolated from their corresponding tissues, we showed that exhausted T cell clones selectively expanded in tumor tissue could recognize antigens presented on cells isolated from either site. The critical antigens appeared to be presented on very few cells close to the detection limit of our assays, which is not surprising since the cell preparations were not enriched for any particular cell type. Supplementary Figure 2 and microscopy (Figure 5) show the majority of cells isolated from rectum tissue were non-lymphocytes. In case a reconstructed TCR did not get activated upon co-incubation, we cannot conclude whether the lack of target antigen was due to the low frequency of antigen-presenting cells or the target antigen indeed not being presented in the investigated tissue. However, *in vivo*, particular expanded T cell clones selectively infiltrated the tumor tissue and were below the detection limits of our technologies at any other site, including peripheral blood. A variety of mechanisms, such as chemo-attraction, selective antigen accessibility *in vivo*, or inhibition of T cell expansion by microenvironment-derived cues, among others, could account for this observation. Recent studies on a variety of solid cancers suggest antigens other than neo-antigens to drive clonal TIL expansion in the tumor environment,<sup>16,43,44</sup> which is in support of our findings. The clinical significance of different phenotype TILs preferentially infiltrating tumor tissue has to be determined along with TCR specificities in future cohorts.

In conclusion, rectal cancer is infiltrated by clonally expanded unique-specificity T cells that show dysfunctional/exhausted immune phenotype patterns and rarely circulate in the peripheral blood. Their target antigens, however, do not seem to be exclusively presented in tumor tissue.

## Patients and methods/materials and methods

### Patients and sample preparation

Surgical specimens (one piece of rectal tumor and one piece of unaffected recto-sigmoidal mucosa per patient) and heparin-anticoagulated peripheral blood at surgery and one follow-up time point were obtained from five treatment-naïve rectal cancer patients. All patients gave written informed consent and the study was approved by the local ethics committee (protocol EA1/007/16 to L.H.). TILs and T<sub>UM</sub> were isolated from fresh specimens immediately after surgery as previously described.<sup>22</sup> In short,

tissue was cut into small pieces (2–4 mm<sup>3</sup>) and incubated in PBS containing 10 mM Ethylenediaminetetraacetic acid (EDTA, Invitrogen) for 30 min. Cells in suspension were passed through a 100  $\mu$ m cell strainer (Corning), tissue was incubated in RPMI1640 containing 5% fetal bovine serum (FBS) and 0.5 mg/ml collagenase (Serva, Collagenase NB 4) for 30 min. Finally, cells were enriched through Percoll (GE Healthcare) gradient centrifugation and cryopreserved. Distances between the tumor and unaffected mucosa specimens varied between patients but unaffected mucosa samples were taken at least 4 cm apart from the macroscopic tumor margin (Figure 1). PBMCs were isolated with Ficoll-Paque PLUS (GE Healthcare) density gradient centrifugation. All cell preparations were cryopreserved in RPMI1640 containing 50% FBS, 10% DMSO before further processing.

### Fluorescence-activated cell sorting

Cells were thawed and stained with multicolor panels (Suppl. Table 1). Antibodies were used according to the manufacturer's instructions. TILs and T<sub>UM</sub> samples from each patient were processed in parallel to minimize instrument and staining variability. For single cell sequencing, single cells were index-sorted directly into 96-well plates pre-filled with OneStep RT-PCR buffer (Qiagen) as previously described.<sup>24</sup> For TCR $\beta$  repertoire sequencing, bulk cells were FACS-sorted into tubes pre-filled with RPMI1640 containing 2% FBS. DNA was isolated immediately after sorting using the DNeasy Blood & Tissue Kit (Qiagen) and stored at 4°C until further processing. All cells were sorted using a FACSAria™ Fusion high-speed cell sorter (BD Biosciences) equipped with a 70  $\mu$ m nozzle.

### Single cell sequencing and phenotyping

PCR amplification, library preparation, and MiSeq (Illumina) sequencing were done as previously described.<sup>22,24</sup> Sequencing data were processed as previously described<sup>24</sup> and scripts can be downloaded from <https://github.com/HansmannLab/TRECA>. Cytokines and transcription factors were determined expressed in single cells if we detected more than 10 reads for the respective cytokine or transcription factor transcript.<sup>22</sup> In case of the seven TCRs chosen for re-expression (Figure 5), transcripts of the second TCR $\alpha$  chain of TCR 1A4 were identified by manually screening the sequencing output. No additional TCR $\alpha$  chains could be identified for the remaining six re-expressed TCRs (Table 2).

Clonal expansion was defined as the detection of at least two cells with identical TCR $\alpha$  and TCR $\beta$  amino acid sequences. Index sorting assigned exact immune phenotypes to every single sorted cell. Notably, some expanded clones showed heterogeneous marker expression and a clone was considered positive for a particular marker based on the majority (> 50%) of cells with a particular TCR sequence.

### TCR $\beta$ repertoire sequencing

TCR $\beta$  repertoire sequencing was done as previously described and the read frequency cutoff for the definition of individual clones was chosen at 10<sup>-4</sup>.<sup>25</sup>

e1586409-10  L. PENTER ET AL.

### Recombinant T cell receptor expression in 58 $\alpha$ <sup>-</sup> $\beta$ <sup>-</sup> cell lines and co-incubation with tumor and unaffected mucosa cell preparations

Selected TCRs were reconstructed by completing the missing leader, V, and constant region parts with sequences downloaded from IMGT,<sup>45</sup> and expressed in 58 $\alpha$ <sup>-</sup> $\beta$ <sup>-</sup> cell lines as previously described.<sup>26</sup> 58 $\alpha$ <sup>-</sup> $\beta$ <sup>-</sup> cell lines also expressed human CD8 $\alpha$  $\beta$  chains<sup>28</sup> and GFP under the control of nuclear factor of activated T cells (NFAT),<sup>26</sup> so they light up green upon activation. TCR-expression was confirmed by CD3 detection with FACS. As positive controls, TCR-recombinant cell lines were stimulated with plate-bound anti-mouse CD3 in 96-well plates for 16 h. IL-2 was measured in cell culture supernatants using the IL-2 Mouse Uncoated ELISA Kit (Thermo Fisher) and GFP expression was detected with FACS and fluorescence microscopy. For co-incubation experiments (Figure 5 and Suppl. Figs. 9–10), TCR-recombinant 58 $\alpha$ <sup>-</sup> $\beta$ <sup>-</sup> cells were incubated with cells isolated from i) corresponding tumor, ii) corresponding unaffected mucosa tissue, or iii) tumor or unaffected mucosa from an HLA-mismatched patient as negative control. For TCRs, corresponding patients, and exact co-incubation cell numbers, see Table 2 and Supplementary Table 4. Numbers of cells isolated from tumor or unaffected mucosa tissues varied between patients due to the size of surgical specimens. The majority of cells isolated from tissues were non-lymphocytes (Suppl. Figure 2). All remaining cells from each patient were used for co-incubation experiments (Figure 5, Suppl. Figs. 9 + 10) to maximize the chance of detection of TCR targets in the available specimens. Co-incubations were done in 96-well plates in a volume of 150  $\mu$ l RPMI1640 containing 10% FBS for 16 h at 37°C and 5% CO<sub>2</sub>.

### Fluorescence microscopy

Bright field and GFP fluorescence images were recorded separately using a Biorevo BZ-9000E instrument (Keyence) equipped with an S Plan Fluor ELWD 20x lens and overlaid for visualization.

### HLA-typing

Genomic DNA samples were amplified using GoTaq Long Range Polymerase (Promega) and HLA-locus-specific primers (NGSgo workflow, GenDx). Pooling of amplicons, fragmentation, adapter ligation, DNA clean-up, indexing PCR, second clean-up, size selection, library pooling, quantification, and denaturation were performed according to the manufacturer's instructions. Sequencing was done on a MiSeq instrument (Illumina) using 300 cycle kits (151 base pairs, paired-end sequencing). Data were analyzed with NGSengine software (GenDx).

### Data accessibility

Single cell sequencing data have been made publicly available (DDBJ/EMBL/GenBank accession KCPL00000000, first version KCPL01000000). TCR $\beta$  repertoire sequencing data are

available online (suppl\_online\_table\_1.xlsx). Single cell cytokine and transcription factor sequencing data along with the corresponding FACS index sort data are available online (suppl\_online\_table\_2.xls).

### Acknowledgments

Major financial support for this research came from Berliner Krebsgesellschaft (HAFF201606 to L.H.). Livius Penter is a Berlin Institute of Health (BIH) Junior Clinician Scientist. Leo Hansmann is a BIH Clinician Scientist and German Cancer Consortium (DKTK) Young Investigator. We thank Hans-Peter Rahn and Kirstin Rautenberg at the Max Delbrück Center for Molecular Medicine, Berlin, for expert assistance with FACS sorting, Christina Lang, Marion Ernst-Schlegel, and Katja Müller at the Institute for Clinical Immunology and Transfusion Medicine at Justus Liebig University Giessen for help with HLA-typing, and Irene Panzer at Labor Berlin for her support with FACS reagents. We thank Iris Otani at UCSF Medical Center and Marika Constant for critically reading the manuscript.

### Disclosure of Potential Conflicts of Interest


No potential conflicts of interest were disclosed.

### Funding

This work was supported by the Berliner Krebsgesellschaft e.V. [HAFF201606 to L.H.].

### ORCID

Livius Penter  <http://orcid.org/0000-0002-9060-0207>

Maria Fernanda Lammoglia Cobo  <http://orcid.org/0000-0002-0369-0364>

Leo Hansmann  <http://orcid.org/0000-0003-3790-0128>

### References

- Howlander N, Noone AM, Krapcho M, Garshell J, Neyman N, Altekruse SE, Kosary CL, Yu M, Ruhl J, Tatalovich Z, et al. SEER cancer statistics review, 1975-2010. National Cancer Institute. Bethesda, MD, [https://seer.cancer.gov/archive/csr/1975\\_2010/](https://seer.cancer.gov/archive/csr/1975_2010/), based on November 2012 SEER data submission, posted to the SEER web site, April 2013.
- Anitei MG, Zeitoun G, Mlecnik B, Marliot F, Haicheur N, Todosi AM, Kirilovsky A, Lagorce C, Bindea G, Ferariu D, et al. Prognostic and predictive values of the immunoscore in patients with rectal cancer. *Clin Cancer Res*. 2014;20:1891–1899. doi:10.1158/1078-0432.CCR-13-2830.
- Bindea G, Mlecnik B, Tosolini M, Kirilovsky A, Waldner M, Obenauf AC, Angell H, Fredriksen T, Lafontaine L, Berger A, et al. Spatiotemporal dynamics of intratumoral immune cells reveal the immune landscape in human cancer. *Immunity*. 2013;39:782–795. doi:10.1016/j.immuni.2013.10.003.
- Fridman WH, Pages F, Sautes-Fridman C, Galon J. The immune contexture in human tumours: impact on clinical outcome. *Nat Rev Cancer*. 2012;12:298–306. doi:10.1038/nrc3245.
- Galon J, Costes A, Sanchez-Cabo F, Kirilovsky A, Mlecnik B, Lagorce-Pages C, Tosolini M, Camus M, Berger A, Wind P, et al. Type, density, and location of immune cells within human colorectal tumors predict clinical outcome. *Science*. 2006;313:1960–1964. doi:10.1126/science.1129139.
- Mlecnik B, Bindea G, Angell HK, Maby P, Angelova M, Tougeron D, Church SE, Lafontaine L, Fischer M, Fredriksen T, et al. Integrative analyses of colorectal cancer show immunoscore is a stronger predictor of patient survival than microsatellite

- instability. *Immunity*. 2016;44:698–711. doi:10.1016/j.immuni.2016.02.025.
7. Pages F, Berger A, Camus M, Sanchez-Cabo F, Costes A, Molitor R, Mlecnik B, Kirilovsky A, Nilsson M, Damotte D, et al. Effector memory T cells, early metastasis, and survival in colorectal cancer. *N Engl J Med*. 2005;353:2654–2666. doi:10.1056/NEJMoa051424.
  8. Davis MM, Boniface JJ, Reich Z, Lyons D, Hampl J, Arden B, Chien Y. Ligand recognition by alpha beta T cell receptors. *Annu Rev Immunol*. 1998;16:523–544. doi:10.1146/annurev.immunol.16.1.523.
  9. Fontenot JD, Gavin MA, Rudensky AY. Foxp3 programs the development and function of CD4+CD25+ regulatory T cells. *Nat Immunol*. 2003;4:330–336. doi:10.1038/ni904.
  10. Ivanov II, McKenzie BS, Zhou L, Tadokoro CE, Lepelletier A, Lafaille JJ, Cua DJ, Littman DR. The orphan nuclear receptor RORgammat directs the differentiation program of proinflammatory IL-17+ T helper cells. *Cell*. 2006;126:1121–1133. doi:10.1016/j.cell.2006.07.035.
  11. Szabo SJ, Kim ST, Costa GL, Zhang X, Fathman CG, Glimcher LH. A novel transcription factor, T-bet, directs Th1 lineage commitment. *Cell*. 2000;100:655–669.
  12. Zheng W, Flavell RA. The transcription factor GATA-3 is necessary and sufficient for Th2 cytokine gene expression in CD4 T cells. *Cell*. 1997;89:587–596.
  13. Giannakis M, Mu XJ, Shukla SA, Qian ZR, Cohen O, Nishihara R, Bahl S, Cao Y, Amin-Mansour A, Yamauchi M, et al. Genomic correlates of immune-cell infiltrates in colorectal carcinoma. *Cell Rep*. 2016;15:857–865. doi:10.1016/j.celrep.2016.03.075.
  14. Maby P, Galon J, Latouche JB. Frameshift mutations, neoantigens and tumor-specific CD8(+) T cells in microsatellite unstable colorectal cancers. *Oncoimmunology*. 2016;5:e1115943. doi:10.1080/2162402X.2015.1115943.
  15. Gros A, Parkhurst MR, Tran E, Pasetto A, Robbins PF, Ilyas S, Prickett TD, Gartner JJ, Crystal JS, Roberts IM, et al. Prospective identification of neoantigen-specific lymphocytes in the peripheral blood of melanoma patients. *Nat Med*. 2016;22:433–438. doi:10.1038/nm.4051.
  16. Gee MH, Han A, Lofgren SM, Beausang JF, Mendoza JL, Birnbaum ME, Bethune MT, Fischer S, Yang X, Gomez-Eerland R, et al. Antigen identification for Orphan T Cell receptors expressed on Tumor-Infiltrating Lymphocytes. *Cell*. 2018;172:549–63 e16. doi:10.1016/j.cell.2017.11.043.
  17. Wu X, Zhang H, Xing Q, Cui J, Li J, Li Y, Tan Y, Wang S. PD-1 (+) CD8(+) T cells are exhausted in tumours and functional in draining lymph nodes of colorectal cancer patients. *Br J Cancer*. 2014;111:1391–1399. doi:10.1038/bjc.2014.416.
  18. Brahmer JR, Tykodi SS, Chow LQ, Hwu WJ, Topalian SL, Hwu P, Drake CG, Camacho LH, Kauh J, Odunsi K, et al. Safety and activity of anti-PD-L1 antibody in patients with advanced cancer. *N Engl J Med*. 2012;366:2455–2465. doi:10.1056/NEJMoa1200694.
  19. Topalian SL, Hodi FS, Brahmer JR, Gettinger SN, Smith DC, McDermott DF, Powderly JD, Carvajal RD, Sosman JA, Atkins MB, et al. Safety, activity, and immune correlates of anti-PD-1 antibody in cancer. *N Engl J Med*. 2012;366:2443–2454. doi:10.1056/NEJMoa1200690.
  20. Holch JW, Ricard I, Stintzing S, Modest DP, Heinemann V. The relevance of primary tumour location in patients with metastatic colorectal cancer: A meta-analysis of first-line clinical trials. *Eur J Cancer*. 2017;70:87–98. doi:10.1016/j.ejca.2016.10.007.
  21. Missiaglia E, Jacobs B, D'Ario G, Di Narzo AF, Soneson C, Budinska E, Popovici V, Vecchione L, Gerster S, Yan P, et al. Distal and proximal colon cancers differ in terms of molecular, pathological, and clinical features. *Ann Oncol*. 2014;25:1995–2001. doi:10.1093/annonc/mdu275.
  22. Han A, Glanville J, Hansmann L, Davis MM. Linking T-cell receptor sequence to functional phenotype at the single-cell level. *Nat Biotechnol*. 2014;32:684–692. doi:10.1038/nbt.2938.
  23. Hansmann L, Han A, Penter L, Liedtke M, Davis MM. Clonal expansion and interrelatedness of distinct B-Lineage compartments in multiple Myeloma Bone Marrow. *Cancer Immunol Res*. 2017;5:744–754. doi:10.1158/2326-6066.CIR-17-0012.
  24. Penter L, Dietze K, Bullinger L, Westermann J, Rahn HP, Hansmann L. FACS single cell index sorting is highly reliable and determines immune phenotypes of clonally expanded T cells. *Eur J Immunol*. 2018;48:1248–1250. doi:10.1002/eji.201847507.
  25. Ritter J, Seitz V, Balzer H, Gary R, Lenze D, Moi S, Pasemann S, Seegebarth A, Wurdack M, Hennig S, et al. Donor CD4 T Cell diversity determines virus reactivation in patients after HLA-matched Allogeneic Stem Cell transplantation. *Am J Transplant*. 2015;15:2170–2179. doi:10.1111/ajt.13241.
  26. Stewert K, Malotka J, Kawakami N, Wekerle H, Hohlfield R, Dornmair K. Unbiased identification of target antigens of CD8+ T cells with combinatorial libraries coding for short peptides. *Nat Med*. 2012;18:824–828. doi:10.1038/nm.2720.
  27. Tran E, Robbins PF, Lu YC, Prickett TD, Gartner JJ, Jia L, Pasetto A, Zheng Z, Ray S, Groh EM, et al. T-Cell transfer therapy targeting mutant KRAS in cancer. *N Engl J Med*. 2016;375:2255–2262. doi:10.1056/NEJMoa1609279.
  28. Friese MA, Jakobsen KB, Friis L, Etzensperger R, Craner MJ, McMahon RM, Jensen LT, Huygelen V, Jones EY, Bell JJ, et al. Opposing effects of HLA class I molecules in tuning autoreactive CD8+ T cells in multiple sclerosis. *Nat Med*. 2008;14:1227–1235. doi:10.1038/nm.1881.
  29. Zhang L, Yu X, Zheng L, Zhang Y, Li Y, Fang Q, Gao R, Kang B, Zhang Q, Huang JY, et al. Lineage tracking reveals dynamic relationships of T cells in colorectal cancer. *Nature*. 2018. doi:10.1038/s41586-018-0694-x.
  30. Sasidharan Nair V, Toor SM, Taha RZ, Shaath H, Elkord E. DNA methylation and repressive histones in the promoters of PD-1, CTLA-4, TIM-3, LAG-3, TIGIT, PD-L1, and galectin-9 genes in human colorectal cancer. *Clin Epigenetics*. 2018;10:104. doi:10.1186/s13148-018-0539-3.
  31. Le DT, Uram JN, Wang H, Bartlett BR, Kemberling H, Eyring AD, Skora AD, Lubner BS, Azad NS, Laheru D, et al. PD-1 Blockade in tumors with mismatch-repair deficiency. *N Engl J Med*. 2015;372:2509–2520. doi:10.1056/NEJMoa1500596.
  32. Haymaker CL, Wu RC, Ritthipichai K, Bernatchez C, Forget MA, Chen JQ, Liu H, Wang E, Marincola F, Hwu P, et al. BTLA marks a less-differentiated tumor-infiltrating lymphocyte subset in melanoma with enhanced survival properties. *Oncoimmunology*. 2015;4:e1014246. doi:10.1080/2162402X.2015.1008371.
  33. Lan X, Li S, Gao H, Nanding A, Quan L, Yang C, Ding S, Xue Y. Increased BTLA and HVEM in gastric cancer are associated with progression and poor prognosis. *Oncotargets Ther*. 2017;10:919–926. doi:10.2147/OTT.S128825.
  34. Oguro S, Ino Y, Shimada K, Hatanaka Y, Matsuno Y, Esaki M, Nara S, Kishi Y, Kosuge T, Hiraoka N. Clinical significance of tumor-infiltrating immune cells focusing on BTLA and Cbl-b in patients with gallbladder cancer. *Cancer Sci*. 2015;106:1750–1760. doi:10.1111/cas.12825.
  35. Ritthipichai K, Haymaker CL, Martinez M, Aschenbrenner A, Yi X, Zhang M, Kale C, Vence LM, Roszik J, Hailemichael Y, et al. Multifaceted role of BTLA in the control of CD8(+) T-cell fate after antigen encounter. *Clin Cancer Res*. 2017;23:6151–6164. doi:10.1158/1078-0432.CCR-16-1217.
  36. Derre L, Rivals JP, Jandus C, Pastor S, Rimoldi D, Romero P, Michielin O, Olive D, Speiser DE. BTLA mediates inhibition of human tumor-specific CD8+ T cells that can be partially reversed by vaccination. *J Clin Invest*. 2010;120:157–167. doi:10.1172/JCI40070.
  37. Fourcade J, Sun Z, Pagliano O, Guillaume P, Luescher IF, Sander C, Kirkwood JM, Olive D, Kuchroo V, Zarour HM. CD8 (+) T cells specific for tumor antigens can be rendered dysfunctional by the tumor microenvironment through upregulation of the inhibitory receptors BTLA and PD-1. *Cancer Res*. 2012;72:887–896. doi:10.1158/0008-5472.CAN-11-2637.
  38. Chen L, Diao L, Yang Y, Yi X, Rodriguez BL, Li Y, Villalobos PA, Cascone T, Liu X, Tan L, et al. CD38-Mediated immunosuppression as a mechanism of Tumor cell escape from PD-1/PD-L1

e1586409-12  L. PENTER ET AL.

- blockade. *Cancer Discov.* 2018;8:1156–1175. doi:10.1158/2159-8290.CD-17-1033.
39. Frohlich M, Gogishvili T, Langenhorst D, Luhder F, Hunig T. Interrupting CD28 costimulation before antigen rechallenge affects CD8(+) T-cell expansion and effector functions during secondary response in mice. *Eur J Immunol.* 2016;46:1644–1655. doi:10.1002/eji.201546232.
40. Maecker HT, McCoy JP, Nussenblatt R. Standardizing immunophenotyping for the Human Immunology Project. *Nat Rev Immunol.* 2012;12:191–200. doi:10.1038/nri3158.
41. Zvyagin IV, Pogorelyy MV, Ivanova ME, Komech EA, Shugay M, Bolotin DA, Shelenkov AA, Kurnosov AA, Staroverov DB, Chudakov DM, et al. Distinctive properties of identical twins' TCR repertoires revealed by high-throughput sequencing. *Proc Natl Acad Sci U S A.* 2014;111:5980–5985. doi:10.1073/pnas.1319389111.
42. Liang X, Weigand LU, Schuster IG, Eppinger E, van der Griendt JC, Schub A, Leisegang M, Sommermeyer D, Anderl F, Han Y, et al. A single TCR alpha-chain with dominant peptide recognition in the allestricted HER2/neu-specific T cell repertoire. *J Immunol.* 2010;184:1617–1629. doi:10.4049/jimmunol.0902155.
43. Simoni Y, Becht E, Fehlings M, Loh CY, Koo SL, Teng KWW, Yeong JPS, Nahar R, Zhang T, Kared H, et al. Bystander CD8(+) T cells are abundant and phenotypically distinct in human tumour infiltrates. *Nature.* 2018;557:575–579. doi:10.1038/s41586-018-0130-2.
44. Scheper W, Kelderman S, Fanchi LF, Linnemann C, Bendle G, de Rooij MAJ, Hirt C, Mezzadra R, Slagter M, Dijkstra K, et al. Low and variable tumor reactivity of the intratumoral TCR repertoire in human cancers. *Nat Med.* 2019;25:89–94. doi:10.1038/s41591-018-0266-5.
45. Li S, Lefranc MP, Miles JJ, Alamyar E, Giudicelli V, Duroux P, Freeman JD, Corbin VD, Scheerlinck JP, Frohman MA, et al. IMGT/HighV QUEST paradigm for T cell receptor IMGT clonotype diversity and next generation repertoire immunoprofiling. *Nat Commun.* 2013;4:2333. doi:10.1038/ncomms3333.



## FULL-LENGTH ARTICLE

## Basic Research

## Rapid single-cell identification of Epstein–Barr virus-specific T-cell receptors for cellular therapy



María Fernanda Lammoglia Cobo<sup>1</sup>, Carlotta Welters<sup>1</sup>, Leonie Rosenberger<sup>2</sup>,  
 Matthias Leisegang<sup>2,3,4</sup>, Kerstin Dietze<sup>1</sup>, Christian Pircher<sup>2</sup>, Livius Penter<sup>1,5</sup>, Regina Gary<sup>6</sup>,  
 Lars Bullinger<sup>1,4</sup>, Anna Takvorian<sup>1</sup>, Andreas Moosmann<sup>7,8</sup>, Klaus Dornmair<sup>9</sup>,  
 Thomas Blankenstein<sup>10</sup>, Thomas Kammertöns<sup>2</sup>, Armin Gerbitz<sup>11</sup>, Leo Hansmann<sup>1,4,\*</sup>

<sup>1</sup> Department of Hematology, Oncology and Tumor Immunology, Charité–Universitätsmedizin Berlin, corporate member of Freie Universität Berlin and Humboldt-Universität zu Berlin, Berlin, Germany

<sup>2</sup> Institute of Immunology, Charité–Universitätsmedizin Berlin, corporate member of Freie Universität Berlin and Humboldt-Universität zu Berlin, Berlin, Germany

<sup>3</sup> David and Lucile Packard Center for Cellular Therapy, The University of Chicago, Chicago, Illinois, USA

<sup>4</sup> German Cancer Consortium (DKTK), partner site Berlin, German Cancer Research Center (DKFZ), Heidelberg, Germany

<sup>5</sup> Dana-Farber Cancer Institute, Boston, Massachusetts, USA

<sup>6</sup> Department of Internal Medicine 5–Hematology/Oncology, University Hospital Erlangen, Erlangen, Germany

<sup>7</sup> Department of Medicine III, Klinikum der Universität München, Munich, Germany

<sup>8</sup> German Center for Infection Research (DZIF), Munich, Germany

<sup>9</sup> Institute of Clinical Neuroimmunology, University Hospital and Biomedical Center, Ludwig Maximilian University of Munich, Munich, Germany

<sup>10</sup> Molecular Immunology and Gene Therapy, Max-Delbrück-Center for Molecular Medicine (MDC), Berlin, Germany

<sup>11</sup> Hans Messner Allogeneic Stem Cell Transplant Program, Princess Margaret Cancer Centre, Toronto, Canada

## ARTICLE INFO

## Article History:

Received 11 December 2021

Accepted 10 March 2022

## Key Words:

adoptive T-cell therapy  
 allogeneic stem cell transplantation  
 Epstein–Barr virus  
 single-cell technologies  
 virus-associated malignancies

## ABSTRACT

**Background and aims:** Epstein–Barr virus (EBV) is associated with solid and hematopoietic malignancies. After allogeneic stem cell transplantation, EBV infection or reactivation represents a potentially life-threatening condition with no specific treatment available in clinical routine. *In vitro* expansion of naturally occurring EBV-specific T cells for adoptive transfer is time-consuming and influenced by the donor's T-cell receptor (TCR) repertoire and requires a specific memory compartment that is non-existent in seronegative individuals.

The authors present highly efficient identification of EBV-specific TCRs that can be expressed on human T cells and recognize EBV-infected cells.

**Methods and Results:** Mononuclear cells from six stem cell grafts were expanded *in vitro* with three HLA-B\*35:01- or four HLA-A\*02:01-presented peptides derived from six EBV proteins expressed during latent and lytic infection. Epitope-specific T cells expanded on average 42-fold and were single-cell-sorted and TCR $\alpha\beta$ -sequenced. To confirm specificity, 11 HLA-B\*35:01- and six HLA-A\*02:01-restricted dominant TCRs were expressed on reporter cell lines, and 16 of 17 TCRs recognized their presumed target peptides. To confirm recognition of virus-infected cells and assess their value for adoptive therapy, three selected HLA-B\*35:01- and four HLA-A\*02:01-restricted TCRs were expressed on human peripheral blood lymphocytes. All TCR-transduced cells recognized EBV-infected lymphoblastoid cell lines.

**Conclusions:** The authors' approach provides sets of EBV epitope-specific TCRs in two different HLA contexts. Resulting cellular products do not require EBV-seropositive donors, can be adjusted to cell subsets of choice with exactly defined proportions of target-specific T cells, can be tracked *in vivo* and will help to overcome unmet clinical needs in the treatment and prophylaxis of EBV reactivation and associated malignancies.

© 2022 International Society for Cell & Gene Therapy. Published by Elsevier Inc. This is an open access article under the CC BY-NC-ND license (<http://creativecommons.org/licenses/by-nc-nd/4.0/>)

## Introduction

Epstein–Barr virus (EBV) belongs to the family of gamma-herpesviruses, and more than 80% of humans over the age of 20 are infected [1]. EBV predominantly infects B cells, resulting in different forms of latent (non-productive) and lytic (virus producing)

\* Correspondence: Leo Hansmann, MD, Department of Hematology, Oncology and Tumor Immunology, Charité–Universitätsmedizin Berlin, Augustenburger Platz 1, Berlin 13353, Germany.

E-mail address: [leo.hansmann@charite.de](mailto:leo.hansmann@charite.de) (L. Hansmann).

<https://doi.org/10.1016/j.jcyt.2022.03.005>

1465–3249/© 2022 International Society for Cell & Gene Therapy. Published by Elsevier Inc. This is an open access article under the CC BY-NC-ND license (<http://creativecommons.org/licenses/by-nc-nd/4.0/>)

infection. Primary EBV infection of a human being is usually self-limiting and controlled by T cell-dominated immune responses, leading to latent virus persistence [2]. Infected cells present characteristic sets of EBV peptides on HLA that can be recognized by EBV-specific T cells [3,4]. In the proliferative latency III program of B-cell infection, six EBV nuclear antigens and three latent membrane proteins (LMPs), among others, are expressed. EBV nuclear antigens regulate replication of the viral genome and are involved in B-cell transformation, disruption of cell cycle checkpoints and lymphoma development [5–8]. Although LMP1 is a major transforming protein, LMP2 can drive proliferation in the absence of B-cell receptor stimulation and is involved in the induction of lymphoma-like phenotypes in B cells [9–11]. During the lytic phase, approximately 70 EBV proteins are expressed, including transcription factors BRLF1 and BZLF1, messenger RNA export factor BMLF1 and DNA polymerase processivity factor BMRF1, which contain peptides that can be presented on HLA [3].

Clinical observations and experiences from adoptive transfer of EBV-specific T-cell products suggest that T-cell responses are critical for controlling EBV infection and maintaining the latent phase [12–16]. Immunodominant EBV epitopes that drive substantial CD8<sup>+</sup> T-cell expansion have been identified in a variety of HLA contexts [17–20]. Expanded EBV epitope-specific T cells persist after acute infection [21] and can constitute up to 5% of circulating CD8<sup>+</sup> T cells in asymptomatic immunocompetent individuals [3].

Apart from often inapparent primary infection, EBV can cause life-threatening complications, including post-transplantation lymphoproliferative disorders (PTLDs), in states of severe immunosuppression associated with solid organ or allogeneic stem cell transplantation (allo-SCT). During the first 100 days after allo-SCT, T cells are typically substantially reduced in numbers and functionally inhibited, allowing EBV reactivation in approximately 30% of patients, with limited, non-specific treatment options available in clinical routine [22]. Especially at risk are EBV-seropositive patients who receive stem cell grafts from seronegative donors—a constellation of increasing relevance with rising numbers of younger haploidentical stem cell donors [23]. PTLDs occur in 1–8% of patients after allo-SCT [24], and close to 100% are EBV-associated when they develop within the first 6 months [25]. In summary, it would be beneficial if clinical conditions demonstrating impaired T-cell immunity and high risk of EBV-associated complications could be bridged with easily accessible, highly specific cellular products.

EBV-specific T-cell products have been shown to be effective in controlling infections and associated malignancies [13,26,27]. Current strategies for the generation of virus-specific T-cell products include *in vitro* expansion of epitope-specific (third-party) T cells from peripheral blood or stem cell grafts [27–29]. However, the following technical and clinical obstacles have prevented broad translation of such products into clinical routine: (i) *in vitro* expansion requires an antigen-experienced memory compartment, (ii) frequencies of epitope-specific T cells can be variable between individuals and products, (iii) donor selection and HLA allotypes are likely to influence functional capacities of the product and (iv) such products are laborious to produce and only directly available at a few specialized centers.

The authors hypothesized that the T-cell compartment of allogeneic stem cell grafts could be used to identify sets of T-cell receptors (TCRs) specific for carefully selected latent and lytic EBV epitopes in the context of pre-defined HLA backgrounds. These TCRs would be available “off-the-shelf” for production of EBV-specific T-cell products within minimum amounts of time. The authors’ approach allows the use of T-cell sources of choice independent of EBV serostatus, guarantees target epitope specificity with clearly defined frequencies of EBV-specific T cells, results in a product that can be tracked *in vivo* by specific antibodies and can

be expanded to other HLA allotypes for prophylaxis or treatment of EBV and associated malignancies.

## Methods

### Stem cell grafts

The authors collected leftover material from six granulocyte colony-stimulating factor-mobilized stem cell grafts of EBV-seropositive donors who expressed either HLA-B\*35:01 or HLA-A\*02:01. Mononuclear cells were isolated using Ficoll-Paque PLUS (GE Healthcare, Chicago, IL, USA) and cryopreserved in human serum albumin (Grifols, Barcelona, Spain) supplemented with 10% dimethyl sulfoxide (Carl Roth GmbH & Co. KG, Karlsruhe, Germany). The study was approved by the local institutional review board (Ethikkommission der Charité–Universitätsmedizin Berlin; approval no. EA2/197/18), all participants gave written informed consent and the entire study was conducted in accordance with the principles of the Declaration of Helsinki.

### Peptide-specific *in vitro* expansion

Mononuclear cells were thawed, washed twice with CellGro DC medium (Sartorius CellGenix GmbH, Freiburg, Germany) and rested for 16 h at 37°C and 5% carbon dioxide (CO<sub>2</sub>). Subsequently,  $5 \times 10^7$  to  $3 \times 10^8$  cells were stimulated for 2 h with synthetic peptides (JPT Peptide Technologies, Berlin, Germany) at 1 µg/mL per peptide. Cells were washed twice and expanded for 9 days at  $2.5 \times 10^6$  cells/mL in CellGro DC medium, 1% GlutaMAX (Life Technologies, Carlsbad, CA, USA), 1% donor serum and 50 IU/mL IL-2 (aldesleukin; Novartis Pharma GmbH, Fehrbellin, Germany) at 37°C and 5% CO<sub>2</sub>. Fresh medium was supplied on day 5. After expansion, cells were cryopreserved.

### Flow cytometry

All flow cytometry reagents, including monoclonal antibodies and live/dead dyes, were titrated and used according to the manufacturers’ instructions. Phycoerythrin- and allophycocyanin-labeled peptide major histocompatibility complex (pMHC) tetramers (National Institutes of Health Tetramer Core Facility, Atlanta, GA, USA) were provided at 1.1–1.5 mg/mL in water and diluted as 20% glycerol (SERVA Electrophoresis GmbH, Heidelberg, Germany) stocks. Per stain, the authors used 0.63 µL of pMHC tetramer stock solution in 150 µL phosphate-buffered saline (Life Technologies) supplemented with 2% fetal bovine serum (FBS) (Life Technologies). Flow cytometry data were acquired on Navios (Beckman Coulter, Brea, CA, USA), LSRFortessa (BD Biosciences, Franklin Lakes, NJ, USA) and Aurora (Cytek Biosciences, Fremont, CA, USA) instruments.

### Fluorescence-activated cell sorting

Cells were thawed, rested in Roswell Park Memorial Institute (RPMI) 1640 with 10% FBS for 1 h at 37°C and 5% CO<sub>2</sub> and stained with monoclonal antibodies. Single cells were index-sorted into 96-well plates pre-filled with OneStep reverse transcription polymerase chain reaction buffer (QIAGEN, Hilden, Germany) using a FACSAria Fusion cell sorter (BD Biosciences) as described previously [30].

### Single-cell TCRαβ sequencing

Polymerase chain reaction amplification, molecular barcoding, library preparation and MiSeq (Illumina, San Diego, CA, USA) sequencing were carried out as previously described [31,32]. Clonal expansion was defined as two or more cells with identical TCRα and TCRβ CDR3 amino acid sequences. Cells that expressed two TCRα

chains in combination with the same TCR $\beta$  chain were defined as one clone if TCR $\alpha$  chains were identical; cells in which only one of these TCR $\alpha$  chains was identified were also included in the clone.

#### TCR expression on 58 $\alpha$ - $\beta$ - cell lines

Missing sequence parts of leader, variable and constant regions of selected TCRs were completed with data downloaded from the international ImmunoGeneTics information system. Reconstructed TCR sequences were synthesized (Thermo Fisher Scientific, Waltham, MA, USA) and expressed in 58 $\alpha$ - $\beta$ - cell lines as previously described [32,33]. The 58 $\alpha$ - $\beta$ - cells expressed human CD8 $\alpha\beta$  chains and green fluorescent protein (GFP) under the control of the nuclear factor of activated T-cell promoter [33], thus indicating T-cell activation by GFP expression. TCR expression was confirmed by mouse CD3 staining and detection by flow cytometry. As positive control for TCR activation, TCR-recombinant cell lines were stimulated with plate-bound anti-mouse CD3 for 16 h at 37°C and 5% CO<sub>2</sub>. GFP expression was measured with flow cytometry and IL-2 production was detected in cell culture supernatants using the DuoSet enzyme-linked immunosorbent assay (ELISA) ancillary reagent kit 2 (R&D Systems, Minneapolis, MN, USA).

#### TCR expression on third-party human T lymphocytes

TCRs were expressed on T cells of a healthy female, EBV-seropositive donor that expressed HLA-A\*02:01 and HLA-B\*35:01. TCR inserts were constructed as described earlier and human TCR constant regions were replaced with mouse constant region sequences to minimize mispairing with endogenous TCR chains. All TCR constructs were codon-optimized for expression in human cells. To generate retroviral vector particles to transduce human cells, 18  $\mu$ g MP71 vector, including the TCR insert, was diluted in 150  $\mu$ L water and 250 mM calcium chloride and combined with 150  $\mu$ L transfection buffer, comprising 1.6 g sodium chloride (Sigma-Aldrich, Burlington, MA, USA), 74 mg potassium chloride (Sigma-Aldrich), 50 mg disodium hydrogen phosphate (Sigma-Aldrich) and 1 g 4-(2-hydroxyethyl)-1-piperazine ethanesulfonic acid (Sigma-Aldrich), and 100 mL water adjusted to pH 6.76. The mixture was added dropwise to  $8.5 \times 10^5$  293Vec-RD114 producer cells (BioVec Pharma, Québec, Canada). Cells were cultured at 37°C and 5% CO<sub>2</sub> for 6 h, and medium was changed afterward.

For transduction,  $1.5 \times 10^6$  human lymphocytes were stimulated with 400 IU/mL IL-2 (Chiron Corporation, Emeryville, CA, USA) in a 24-well plate pre-coated with 5  $\mu$ g/mL anti-CD3 (BD Pharmingen, San Diego, CA, USA) and 1  $\mu$ g/mL anti-CD28 (BD Pharmingen) for 2 days. Afterward, cells were spinoculated on two consecutive days for 90 min at 800  $\times$  g and 32°C with 1 mL filtered (0.45  $\mu$ m pore size) RD114 retroviral vector supernatant, 400 IU/mL IL-2 and 8  $\mu$ g/mL protamine sulfate (Sigma-Aldrich). Spinoculated cells were expanded in cell culture medium supplemented with 400 IU/mL IL-2 for 10 days and rested for 2 days with 40 IU/mL IL-2 before cryopreservation. Efficiency of TCR transduction was determined with flow cytometry by mouse TCR $\beta$  constant region staining.

#### Lymphoblastoid and mini-lymphoblastoid cell lines

Lymphoblastoid cell lines (LCLs) were generated by transformation of peripheral blood mononuclear cells with supernatant of the EBV strain B95.8 as previously described [34]. Mini-LCLs were prepared by immortalizing HLA-B\*35:01\* or HLA-A\*02:01\* B cells with the recombinant mini-EBV plasmid p1495.4 [35,36]. Mini-EBV plasmids contained less than half of the EBV genome, and mini-LCLs could not produce infectious particles [37]. Detailed HLA class I data of all LCLs and mini-LCLs used in this study are included in the supplementary material.

#### Co-culture of TCR-recombinant cells with target cells

A total of 60 000 TCR-recombinant 58 $\alpha$ - $\beta$ - cells were cultured with 100 000 antigen-presenting cells. Cells were co-cultured in 150  $\mu$ L RPMI 1640 and 10% FBS in 96-well plates for 16 h at 37°C and 5% CO<sub>2</sub>. For target peptide loading,  $3 \times 10^6$  antigen-presenting cells were incubated with the respective target peptide at 7.5  $\mu$ mol/L for 30 min prior to co-culture.

TCR-transduced human lymphocytes were cultured at 50 000 T cells with 10 000 potential target cells in 200  $\mu$ L RPMI 1640 and 10% FBS in 96-well plates at 37°C and 5% CO<sub>2</sub> for 20 h. Exact effector-to-target ratios of individual co-cultures depended on frequencies of CD8<sup>+</sup> and TCR-transduced T cells within individual T-cell preparations and can be found in the supplementary material. Interferon gamma (IFN- $\gamma$ ), granzyme B and tumor necrosis factor alpha (TNF- $\alpha$ ) were determined in cell culture supernatants using a human IFN- $\gamma$  ELISA set (BD Biosciences), human granzyme B DuoSet ELISA kit (R&D Systems) and human TNF- $\alpha$  DuoSet ELISA kit (R&D Systems).

## Results

#### Expansion of EBV epitope-specific T cells from stem cell grafts

Efficient identification of EBV epitope-specific TCRs requires sufficient frequencies of specific T-cell clones. Therefore, the authors used *in vitro* expansion of  $5 \times 10^7$  to  $3 \times 10^8$  mononuclear cells from five EBV-seropositive allogeneic stem cell grafts in the presence of three synthetic EBV-derived peptides presented on HLA-B\*35:01 and one additional graft with four synthetic peptides presented on HLA-A\*02:01 (Table 1). The peptides used were selected immunodominant epitopes expressed during lytic and latent infection phases, and frequencies of specific CD8<sup>+</sup> T cells were determined by flow cytometry using pMHC tetramer staining.

During *in vitro* expansion, absolute numbers of CD8<sup>+</sup> T cells increased (Figure 1A), and peptide-specific CD8<sup>+</sup> T cells expanded on average 42-fold (range, 1–228). Degrees of expansion varied between stem cell grafts and individual peptides (Figure 1B,C). Frequencies of HPV-, YPL- and EPL-specific HLA-B\*35:01-restricted CD8<sup>+</sup> T cells increased on average 25-, 10- and 108-fold, respectively (Figure 1B). Frequencies of GLC-, CLG-, FLY- and YVL-specific HLA-A\*02:01-restricted CD8<sup>+</sup> T cells increased 14-, 8-, 26- and 27-fold, respectively (Figure 1C). Detailed cell numbers for each stem cell graft before and after expansion can be found in supplementary Table 1. Representative pMHC tetramer staining is shown in Figure 1D (see supplementary Figure 1; see supplementary Table 2).

#### Single-cell identification of EBV epitope-specific TCRs

Reliable and efficient identification of paired TCR $\alpha\beta$  sequences from complex T-cell populations requires single-cell resolution. The authors isolated epitope-specific CD8<sup>+</sup> T cells by pMHC tetramer staining of stem cell grafts expanded *in vitro* and subsequent fluorescence-activated cell sorting (see supplementary Table 2). Gating for single-cell sorting is illustrated in Figure 2A. TCR $\alpha\beta$  genes of every

**Table 1**  
Peptides for EBV epitope-specific *in vitro* expansion.

Label	Amino acid sequence	Protein	Virus phase	Presented on HLA
HPV	HPVGEADYFEY	EBNA1	Latency I, II, III	B*35:01
YPL	YPLHEQHGGM	EBNA3A	Latency III	B*35:01
EPL	EPLPQGLTAY	BZLF1	lytic	B*35:01
GLC	GLCTLVAML	BMLF1	lytic	A*02:01
CLG	CLGGLTMV	LMP2A	Latency II, III	A*02:01
FLY	FLYALALL	LMP2A	Latency II, III	A*02:01
YVL	YVLDHLIV	BRLF1	lytic	A*02:01



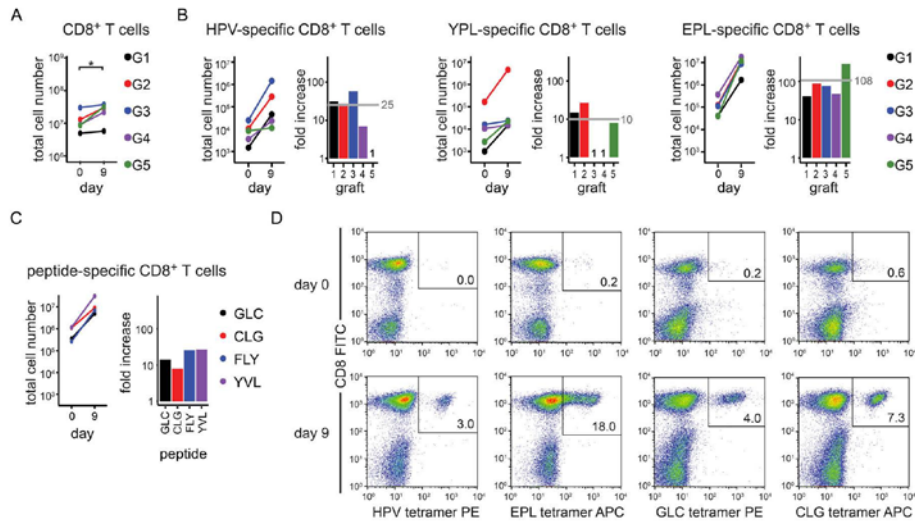


**Figure 1.** Expansion of EBV peptide-specific T cells from stem cell grafts. Mononuclear cells from allogeneic stem cell grafts were expanded *in vitro* in the presence of EBV-derived peptides for 9 days. (A) Total numbers of CD8<sup>+</sup> T cells from five stem cell grafts (G1–5). Gray lines and gray numbers indicate averages. (B) Total numbers and fold expansion of HLA-B\*35:01-restricted peptide-specific T cells from five stem cell grafts (G1–5). Gray lines and gray numbers indicate averages. (C) Total cell number and fold expansion of HLA-A\*02:01-restricted peptide-specific T cells from stem cell graft G6. (D) Frequencies of peptide-specific CD8<sup>+</sup> T cells before (day 0) and after (day 9) expansion as determined by pMHC tetramer staining. HPV- and EPL (presented on HLA-B\*35:01)-specific expansions from stem cell graft G3 are shown as an example along with GLC- and CLG (presented on HLA-A\*02:01)-specific expansions from stem cell graft G6. Plots are pre-gated on live single T cells. Numbers within gates indicate percentages. Significance determined by two-sided paired sample *t*-test. \**P* < 0.05. APC, allophycocyanin; FITC, fluorescein isothiocyanate; PE, phycoerythrin.

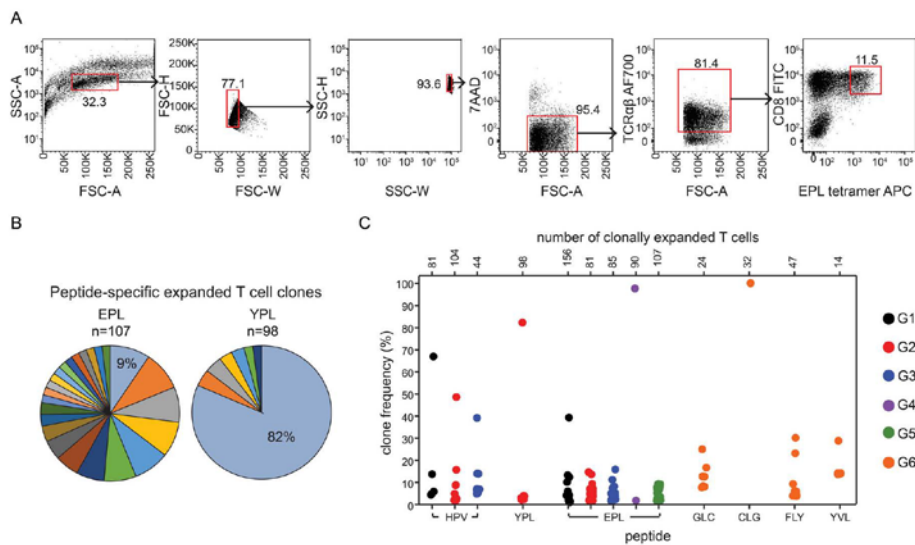


**Figure 2.** Identification of EBV epitope-specific TCRs. (A) Gates for single-cell sorting are shown in red. Selection of peptide-specific CD8<sup>+</sup> TCRαβ<sup>+</sup> cells after gating on single lymphocytes and exclusion of dead cells. Data for single-cell sorting of EPL-specific cells from stem cell graft G3 are shown as a representative example of all sorts (n = 13). Numbers adjacent to gates indicate percentages. (B) Frequencies of T-cell clones after pMHC tetramer-specific single-cell sorting and sequencing. Expanded clones share identical TCRαβ CDR3 amino acid sequences. Results from EPL-specific clonal expansion of stem cell graft G5 and YPL-specific clonal expansion of stem cell graft G2 are shown as examples. Numbers of clonally expanded cells are indicated above each chart. Percentages indicate percentages of clonally expanded cells. (C) Frequencies of expanded epitope-specific T-cell clones of all expansions (n = 13). Data points indicate individual expanded clones. Frequencies represent frequencies within clonally expanded cells for each peptide specificity. Numbers above the plot indicate total numbers of clonally expanded T cells. APC, allophycocyanin; FITC, fluorescein isothiocyanate; FSC-A, forward scatter area; FSC-H, forward scatter height; FSC-W, forward scatter width; 7AAD, 7-aminoactinomycin D; SSC-A, side scatter area; SSC-H, side scatter height; SSC-W, side scatter width.

single sorted cell were sequenced using next-generation sequencing (see supplementary Table 3), and clonal expansion was defined as detection of identical TCR $\alpha\beta$  CDR3 amino acid sequences in at least two cells.

Numbers and sizes of expanded T-cell clones varied between stem cell grafts and between epitope specificities (Figure 2B,C). Although *in vitro* expansion resulted in, for example, 24 different EPL-specific T-cell clones, with dominant clones accounting for only 9% of clonally expanded cells (EPL-specific expansion of stem cell graft G5), another expansion contained seven different YPL-specific clones, with the dominant clone comprising 82% of clonally expanded cells (Figure 2B). Frequencies of epitope-specific T-cell clones from all *in vitro* expansions are summarized in Figure 2C. The strongest clonal expansion was observed for CLG-specific T cells from stem cell graft G6, where only one expanded clone could be detected.

When comparing TCR sequences of epitope-specific clones between individual grafts, five TCRs (two HPV- and three EPL-specific) were found in more than one stem cell graft, and their degree of clonal expansion did not exceed 11% of clonally expanded T cells (see supplementary Table 4). In summary, clonal expansion was stem cell graft- and peptide-dependent and showed two patterns: (i) expansion of a few dominant clones comprising almost the entire clonally expanded T-cell compartment and (ii) expansion of a variety of less dominant clones, each accounting for less than approximately 35% of clonally expanded T cells.

#### Confirmation of target epitope specificity of expanded T-cell clones

Although identification of largely expanded dominant clones within pMHC tetramer-sorted T cells suggested target peptide specificity, specificities of smaller size clones were less clear. To confirm target peptide specificity, the authors expressed TCRs of 17 expanded T-cell clones covering specificities for all peptides that had been used for *in vitro* expansion on 58 $\alpha^{-}\beta^{-}$  reporter T cells with nuclear factor of activated T-cell-driven GFP expression (Table 2, Figure 3A). TCR-recombinant cell lines were named “58-[name of the TCR]” and incubated with antigen-presenting cells loaded with the respective peptides. GFP expression and IL-2 production were measured as indicators of T-cell activation. Mini-LCLs were used as antigen-presenting cells and loaded with peptides of choice.

All TCR-recombinant cell lines produced GFP and IL-2 upon stimulation with plate-bound anti-CD3 (see supplementary Figure 2). Upon co-incubation with target peptide-loaded antigen-presenting cells,

16 of 17 TCRs were activated, and no activation could be detected upon incubation with non-target peptide-loaded antigen-presenting cells (Figure 3B,C; also see supplementary Figure 3). TCR EPL7A4 could not be activated by its presumed target peptide and was excluded from further analysis. Notably, 58-GLC1B1 and 58-GLC1B4 shared an identical TCR $\beta$  chain but expressed different alpha chains (Table 2). The authors expressed both alpha chains individually together with the corresponding TCR $\beta$  chain, and both combinations resulted in productive TCRs specific for the same target peptide. In summary, the authors confirmed specificity for a panel of 16 TCRs targeting EBV epitopes presented during the latent and lytic infection phase.

#### TCR-transduced third-party human lymphocytes recognize EBV-infected cell lines

To determine their translational potential, the authors selected three HLA-B\*35:01- and four HLA-A\*02:01-restricted TCRs, confirmed that they were not broadly cross-reactive with HLA other than the target HLA (see supplementary Figure 4; see supplementary Table 5), expressed them in human lymphocytes and tested their reactivity with EBV-infected cells. TCRs were expressed on CD4-depleted human lymphocytes, and TCR-transduced T cells were co-cultured with four EBV-infected LCLs (named B01, JY, B03 and DJS). TCR-transduced lymphocytes were named “hL-[name of the TCR],” and recombinant TCR expression was detectable on average on 34% of CD8<sup>+</sup> T cells (see supplementary Figure 5). CD137 expression on CD8<sup>+</sup> T cells and IFN- $\gamma$  in cell culture supernatants were measured as readouts for T-cell activation, and activation was assumed if either of them was detectable.

TCR-transduced T cells of all six epitope specificities significantly upregulated CD137 expression when incubated with at least one of the corresponding LCLs (Figure 4A; also see supplementary Figure 6). T cells specific for EPL, GLC, CLG, YVL and FLY also produced significant amounts of IFN- $\gamma$  in comparison with non-transduced T cells (Figure 4B). T cells expressing the HPV-specific TCR (hL-HPV13A10) were activated, as indicated by CD137 expression; however, IFN- $\gamma$  production was low and did not reach statistical significance because of relatively high background IFN- $\gamma$  levels of non-transduced T cells, which varied between different LCL and co-incubation experiments.

To further characterize the activation response of TCR-transduced human T cells, the authors selected hL-EPL11A7 as an example and

**Table 2**  
Epitope-specific, recombinantly expressed TCRs.

Label	HLA restriction	G	TRAV	CDR3 $\alpha$ AA sequence	TRAJ	TRBV	CDR3 $\beta$ AA sequence	TRBJ	% cF <sup>a</sup>
HPV13A10	B*35:01	G1	5*01	CAESYTGKFKTIF	9*01	6-1*01	CASGTEAFF	1-1*01	67
HPV13B12	B*35:01	G1	10*01	CVVSEEGFKTIF	9*01	12-5*01	CASGLGGSNEQFF	2-1*01	14
HPV9A2	B*35:01	G3	20*01	CAVQELVTSSGRLTF	58*01	9*01	CASGAGEGPPF	1-1*01	39
HPV9C10	B*35:01	G3	20*01	CAVQAMTSSNYKLTIF	53*01	9*01	CASSARTGELFF	2-2*01	14
YPL3D3	B*35:01	G2	19*01	CAISEAGFGNEKLTIF	48*01	10-3*01	CAISDPRDSVEQYF	2-7*01	82
EPL11A7	B*35:01	G1	1-2*01	CAVMSSGGSYIPTF	6*01	10-3*01	CAISTGDSNQPHF	1-5*01	13
EPL11A12	B*35:01	G1	24*01	CAFPGGNKLVF	47*01	10-3*01	CAISEWDSPTLNSPLHF	1-6*01	10
EPL7A4	B*35:01	G3	19*01	CAISRNYGQNFVF	26*01	12-3*01	CASSLAATYNEQFF	2-1*01	5
EPL7A10	B*35:01	G3	1-2*01	CAVRGSGGSYIPTF	6*01	10-3*01	CATGTGDSNQPHF	1-5*01	11
EPL11A10	B*35:01	G4	24*01	CALNAGGTSYGKLTIF	52*01	7-3*01	CASSRDFYAYNEQFF	2-1*01	98
EPL13B9	B*35:01	G5	2*01	CAVEDMNSGGYQKVTIF	13*02	28*01	CASKRATYEQYF	2-7*01	8
GLC1B11	A*02:01	G6	5*01	CAESTGKLIFF	37*01	29-1*01	CSVGTGGTNEKLIFF	1-4*01	17
GLC1B4	A*02:01	G6	5*01	CAESTSWGKLIFF	24*02	29-1*01	CSVGTGGTNEKLIFF	1-4*01	25
CLG3A10	A*02:01	G6	21*01	CAILMDSNYQLIWF	33*01	10-2*02	CASSEDGMNTEAFF	1-1*01	100
FLY5D11	A*02:01	G6	17*01	CATEGDSGYSLTIF	11*01	6-5*01	CASSYQGGNYGYTF	1-2*01	30
FLY5B5	A*02:01	G6	17*01	CATVGNSSGYSLTIF	11*01	6-5*01	CASSKQGGNIQYF	2-4*01	23
YVL16D1	A*02:01	G6	38-2/DV8*01	CAYRSFKLIFF	48*01	30*01	CAWSVPLGRREKLIFF	1-4*01	14

AA, amino acid; cF, clone frequency; G, stem cell graft; TRAJ, TCR $\alpha$  J-gene and allele; TRAV, TCR $\alpha$  V-gene and allele; TRBJ, TCR $\beta$  J-gene and allele; TRBV, TCR $\beta$  V-gene and allele.

<sup>a</sup> Among clonally expanded cells specific for the respective epitope.

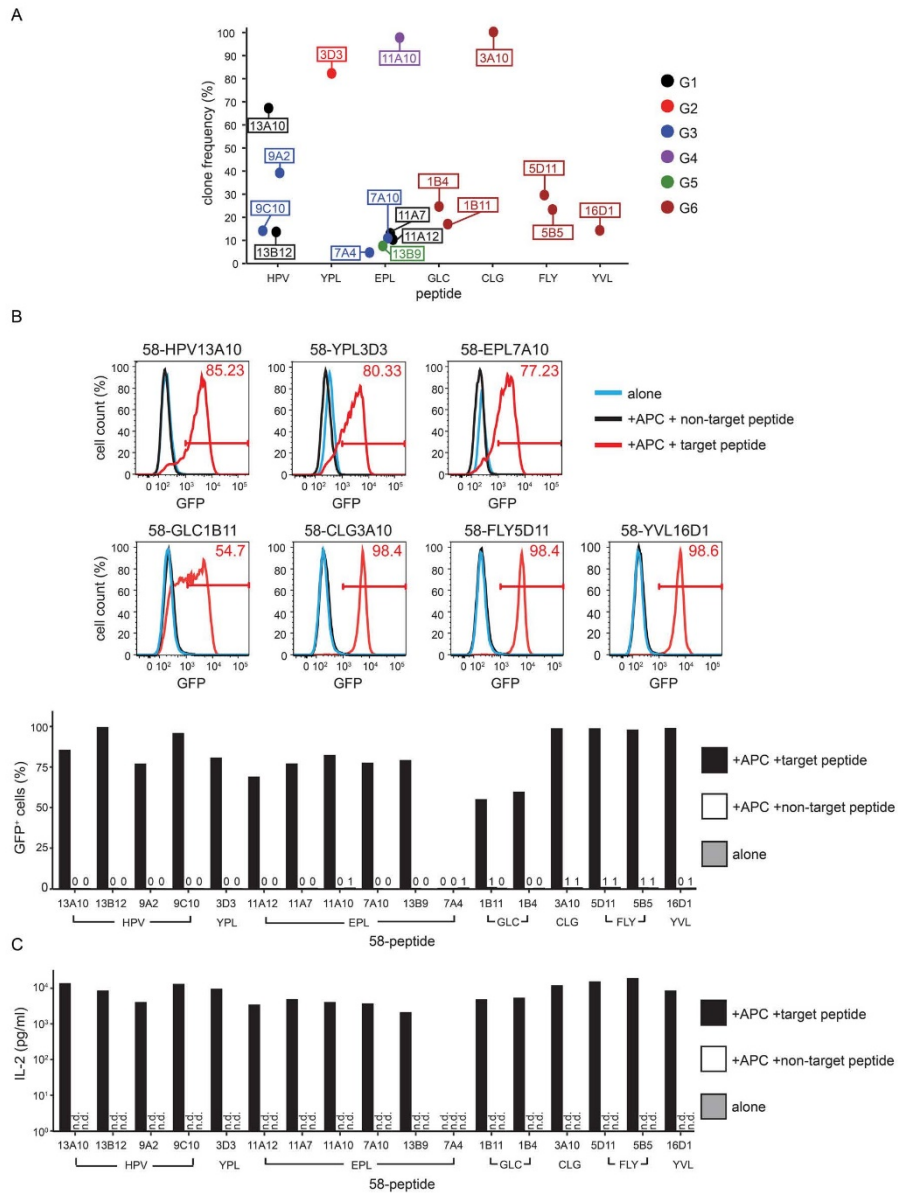


**Figure 3.** Confirmation of target peptide specificity of expanded T-cell clones. (A) TCRs selected for expression in 58 $\alpha$ - $\beta$  reporter T cells. Data points indicate individual T-cell clones. Clone frequencies are indicated as frequencies of each individual clone within clonally expanded pMHC tetramer-sorted cells. (B) TCR-recombinant cell lines were co-incubated with peptide-loaded antigen-presenting cells, and GFP expression was measured by flow cytometry as an indicator for T-cell activation. "Alone" refers to TCR-recombinant 58 $\alpha$ - $\beta$  reporter cell lines alone. All histograms are pre-gated on live TCR $\alpha$  $\beta$ CD8<sup>+</sup> cells. One co-culture per peptide specificity is shown as an example. (C) IL-2 production as measured by ELISA in cell culture supernatants corresponding to (B) TCR-recombinant data. APC, allophycocyanin; n.d., not detectable.

additionally determined CD107a expression and granzyme B and TNF- $\alpha$  secretion after stimulation with two HLA-A\*02:01-matched LCLs (B01 and DJS) and one HLA-A\*02:01-mismatched LCL (JY) in the presence of increasing target peptide concentrations. As expected, responses were substantially stronger when LCLs were artificially

loaded with the target peptide. However, significant CD137 and CD107a expression as well as IFN- $\gamma$ , granzyme B and TNF- $\alpha$  secretion could already be detected without target peptide loading, and T-cell activation was detectable only upon co-culture with HLA-matched LCLs (see supplementary Figure 7).

824

M.F. Lammoglia-Cobo et al. / Cytotherapy 24 (2022) 818–826

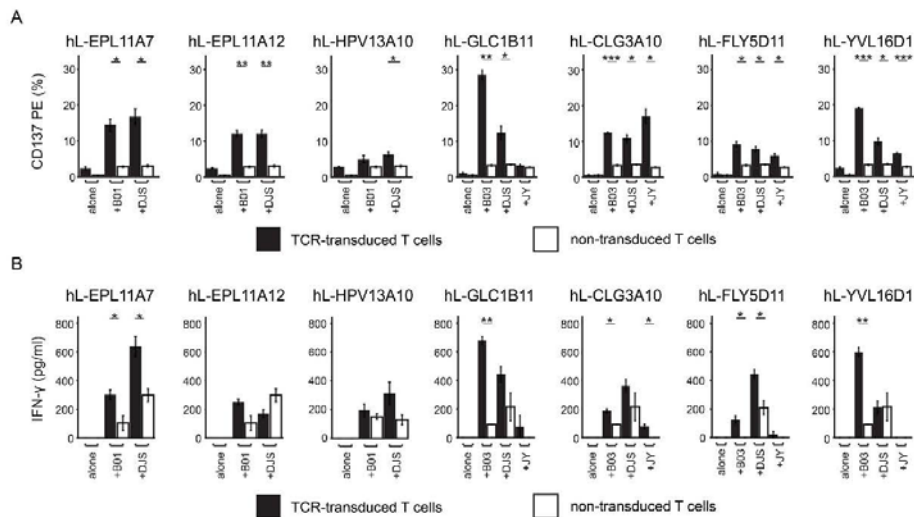


**Figure 4.** Human T cells transduced with EBV epitope-specific TCRs recognize EBV-infected cells. Three HLA-B\*35:01-restricted (EPL11A7, EPL11A12, HPV13A10) and four HLA-A\*02:01-restricted (GLC1B11, CLG3A10, FLY5D11, YVL16D1) TCRs were expressed in human lymphocytes (named “hL-[name of the TCR]”) and cultured with LCLs (B01, B03, DJS, JY). HLA-B\*35:01-restricted TCRs were cultured with HLA-B\*35:01-expressing B01 and DJS LCLs. HLA-A\*02:01-restricted TCRs were cultured with HLA-A\*02:01-expressing B03, DJS and JY LCLs. Non-transduced T cells were used as negative controls. (A) CD137 expression determined by flow cytometry. Plots are pre-gated on live CD8<sup>+</sup> lymphocytes. Data show three replicates from one experiment. (B) IFN- $\gamma$  in cell culture supernatants was measured by ELISA. Data are representative of independent experiments ( $n = 3$ ). Co-cultures of each experiment were done in triplicate. All bars represent mean values  $\pm$  standard error. Significance determined by Welch two-sample  $t$ -test. \* $P < 0.05$ , \*\* $P < 0.01$ , \*\*\* $P < 0.001$ . PE, phycoerythrin.

## Discussion

The authors' research addresses the unmet clinical need of availability of highly specific T-cell products with reliable and reproducible characteristics for prophylaxis and treatment of EBV infection and associated malignancies within minimum amounts of time. The authors defined sets of TCRs that guarantee EBV epitope specificity, recognize EBV-infected cells in two different HLA contexts and can be expressed in T-cell sources of choice.

There are a variety of elegant methodologies for identification of virus-specific TCRs and in-depth characterization of their immune phenotypes [38–40]. The authors decided to use stem cell grafts for epitope-specific T-cell expansion, which was especially helpful for identification of otherwise potentially low-frequency T-cell clones against target antigens (e.g., derived from LMP2A). Although in theory any T-cell source, including peripheral blood, may be sufficient, stem cell grafts have considerable advantages: (i) detailed HLA typing is readily available, (ii) EBV serostatus is provided, (iii) they are characterized with regard to T-cell content and (iv) leftover material from one routine stem cell transplantation is sufficient for epitope-specific T-cell expansion, circumventing otherwise unnecessary higher volume blood draws from healthy individuals. Access to already HLA-typed stem cell donors can be especially helpful for identification of epitope-specific TCRs in the context of uncommon HLA types. In addition to these rather technical advantages, virus-specific T cells generated from stem cell donor specimens have already been used for clinically effective treatment [41–43], making them T-cell sources of choice for the authors' purposes.

To increase the chances of successful epitope-specific T-cell expansion and broad applicability of potentially resulting T-cell products, the authors chose target epitopes that had previously been well characterized, are known to strongly contribute to life-long EBV-specific T-cell memory and effector repertoires in infected individuals [3,20,44–46] and are presented on HLA types covering

approximately 30–40% of the population (HLA-A\*02: 29%, HLA-B\*35: 6%) [47].

Reliable identification of EBV-specific TCRs required identification of epitope-specific T cells and highly efficient TCR $\alpha\beta$  sequencing at the single-cell level. The authors used pMHC tetramer staining for fluorescence-activated cell sorting index sorting of single peptide-specific T cells and subsequent paired TCR $\alpha\beta$  single-cell sequencing [30,48]. The authors have previously demonstrated that the combination of these technologies represents one of the most reliable and efficient approaches for identification of paired TCR $\alpha\beta$  sequences and associated immune phenotypes of single cells [31, 32]. In theory, epitope-specific T cells could have been sorted without prior *in vitro* expansion; however, frequencies of epitope-specific T cells were low before expansion (<1% of T cells), and accuracy and efficiency of single-cell sorting and TCR $\alpha\beta$  sequencing increase substantially with higher frequencies of target populations [49]. Degrees of clonal expansion varied between stem cell grafts and peptides used for *in vitro* expansion, yet epitope-specific TCRs could be successfully identified even in cases of oligoclonal expansions, in which clones of interest occupied less than 35% of CD8<sup>+</sup> clonally expanded T cells.

Five TCRs were expanded across different stem cell grafts. In the setting of only partially matched HLA types and peptide-driven *in vitro* expansion followed by pMHC tetramer-specific sorting, overlap of TCR repertoires of sorted populations is difficult to predict and will be influenced by the diversity of TCR repertoires and limited overlap between individuals. For nine of the re-expressed TCRs, the TCR $\alpha$  and/or TCR $\beta$  chains had already been deposited in the public database VDJdb; however, paired TCR $\alpha\beta$  information, which is critical for specificity, was available only for TCRs GLC1B11 and FLY5D11 [50]. For example, the TCR $\beta$  chain of TCR HPV13A10 has been described as part of a Melan A-specific TCR, whereas the alpha chain of the same TCR can be part of a cytomegalovirus IE1-specific TCR. The authors proved experimentally that, in combination, these alpha and beta chains compose the EBV epitope-specific TCR HPV13A10,

underlining the importance of paired TCR $\alpha\beta$  single-cell sequencing. Furthermore, among pMHC tetramer-sorted cells, the authors identified TCR $\beta$  chains that paired with two different TCR $\alpha$  chains. For one of these TCR $\beta$  chains, the authors showed experimentally that combining with either TCR $\alpha$  chain resulted in the productive TCRs GLC1B4 and GLC1B11, which were specific for the same epitope.

To confirm epitope specificity of selected TCRs, the authors used modified 58 $\alpha^- \beta^-$  cells as reporter cells and mini-LCLs as antigen-presenting cells. Mini-LCLs contain a selected set of latent EBV genes [35]; however, none of the TCR-recombinant 58 $\alpha^- \beta^-$  cell lines were activated by mini-LCLs, most likely due to low target antigen expression/presentation. Nevertheless, mini-LCLs could efficiently present artificially loaded peptides.

EBV epitope specificity for a variety of publicly available TCRs has already been demonstrated using artificially peptide-loaded antigen-presenting cells; however, data on TCRs that recognize EBV-infected cells without additional peptide loading are limited. The single-cell resolution of the authors' approach yielded sets of candidate TCRs specific for the target peptides of choice. To demonstrate that the identified TCRs could indeed recognize virus-infected cells, seven TCRs against latent and lytic phase epitopes were expressed on human lymphocytes and incubated with LCLs that expressed the required HLA-A\*02:01 or B\*35:01 allele. LCLs show a latency III EBV gene expression pattern and a general cellular phenotype that closely correspond to PTLDs [51]. All tested TCRs showed *in vitro* reactivity with LCLs by CD137 upregulation and/or IFN- $\gamma$  production, making them promising candidates for translation into highly specific T-cell products for adoptive transfer. The authors chose IFN- $\gamma$  secretion as the readout for T-cell activation because it requires triggering of at least 20–50% of TCRs on a T cell, and cytotoxic activity can be assumed if IFN- $\gamma$  secretion is detectable [52]. As an example, for one TCR, the authors showed that in case of target antigen recognition, both CD107a expression and granzyme B and TNF- $\alpha$  secretion were also detectable. Although the majority of LCLs are not in the lytic infection phase, it has already been shown that LCLs can efficiently activate T cells recognizing lytic phase epitopes [53].

With respect to potential TCR cross-reactivity with HLAs other than the target HLA, the authors could not detect T-cell activation upon incubation with HLA-mismatched mini-LCLs for all seven TCRs that were transduced into human peripheral blood lymphocytes. However, more detailed studies of HLA cross-reactivity are likely required before therapeutic application can be implemented. For TCR expression in human peripheral blood lymphocytes, the authors replaced the human TCR constant regions with their murine counterparts to (i) avoid mispairing of TCR $\alpha\beta$  chains [54] and (ii) allow staining with mouse TCR $\beta$  constant region antibodies. Whether expression of the murine constant regions could result in therapeutically relevant immunogenicity has to be determined in further studies; however, TCR $\alpha\beta$  mispairing could also be avoided by using minimally murinized TCR constant regions, reducing the risk of immunogenicity [55].

In addition to EBV infection and PTLDs, there are a variety of EBV-associated solid malignancies in which the pathophysiological role of EBV is still a matter of debate. Especially in Hodgkin lymphoma, natural killer/T-cell lymphoma and nasopharyngeal carcinoma, not all EBV antigens can be assumed to be equally expressed and presented [40,56]. Nevertheless EBV-directed T-cell therapy might represent a targeted therapeutic option with tolerable side effects and promising results in (pre-)clinical applications [57,58].

### Conclusions

The authors present efficient identification of EBV-specific TCRs for translation into highly specific cellular therapeutics that can be available within minimum amounts of time. T-cell

products will have exactly defined EBV epitope-specific T-cell content and can be tracked *in vivo* by mouse TCR $\beta$  constant region staining. T-cell sources for TCR expression and compositions of T-cell subsets are the investigator's choice and can potentially be adjusted and functionally manipulated before adoptive transfer. The authors' methodologies can be expanded to other epitopes and HLA types and might be successfully applied beyond EBV and other viral infections.

### Funding

IH received major financial support from Deutsche Krebshilfe e.V. (70113355), Berliner Krebsgesellschaft e.V. (HAFF202013 MM) and the German Cancer Consortium. MFLC was supported by scholarships from the Berlin School of Integrative Oncology, Charité–Universitätsmedizin Berlin and the Mexican National Council of Science and Technology. LP is supported by a research fellowship from the German Research Foundation (PE 3127/1-1) and is a scholar of the American Society of Hematology. KDo was supported by SyNergy (EXC 2145 SyNergy, 390857198).

### Declaration of Competing Interest

LB is on the advisory committees of AbbVie, Amgen, Astellas, Bristol Myers Squibb, Celgene, Daiichi Sankyo, Gilead, Hexal, Janssen, Jazz Pharmaceuticals, Menarini, Novartis, Pfizer, Sanofi and Seattle Genetics and supports research at Bayer and Jazz Pharmaceuticals.

### Author Contributions

Conception and design of the study: MFLC, AG and IH. Acquisition of data: MFLC, CW, LR, KDi, CP, AT and IH. Analysis and interpretation of data: MFLC, CW, LR, ML, CP, LP, RG, LB, JM, AM, KDo, TB, TK, AG and LH. Drafting or revising the manuscript: MFLC, AM, TB and LH. All authors have approved the final article.

### Acknowledgments

The authors thank Kirstin Rautenberg and Hans-Peter Rahn at the preparative flow cytometry unit at the Max Delbrück Center for Molecular Medicine, Berlin, Germany, for expert fluorescence-activated cell sorting support. The authors also thank the National Institutes of Health Tetramer Core Facility for providing the pMHC tetramers.

### Supplementary materials

Supplementary material associated with this article can be found in the online version at doi:10.1016/j.jcyt.2022.03.005.

### References

- [1] Tzellos S, Farrell PJ. Epstein–Barr virus sequence variation–biology and disease. *Pathogens* 2012;1:156–74.
- [2] Young LS, Rickinson AB. Epstein–Barr virus: 40 years on. *Nat Rev Cancer* 2004;4:757–68.
- [3] Hislop AD, Annels NE, Gudgeon NH, et al. Epitope-specific evolution of human CD8(+) T cell responses from primary to persistent phases of Epstein–Barr virus infection. *J Exp Med* 2002;195:893–905.
- [4] Kurth J, Spieker T, Wustrow J, et al. EBV-infected B cells in infectious mononucleosis: viral strategies for spreading in the B cell compartment and establishing latency. *Immunity* 2000;13:485–95.
- [5] Kennedy G, Komano J, Sugden B. Epstein–Barr virus provides a survival factor to Burkitt's lymphomas. *Proc Natl Acad Sci U S A* 2003;100:14269–74.
- [6] Mannick JB, Cohen JL, Birkenbach M, et al. The Epstein–Barr virus nuclear protein encoded by the leader of the EBNA RNAs is important in B-lymphocyte transformation. *J Virol* 1991;65:6826–37.
- [7] Parker GA, Toutou R, Allday MJ. Epstein–Barr virus EBNA3C can disrupt multiple cell cycle checkpoints and induce nuclear division divorced from cytokinesis. *Oncogene* 2000;19:700–9.

- [8] Tomkinson B, Robertson E, Kieff E. Epstein–Barr virus nuclear proteins EBNA-3A and EBNA-3C are essential for B-lymphocyte growth transformation. *J Virol* 1993;67:2014–25.
- [9] Caldwell RG, Wilson JB, Anderson SJ, et al. Epstein–Barr virus LMP2A drives B cell development and survival in the absence of normal B cell receptor signals. *Immunity* 1998;9:405–11.
- [10] Portis T, Dyck P, Longnecker R. Epstein–Barr Virus (EBV) LMP2A induces alterations in gene transcription similar to those observed in Reed–Sternberg cells of Hodgkin lymphoma. *Blood* 2003;102:4166–78.
- [11] Portis T, Longnecker R. Epstein–Barr virus LMP2A interferes with global transcription factor regulation when expressed during B-lymphocyte development. *J Virol* 2003;77:105–14.
- [12] Heslop HE, Ng CY, Li C, et al. Long-term restoration of immunity against Epstein–Barr virus infection by adoptive transfer of gene-modified virus-specific T lymphocytes. *Nat Med* 1996;2:551–5.
- [13] Leen AM, Christin A, Myers GD, et al. Cytotoxic T lymphocyte therapy with donor T cells prevents and treats adenovirus and Epstein–Barr virus infections after haploidentical and matched unrelated stem cell transplantation. *Blood* 2009;114:4283–92.
- [14] Rooney CM, Smith CA, Ng CY, et al. Use of gene-modified virus-specific T lymphocytes to control Epstein–Barr-virus-related lymphoproliferation. *Lancet* 1995;345:9–13.
- [15] Ouyang Q, Wagner WM, Walter S, et al. An age-related increase in the number of CD8<sup>+</sup> T cells carrying receptors for an immunodominant Epstein–Barr virus (EBV) epitope is counteracted by a decreased frequency of their antigen-specific responsiveness. *Mech Ageing Dev* 2003;124:477–85.
- [16] Tomkinson BE, Wagner DK, Nelson DL, et al. Activated lymphocytes during acute Epstein–Barr virus infection. *J Immunol* 1987;139:3802–7.
- [17] Burrows SR, Gardner J, Khanna R, et al. Five new cytotoxic T cell epitopes identified within Epstein–Barr virus nuclear antigen 3. *J Gen Virol* 1994;75(Pt 9):2489–93.
- [18] Lee SP, Thomas WA, Murray RJ, et al. HLA A2.1-restricted cytotoxic T cells recognizing a range of Epstein–Barr virus isolates through a defined epitope in latent membrane protein LMP2. *J Virol* 1993;67:7428–35.
- [19] Saulquin X, Birsch C, Peyrat MA, et al. A global appraisal of immunodominant CD8 T cell responses to Epstein–Barr virus and cytomegalovirus by bulk screening. *Eur J Immunol* 2000;30:2531–9.
- [20] Steven NM, Anells NE, Kumar A, et al. Immediate early and early lytic cycle proteins are frequent targets of the Epstein–Barr virus-induced cytotoxic T cell response. *J Exp Med* 1997;185:1605–17.
- [21] Tangye SG, Palendira U, Edwards ES. Human immunity against EBV: lessons from the clinic. *J Exp Med* 2017;214:269–83.
- [22] Ogonek J, Kralj Juric M, Ghimire S, et al. Immune Reconstitution after Allogeneic Hematopoietic Stem Cell Transplantation. *Front Immunol* 2016;7:507.
- [23] Comoli P, Basso S, Zecca M, et al. Preemptive therapy of EBV-related lymphoproliferative disease after pediatric haploidentical stem cell transplantation. *Am J Transplant* 2007;7:1646–55.
- [24] Landgren O, Gilbert ES, Rizzo JD, et al. Risk factors for lymphoproliferative disorders after allogeneic hematopoietic cell transplantation. *Blood* 2009;113:4992–5001.
- [25] Young L, Alfieri C, Hennessy K, et al. Expression of Epstein–Barr virus transformation-associated genes in tissues of patients with EBV lymphoproliferative disease. *N Engl J Med* 1989;321:1080–5.
- [26] Burns DM, Ryan GB, Harvey CM, et al. Non-uniform *in vivo* Expansion of Epstein–Barr Virus-Specific T-Cells Following Donor Lymphocyte Infusion for Post-transplant Lymphoproliferative Disease. *Front Immunol* 2019;10:2489.
- [27] Moosmann A, Bigalke I, Tischer J, et al. Effective and long-term control of EBV PTLD after transfer of peptide-selected T cells. *Blood* 2010;115:2960–70.
- [28] Gary R, Agner M, Moi S, et al. Clinical-grade generation of peptide-stimulated CMV/EBV-specific T cells from G-CSF mobilized stem cell grafts. *J Transl Med* 2018;16:124.
- [29] Schultze-Florey RE, Tischer S, Kuhlmann L, et al. Dissecting Epstein–Barr Virus-Specific T-Cell Responses After Allogeneic EBV-Specific T-Cell Transfer for Central Nervous System Posttransplant Lymphoproliferative Disease. *Front Immunol* 2018;9:1475.
- [30] Han A, Glanville J, Hansmann L, et al. Linking T-cell receptor sequence to functional phenotype at the single-cell level. *Nat Biotechnol* 2014;32:684–92.
- [31] Penter L, Dietze K, Bullinger L, et al. FACS single cell index sorting is highly reliable and determines immune phenotypes of clonally expanded T cells. *Eur J Immunol* 2018;48:1248–50.
- [32] Penter L, Dietze K, Ritter J, et al. Localization-associated immune phenotypes of clonally expanded tumor-infiltrating T cells and distribution of their target antigens in rectal cancer. *Oncimmunology* 2019;8:e1586409.
- [33] Siewert K, Malocka J, Kawakami N, et al. Unbiased identification of target antigens of CD8<sup>+</sup> T cells with combinatorial libraries coding for short peptides. *Nat Med* 2012;18:824–8.
- [34] Feederle R, Kost M, Baumann M, et al. The Epstein–Barr virus lytic program is controlled by the co-operative functions of two transactivators. *Embo J* 2000;19:3080–9.
- [35] Moosmann A, Khan N, Cobbold M, et al. B cells immortalized by a mini-Epstein–Barr virus encoding a foreign antigen efficiently reactivate specific cytotoxic T cells. *Blood* 2002;100:1755–64.
- [36] Wiesner M, Zentz C, Hammer MH, et al. Selection of CMV-specific CD8<sup>+</sup> and CD4<sup>+</sup> T cells by mini-EBV-transformed B cell lines. *Eur J Immunol* 2005;35:2110–21.
- [37] Kempkes B, Pich D, Zeidler R, et al. Immortalization of human primary B lymphocytes *in vitro* with DNA. *Proc Natl Acad Sci U S A* 1995;92:5875–9.
- [38] Kobayashi E, Mizukoshi E, Kishi H, et al. A new cloning and expression system yields and validates TCRs from blood lymphocytes of patients with cancer within 10 days. *Nat Med* 2013;19:1542–6.
- [39] Ma KY, Schonnesen AA, He C, et al. High-throughput and high-dimensional single-cell analysis of antigen-specific CD8<sup>(+)</sup> T cells. *Nat Immunol* 2021;22:1590–8.
- [40] Zhang C, Tan Q, Li S, et al. Induction of EBV latent membrane protein-2A (LMP2A)-specific T cells and construction of individualized TCR-engineered T cells for EBV-associated malignancies. *J Immunother Cancer* 2021;9(7):e002516.
- [41] Doubrovina E, Ofiaz-Sozmen B, Prockop SE, et al. Adoptive immunotherapy with unselected or EBV-specific T cells for biopsy-proven EBV<sup>+</sup> lymphomas after allogeneic hematopoietic cell transplantation. *Blood* 2012;119:2644–56.
- [42] Gustafsson A, Levitsky V, Zou JZ, et al. Epstein–Barr virus (EBV) load in bone marrow transplant recipients at risk to develop posttransplant lymphoproliferative disease: prophylactic infusion of EBV-specific cytotoxic T cells. *Blood* 2000;95:807–14.
- [43] Walter EA, Greenberg PD, Gilbert MJ, et al. Reconstitution of cellular immunity against cytomegalovirus in recipients of allogeneic bone marrow by transfer of T-cell clones from the donor. *N Engl J Med* 1995;333:1038–44.
- [44] Bharadwaj M, Burrows SR, Burrows JM, et al. Longitudinal dynamics of antigen-specific CD8<sup>+</sup> cytotoxic T lymphocytes following primary Epstein–Barr virus infection. *Blood* 2001;98:2588–9.
- [45] Catalina MD, Sullivan JL, Bak KR, et al. Differential evolution and stability of epitope-specific CD8<sup>(+)</sup> T cell responses in EBV infection. *J Immunol* 2001;167:4450–7.
- [46] Pudney VA, Leese AM, Rickinson AB, et al. CD8<sup>+</sup> immunodominance among Epstein–Barr virus lytic cycle antigens directly reflects the efficiency of antigen presentation in lytically infected cells. *J Exp Med* 2005;201:349–60.
- [47] Hurley CK, Kempenich J, Wadsworth K, et al. Common, intermediate and well-documented HLA alleles in world populations: CIWD version 3.0.0. *HLA* 2020;95:516–31.
- [48] Hansmann L, Han A, Penter L, et al. Clonal Expansion and Interrelatedness of Distinct B-Lineage Compartments in Multiple Myeloma Bone Marrow. *Cancer Immunol Res* 2017;5:744–54.
- [49] Cossarizza A, Chang HD, Radbruch A, et al. Guidelines for the use of flow cytometry and cell sorting in immunological studies (second edition). *Eur J Immunol* 2019;49:1457–973.
- [50] Bagaev DV, Vroomans RMA, Samir J, et al. VDJdb in 2019: database extension, new analysis infrastructure and a T-cell receptor motif compendium. *Nucleic Acids Res* 2020;48:D1057–D62.
- [51] Mrozek-Gorska P, Buschle A, Pich D, et al. Epstein–Barr virus reprograms human B lymphocytes immediately in the prelatent phase of infection. *Proc Natl Acad Sci U S A* 2019;116:16046–55.
- [52] Valitutti S, Muller S, Dessing M, et al. Different responses are elicited in cytotoxic T lymphocytes by different levels of T cell receptor occupancy. *J Exp Med* 1996;183:1917–21.
- [53] Adhikary D, Behrends U, Moosmann A, et al. Control of Epstein–Barr virus infection *in vitro* by T helper cells specific for virion glycoproteins. *J Exp Med* 2006;203:995–1006.
- [54] Cohen CJ, Zhao Y, Zheng Z, et al. Enhanced antitumor activity of murine-human hybrid T-cell receptor (TCR) in human lymphocytes is associated with improved pairing and TCR/CD3 stability. *Cancer Res* 2006;66:8878–86.
- [55] Sommermeier D, Uckert W. Minimal amino acid exchange in human TCR constant regions fosters improved function of TCR gene-modified T cells. *J Immunol* 2010;184:6223–31.
- [56] Smith C, Khanna R. Generation of cytotoxic T lymphocytes for immunotherapy of EBV associated malignancies. *Methods Mol Biol* 2010;651:49–59.
- [57] Sinha D, Srihari S, Beckett K, et al. Off-the-shelf allogeneic antigen-specific adoptive T-cell therapy for the treatment of multiple EBV-associated malignancies. *J Immunother Cancer* 2021;9(2):e001608.
- [58] Smith C, McGrath M, Neller MA, et al. Complete response to PD-1 blockade following EBV-specific T-cell therapy in metastatic nasopharyngeal carcinoma. *NPJ Precis Oncol* 2021;5:24.

# PLOS PATHOGENS

## RESEARCH ARTICLE

# Reconstitution of EBV-directed T cell immunity by adoptive transfer of peptide-stimulated T cells in a patient after allogeneic stem cell transplantation for AITL

María Fernanda Lammoglia Cobo<sup>1</sup>✉, Julia Ritter<sup>2</sup>✉, Regina Gary<sup>3</sup>, Volkhard Seitz<sup>2,4</sup>, Josef Mautner<sup>5,6</sup>, Michael Aigner<sup>3</sup>, Simon Vökl<sup>3</sup>, Stefanie Schaffer<sup>3</sup>, Stephanie Moi<sup>3</sup>, Anke Seegebarth<sup>2</sup>, Heiko Bruns<sup>3</sup>, Wolf Rösler<sup>3</sup>, Kerstin Amann<sup>7</sup>, Maike Büttner-Herold<sup>7</sup>, Steffen Hennig<sup>4</sup>, Andreas Mackensen<sup>3</sup>, Michael Hummel<sup>2</sup>, Andreas Moosmann<sup>5,6</sup>\*, Armin Gerbitz<sup>8,†,\*</sup>



**1** Department of Hematology, Oncology, and Tumor Immunology, Charité–Universitätsmedizin Berlin, corporate member of Freie Universität Berlin and Humboldt-Universität zu Berlin, Berlin, Germany, **2** Institute of Pathology, Charité–Universitätsmedizin Berlin, corporate member of Freie Universität Berlin and Humboldt-Universität zu Berlin, Berlin, Germany, **3** Department of Internal Medicine 5–Hematology/Oncology, University Hospital Erlangen, Erlangen, Germany, **4** HS Diagnostics GmbH, Berlin, Germany, **5** Department of Medicine III, LMU-Klinikum, Munich, Germany, **6** German Centre for Infection Research, Munich, Germany, **7** Department of Nephropathology, Institute of Pathology, University of Erlangen, Erlangen, Germany, **8** Division of Medical Oncology and Hematology, Princess Margaret Cancer Center, Toronto, Ontario, Canada

## OPEN ACCESS

**Citation:** Lammoglia Cobo MF, Ritter J, Gary R, Seitz V, Mautner J, Aigner M, et al. (2022) Reconstitution of EBV-directed T cell immunity by adoptive transfer of peptide-stimulated T cells in a patient after allogeneic stem cell transplantation for AITL. *PLoS Pathog* 18(4): e1010206. <https://doi.org/10.1371/journal.ppat.1010206>

**Editor:** Micah A. Luftig, Duke University Medical Center, UNITED STATES

**Received:** December 16, 2021

**Accepted:** March 31, 2022

**Published:** April 22, 2022

**Peer Review History:** PLOS recognizes the benefits of transparency in the peer review process; therefore, we enable the publication of all of the content of peer review and author responses alongside final, published articles. The editorial history of this article is available here: <https://doi.org/10.1371/journal.ppat.1010206>

**Copyright:** © 2022 Lammoglia Cobo et al. This is an open access article distributed under the terms of the [Creative Commons Attribution License](https://creativecommons.org/licenses/by/4.0/), which permits unrestricted use, distribution, and reproduction in any medium, provided the original author and source are credited.

**Data Availability Statement:** All relevant data are within the manuscript and its [Supporting Information](#) files.

✉ These authors contributed equally to this work.  
 † AM and AG also contributed equally to this work.  
 \* [armin.gerbitz@uhn.ca](mailto:armin.gerbitz@uhn.ca)

## Abstract

Reconstitution of the T cell repertoire after allogeneic stem cell transplantation is a long and often incomplete process. As a result, reactivation of Epstein-Barr virus (EBV) is a frequent complication that may be treated by adoptive transfer of donor-derived EBV-specific T cells. We generated donor-derived EBV-specific T cells by stimulation with peptides representing defined epitopes covering multiple HLA restrictions. T cells were adoptively transferred to a patient who had developed persisting high titers of EBV after allogeneic stem cell transplantation for angioimmunoblastic T-cell lymphoma (AITL). T cell receptor beta (TCR $\beta$ ) deep sequencing showed that the T cell repertoire of the patient early after transplantation (day 60) was strongly reduced and only very low numbers of EBV-specific T cells were detectable. Manufacturing and *in vitro* expansion of donor-derived EBV-specific T cells resulted in enrichment of EBV epitope-specific, HLA-restricted T cells. Monitoring of T cell clonotypes at a molecular level after adoptive transfer revealed that the dominant TCR sequences from peptide-stimulated T cells persisted long-term and established an EBV-specific TCR clonotype repertoire in the host, with many of the EBV-specific TCRs present in the donor. This reconstituted repertoire was associated with immunological control of EBV and with lack of further AITL relapse.

**Funding:** AG was supported by the ZIM fund (KF 2766401FRO, Federal Ministry for Economic Affairs and Energy Germany), the BayImmuNet Consortium of the Bayerische Staatsministerium für Bildung und Kultur, Wissenschaft und Kunst (Government of Bavaria), and the Deutsche Forschungsgemeinschaft (DFG, German Research Foundation) - Projektnummer 324392634 - TRR 221 and SFB643. MFLC was supported by scholarships from Berlin School of Integrative Oncology (BSIO), Charité – Universitätsmedizin Berlin, and the Mexican National Council of Science and Technology (CONACYT). AMo was supported by Wilhelm Sander-Stiftung (project 2018.135.1). The funders had no role in study design, data collection and analysis, decision to publish, or preparation of the manuscript.

**Competing interests:** I have read the journal's policy and the authors of this manuscript have the following competing interests: AMo receives project funding from Biosyngen Pte. Ltd. for preclinical development of EBV-specific TCRs not related to this study.

## Author summary

A characteristic feature of all herpesviruses is their persistence in the host's body after primary infection. Hence, the host's immune system is confronted with the problem to control these viruses life-long. When the immune system is severely compromised, for example after stem cell transplantation from a foreign (allogeneic) donor, these viruses can reappear, as they persist in the host's body life-long after primary infection. Epstein-Barr virus (EBV) is a herpesvirus that can cause life-threatening complications after stem cell transplantation and only reinforcement of the host's immune system can reestablish control over the virus. Here we show that *ex vivo* manufactured EBV-specific T cells can reestablish long-term control of EBV and that these cells persist in the host's body over months. These results give us a better understanding of viral immune reconstitution post-transplant and of clinically-relevant T cell populations against EBV.

## Introduction

Linked to its high prevalence in adults, approximately 30–40% of patients reactivate Epstein-Barr virus (EBV) after MHC-matched allogeneic stem cell transplantation (allo-SCT), as determined by virus-specific PCR of cells of the peripheral blood [1]. Reactivation of EBV worsens outcome after allo-SCT, since it imposes the risk of EBV-associated post-transplant lymphoproliferative disorder (PTLD) and is associated with malignancies such as angioimmunoblastic T cell lymphoma (AITL) [2]. AITL is a rare form of T cell non-Hodgkin Lymphoma in which concomitant EBV infection often occurs [3]. EBV appears to play a role in AITL pathogenesis and histological development [2,4], either through EBV-infected B immunoblasts found at early AITL stages adjacent to neoplastic T cells [5–7] or infection of both cells types [8]. For this reason, EBV serostatus and viral loads serve as important prognostic factors [9,10], especially among young patients [11].

EBV DNA load in peripheral blood is routinely monitored by polymerase chain reaction (PCR) in patients after allo-SCT to allow for pre-emptive treatment strategies [12]. Since no specific antiviral therapy is available to date, treatment of EBV-related disease in patients after allo-SCT focuses on three major strategies: (i) in-patient depletion of EBV-transformed B cells with antibodies—with depletion of other B cells as collateral damage—(ii) reduction of immunosuppression, or (iii) application of EBV-specific, donor-derived T cells [13–16].

The availability of B cell-depleting antibodies has reduced the occurrence of PTLD after allo-SCT [17], but comes with severe side effects and costs. Due to the long-term depletion of B cells, antibody generation is abolished and patients are at risk of severe infections, especially with encapsulated bacteria whose control requires antibody opsonization [18,19]. Therefore, frequent application of intravenous immunoglobulins is necessary. Furthermore, the problem of failing immunological control of EBV is not resolved.

As an alternative strategy, several groups have focused on the development of EBV-specific T cell transfer, as reactivation of EBV is associated with use of T cell-depleted grafts or insufficient T cell reconstitution after transplantation. This approach does not bear the risk of developing *de novo* graft versus host disease [20–24]. Adoptive transfer of natural EBV-specific T cells from EBV-positive donors has been performed and is considered overall a success due to its effectiveness and safety [23]. For patients with EBV-seronegative donors, where natural EBV-specific T cells are not available, adoptive transfer of EBV TCR-transduced T cells is a promising alternative [25–29].



We have recently described a Good Manufacturing Practice (GMP)-compliant method for the generation of CMV- and EBV-specific T cells by stimulation of G-CSF mobilized allogeneic stem cell grafts or conventional PBMC with MHC-I- and MHC-II-restricted epitope peptides derived from viral proteins [24]. We selected peptides that allow for comprehensive quality control of the product and subsequent follow-up within the patient after adoptive transfer, using flow cytometry with peptide-MHC multimers. However, little is known about the detailed structure of the EBV-specific T cell repertoire recognizing each epitope and its fate after adoptive transfer into the patient.

Here, we generated multi-epitope-specific T cells by peptide stimulation and adoptively transferred them to a patient with severe EBV reactivation after allo-SCT. We selected several peptides for defined latent and lytic epitopes of multiple well-established HLA restrictions. Using peptide-MHC multimer binding in flow cytometry and high-throughput sequencing of the TCR $\beta$  repertoire, we show that stimulation of T cells with EBV peptides generates a product with a clonotypic TCR $\beta$  repertoire that is strongly focused on EBV-specific sequences, and that this repertoire can be tracked long-term *in vivo* after adoptive transfer in the patient to demonstrate immune reconstitution.

## Results

### Manufacturing of EBV-specific T cells

A 55-year-old, EBV-seropositive patient suffered from biopsy-confirmed chemotherapy-refractory AITL (Stage IVB, EBV<sup>-</sup>, see [S1](#) and [S2](#) Figs) and was transplanted with G-CSF-mobilized peripheral blood stem cells from an HLA 10/10 matched unrelated donor. Concomitant with leukemic relapse shortly after transplantation (day 42), the patient developed high EBV titers in peripheral blood on day 66 and received conventional unmanipulated donor lymphocyte infusion (DLI) on day 76 and Rituximab four times weekly on days 68–89. As major symptoms of EBV reactivation (night sweats, fever, itching of the skin, and elevated liver enzymes) were not controlled, we decided to prepare and adoptively transfer peptide-stimulated EBV-specific T cells (ATCT) on day 105. An overview of the patient history is provided in [S1 Table](#) and [S3 Fig](#).

To prepare EBV-specific T cells, a total of 600 million conventional PBMC (frozen fraction of the preparation for conventional DLI) were stimulated with a pool of defined EBV-derived peptides (1  $\mu$ g/ml per peptide, [Table 1](#)), similar to the procedure published previously [24]. Peptide-stimulated cells were subsequently expanded in a closed bag system for 9 days. [Fig 1A](#) (left panel) shows the composition of the PBMC before peptide stimulation (day 0) and of the resulting cell composition after 9 days of expansion. The dominant fraction of cells in the product were CD3<sup>+</sup> T cells (84.8%). B cells, NK cells and monocytes were reduced to 5.8% of all cells. Other cells (9.4%) were mainly macrophages, activated monocytes, neutrophils (all CD11b<sup>+</sup>, CD68<sup>+</sup>), and few remaining granulocytes. As shown in [Fig 1A](#) (right panel), total CD3<sup>+</sup> T cell number increased from approximately 315 million to 631 million cells over the 9-day period, and a total of approximately 750 million cells were harvested.

The T cell product was analyzed before and after peptide stimulation with peptide-MHC multimers ([Fig 1B](#)) corresponding to the six peptides of the stimulation pool that were restricted through HLAs present in transplant donor and recipient ([Table 1](#)). On day 0, 2.4% of CD8<sup>+</sup> T cells, mainly in the CCR7-negative subset, specifically bound peptide-MHC multimers. By day 9, T cells specific for five of the six epitopes had strongly expanded and now amounted to 64.6% of all CD8<sup>+</sup> T cells. Two epitopes (RAK and EPL) from the immediate-early protein BZLF1 and one epitope (HPV) from the latent antigen EBNA1 were particularly dominant. Intracellular cytokine staining after restimulation demonstrated, as expected [44],

Table 1. Peptide pool used for T cell stimulation.

label	AA Sequence	peptide length	protein	presented on HLA	reference	matched with patient
CLG	CLGGLTVMV	9	LMP2	A*02:01	[30]	
GLC	GLCTLVAML	9	BMLF1	A*02:01	[31,32]	
YVL	YVLDHLIVV	9	BRLF1	A*02:01	[33]	
FLY	FLYALALL	9	LMP2	A*02:01	[34]	
RLR	RLRAEAQVK	9	EBNA3A	A*03:01	[35]	+
RPP	RPPIFIRRL	9	EBNA3A	B*07:02	[35]	
QAK	QAKWRLQTL	9	EBNA3A	B*08:01	[36]	+
RAK	RAKFKQLL	8	BZLF1	B*08:01	[37]	+
YPL	YPLHEQHGM	9	EBNA3A	B*35:01	[36]	+
HPV	HPVGEADYFEY	11	EBNA1	B*35:01	[38]	+
EPL	EPLPQGQLTAY	11	BZLF1	B*35:01	[33]	+
PYYV	PYYVVDLSVRGM	12	BHRF1	DR*4	[39]	
VVRM	VVRMFMRERQLPQS	14	EBNA3C	DR*11	[40]	
FGQL	FGQLTPHTKAVYQPR	15	BLLF1	DR*13	[41]	
IPQC	IPQCRLTPLSRLPFG	15	EBNA1	DR*13	[42]	
TDAW	TDAWRFAMNYPRNPT	15	BNRF1	DR*15	[43]	

AA: amino acid sequence.

<https://doi.org/10.1371/journal.ppat.1010206.t001>

that a variable proportion of CD8<sup>+</sup> T cells specific for these epitopes secreted IFN- $\gamma$  in response to single peptide stimulation (Fig 1C). A high proportion of IFN- $\gamma$ -secreting CD8<sup>+</sup> cells (13.2%, compared to 24.1% of multimer-staining cells) was seen for the EPL epitope. An increase of IFN- $\gamma$  concentration and other cytokines was also detected in patient serum after adoptive transfer (S4 Fig). While more than half (53.6%) of CD3<sup>+</sup> T cells of the PBMCs (day 0) had initially a naive phenotype (CCR7<sup>+</sup>/CD45RA<sup>+</sup>), these were reduced to 15.4% on day 9 (Fig 1D). In contrast, the proportion of T cells with effector/effector memory phenotype (CCR7<sup>-</sup>/CD45RA<sup>-</sup>) changed from 22.8% to 80.0%. The three most dominant multimer-binding CD8<sup>+</sup> T cell populations (EPL, RAK, and HPV) had a dominating effector memory phenotype in the cellular product, despite a stronger CD62L expression in EPL- and RAK-specific T cells as compared to HPV-specific T cells (S5 Fig).

Separate analysis showed that T cell memory phenotypes were extensively changed in the CD8<sup>+</sup> but hardly in the CD4<sup>+</sup> T cell subset (Fig 1E), while expression of the activation markers CD25, HLA-DR and CD38 was also largely limited to the CD8<sup>+</sup> subset (Fig 1E). As far as is known (and disregarding the possibility of promiscuous HLA class II restriction [45]), peptides presented on HLA-DR to CD4<sup>+</sup> T cells and which were used for stimulation (Table 1) were not restricted for any donor or patient HLA-ABC molecule. Consequently, EBV-specific CD4<sup>+</sup> T cells may not have been stimulated by the EBV peptide pool, and therefore memory and activation markers on CD4<sup>+</sup> T cells were not altered.

### Analysis of the TCR repertoire of the T cell product

Having demonstrated that stimulation of T cells with a pool of EBV peptides results in strong expansion of peptide-specific CD8<sup>+</sup> effector and effector/effector-memory T cells, we next analyzed the T cell receptor  $\beta$ -chain (TCR $\beta$ ) repertoire before and after peptide stimulation. To this end, we amplified the TCR $\beta$  of flow cytometry-sorted CD8<sup>+</sup> T cells via high-throughput sequencing (HTS) (see S6 Fig for multimer sorting gating strategy and purity). For comparability, the same amount of DNA (100 ng per analysis)—representing the equivalent number of

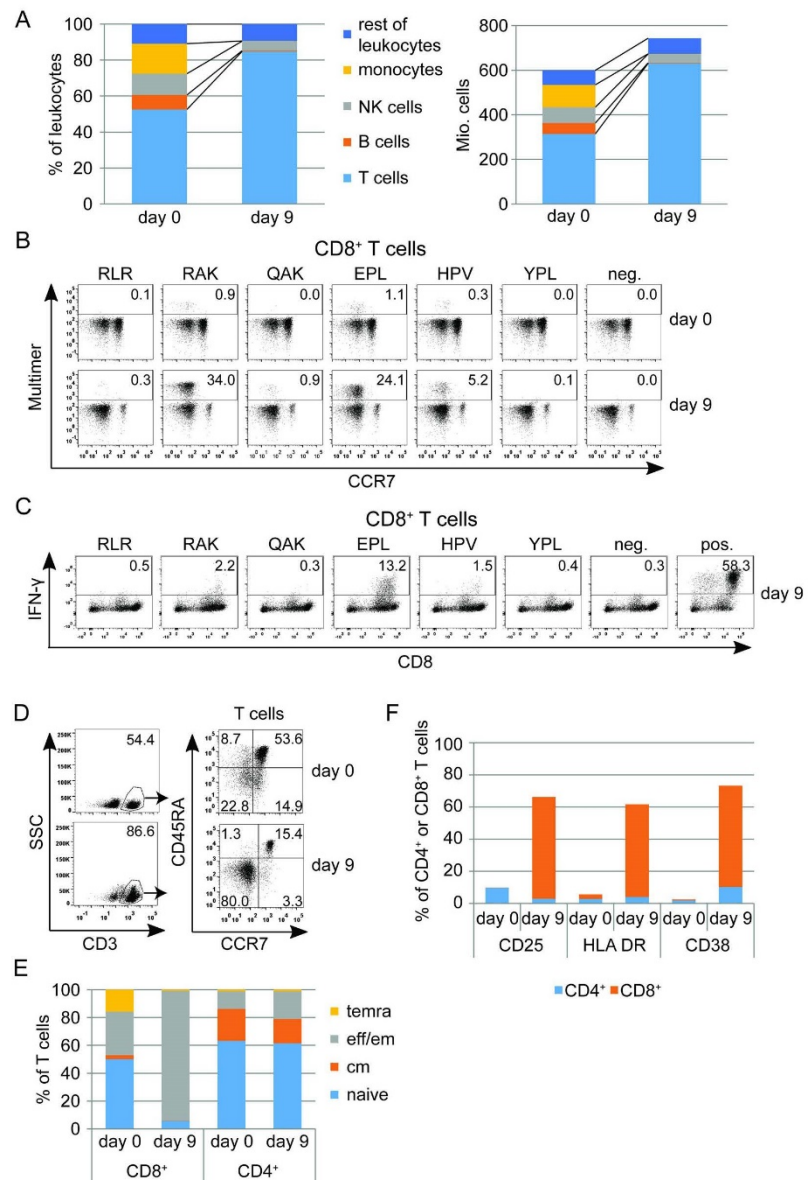


**Fig 1. Manufacture of EBV-specific T cells.** (A) Composition of the apheresis product that served as starting material (day 0) and the resulting T cell culture after stimulation with EBV peptides (day 9). Left panel: Proportions of different cell types in CD45<sup>+</sup> cells (monocytes: CD14<sup>+</sup>SSC<sup>low</sup>, NK cells: CD56<sup>+</sup>, B cells: CD19<sup>+</sup>, T cells: CD3<sup>+</sup>, rest of leukocytes). Right panel: Composition in absolute cell numbers. (B) Percentage of peptide-specific T cells assessed by flow cytometry using peptide-MHC multimers (RLR, HLA-A\*03:01; QAK, RAK, HLA-B\*08:01; YPL, HPV, EPL, HLA-B\*35:01) on day 0 and

day 9. (C) IFN- $\gamma$  secretion of peptide-specific T cells after restimulation with single peptides on day 9, assessed by intracellular cytokine staining (neg.: unstimulated CD8<sup>+</sup> T cells, pos.: stimulation of T cells with ionomycin). (D) Flow cytometric analysis of T cell memory/differentiation markers on day 0 and day 9. Plots on the right side are pre-gated on CD3<sup>+</sup> cells. temra = terminally differentiated effector memory T cells (CCR7<sup>-</sup> CD45RA<sup>+</sup>), eff/em = effector/effector memory T cells (CCR7<sup>+</sup> CD45RA<sup>+</sup>), cm = central memory T cells (CCR7<sup>+</sup> CD45RA<sup>-</sup>), naïve = naïve T cells (CCR7<sup>+</sup> CD45RA<sup>-</sup>). (E) Percentage of T cell subsets within CD4<sup>+</sup> and CD8<sup>+</sup> T cells. (F) Flow cytometric analysis of T cell activation markers CD25, HLA-DR and CD38 within the CD4<sup>+</sup> and CD8<sup>+</sup> T cell compartment.

<https://doi.org/10.1371/journal.ppat.1010206.g001>

T cell rearrangements (approximately 14,500 T cells)—was employed for each library preparation. Within a first study, we were able to demonstrate that analyzing this constant amount of T cells reliably reflects T cell composition and T cell diversity [46].

Following this approach, we observed a strong change in the usage of TCR V $\beta$  segments of the sorted CD8<sup>+</sup> T cells before and after EBV peptide stimulation (Fig 2A, left panel). While the proportion of V $\beta$ 19, 20, and 4 was reduced over 9 days of cultivation, we observed an expansion of V $\beta$ 6 and V $\beta$ 7 chains. Next, we enriched EBV epitope-specific CD8<sup>+</sup> T cells by flow cytometry cell sorting based on peptide-MHC multimer binding on day 9. Interestingly, individual patterns of V $\beta$  usage were characteristic for each EBV epitope (Fig 2A, right panel), with predominant V $\beta$ 6 usage in EPL and HPV multimer-enriched CD8<sup>+</sup> T cells, and V $\beta$ 7 and V $\beta$ 4 predominant in RAK-enriched T cells.

Individual clonotypes were defined as TCR $\beta$  complementarity-determining regions 3 (CDR3) DNA sequences with a percentage of reads equal to or above the cut-off of 0.01%. We compared the frequencies of the 25 most abundant TCR $\beta$  clonotypes at day 0 and day 9 of the CD8<sup>+</sup> T cells, ordered by read frequency in descending order (Fig 2B, left panel). While the percentage of the most common clonotype (labeled by arrow) of the total CD8<sup>+</sup> T cell fraction on day 0 was 1.4%, the most dominant clonotype on day 9 reached 14.5%.

Analysis of the clonotype distribution of multimer-sorted T cells (Fig 2B, right panel) revealed a steep distribution curve for epitope HPV-sorted T cells with the most dominant single TCR $\beta$  clonotype (CASGTEAFF) representing 38.8% of all HPV-sorted TCR $\beta$  sequence reads. In contrast, RAK- and EPL-sorted CD8<sup>+</sup> T cells showed a less steep distribution curve, indicating a higher variety of different TCR $\beta$  clonotypes.

A higher percentage of the most common clonotype correlated with a lower total number of different clonotypes per sample. This correlation was also present in clonotype numbers in CD8<sup>+</sup> T cells before and after peptide stimulation (Fig 2C, left panel). At day 0, we identified 1,957 different TCR $\beta$  clonotypes (cutoff 0.01% of reads) derived from an equivalent of approximately 14,500 T cells (100 ng input DNA). This number was reduced to 471 clonotypes after stimulation, and 276 of these were shared in both samples. These 276 clonotypes accounted for 27.4% of total sequence reads on day 0 and for 80.8% of reads on day 9. Of these 276 clonotypes, 208 were found in multimer-sorted populations: 108 in EPL-, 97 in RAK-, and 96 in HPV peptide-MHC multimer-binding T cells (overlapped clonotypes had only minor frequencies). These 208 clonotypes accounted for 16.2% of all CD8<sup>+</sup> TCR $\beta$  sequence reads of the healthy donor (day 0). This fraction increased to 77.5% of all detected CD8<sup>+</sup> T cell TCRs in the peptide-stimulated T cell product (day 9).

After flow cytometric cell sorting with the three peptide-MHC multimers, a total of 327 clonotypes were present in cells sorted with EPL multimer, 341 clonotypes in RAK-sorted cells, and 313 clonotypes in HPV-sorted cells. Multimer sorting gate was kept stringent to achieve a sorting purity above 98% (S6 Fig). To clearly identify epitope-specific clonotypes and remove both overlapping and contaminant cells in multimer-sorted populations, we established two additional filters: (1) a frequency cutoff of 0.1% before and after multimer sorting, and (2) a requirement that epitope-specific clonotypes were at least ten times more highly enriched in

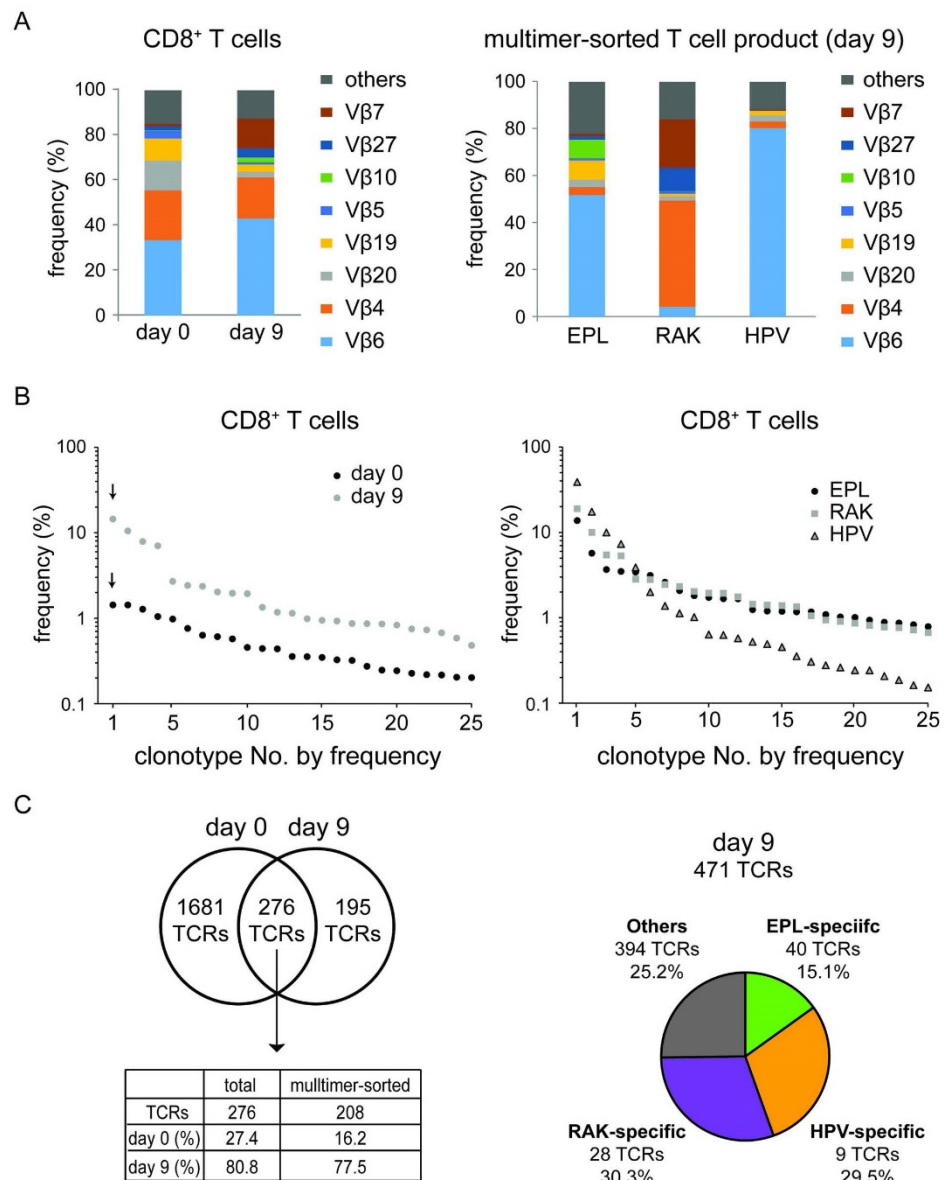


**Fig 2. Global and EBV-specific TCR repertoire of the T cell product.** (A) Vβ usage. Left panel: Percentage of Vβ subgroup usage within CD8<sup>+</sup> T cells before (day 0) and after (day 9) peptide stimulation. Right panel: Vβ subgroup analysis of flow cytometry-sorted MHC multimer binding T cells (EPL, RAK, and HPV) on day 9 after peptide stimulation. (B) Individual clonotype distribution within CD8<sup>+</sup> T cells on day 0 and day 9 (left panel) and in multimer-sorted T cells on day 9 (right panel). Each dot represents the frequency (percentage of all sequencing reads) of a single TCRβ clonotype. The 25 most frequent clonotypes of each sample are illustrated. (C) Left panel: Overlap of the number of

TCR $\beta$  clonotypes within CD8<sup>+</sup> T cells on day 0 and day 9. The table shows the presence of the 276 shared TCRs from days 0 and 9 in total CD8<sup>+</sup> T cells and in multimer-sorted CD8<sup>+</sup> T cells from day 9, along with their cumulative percentage in total CD8<sup>+</sup> T cells per day. Right panel: Number of epitope-specific TCR $\beta$  clonotypes and their proportion of cumulative TCR $\beta$  sequence reads within the overall CD8<sup>+</sup> T cell product on day 9.

<https://doi.org/10.1371/journal.ppat.1010206.g002>

one of the multimer-sorted cultures than in the other two (ternary exclusion criterion). This analysis resulted in the identification of 40 EPL-, 28 RAK-, and 9 HPV-specific TCRs. (Fig 2C, right panel, epitope-specific clonotype identification in S7 Fig, TCR overview in S2–S4 Tables). Notably, the 77 epitope-specific clonotypes represented 74.7% of all TCR $\beta$  reads on day 9. This finding confirmed that day 9 peptide-expanded T cells were dominated by EBV epitope-specific CD8<sup>+</sup> T cells. Among these, the 9 HPV-specific clonotypes accounted for 29.5% of all CD8<sup>+</sup> clonotypes on day 9, which again reflects the steep distribution curve shown in Fig 2B (right panel) and the high proportion of dominant clonotypes such as CASGTEAFF in the HPV-sorted fraction.

To illustrate how EBV peptide-sorted T cell clonotypes expanded after peptide stimulation, the 30 most common TCR $\beta$  clonotypes on day 0 and day 9 as well as the 10 most common clonotypes of EPL-, RAK-, and HPV-sorted T cells are listed in Table 2. Therein, the most dominant TCR $\beta$  clonotype for 3 EBV peptides is color-coded according to the peptide. Peptide stimulation resulted in a strong expansion of the dominant clonotypes for the three peptides. The dominant HPV-sorted TCR $\beta$  clonotype (CASGTEAFF) was also the most dominant one in day 9 CD8<sup>+</sup> T cells and had been expanded 24-fold as compared to day 0. Within the multimer-sorted T cell fraction, this specific clonotype accounted for 38.8% of sequencing reads. Similar results were obtained for EPL and RAK dominant clonotypes. However, the HPV-specific TCR $\beta$  clonotype CASGTEAFF was found three times due to different DNA sequences coding for the identical amino acid sequence. Overall, these three clonotypes accounted for 66.2% within the HPV-sorted fraction.

### T cell expansion after adoptive T cell transfer

To follow the *in vivo* fate of adoptively transferred peptide-stimulated T cells, we analyzed the peripheral blood of the patient before and after transfer. Fig 3A shows T cell immune reconstitution in absolute T cell numbers after allo-SCT. Between day 34 and day 89, we observed massive expansion of CD4<sup>+</sup> cells that was caused by the relapse of the underlying CD4<sup>+</sup> AITL, as confirmed on a molecular level by preponderance of a single T-cell clonotype in a lymph node (S1 Fig). This hematologic relapse was accompanied by high fever and EBV reactivation emerging on day 66 and peaking on day 89 with 140,000 copies per ml peripheral blood (Fig 3A). The patient received four Rituximab doses weekly, starting on day 68, and an unseparated donor lymphocyte infusion (DLI) containing 5.0 Mio. CD3<sup>+</sup> T cells/kg body weight on day 76 (S1 Table). No further therapy was given at that point. Over the course of the following 21 days, T cell counts strongly decreased. We therefore decided to generate an EBV-derived peptide-stimulated T cell product from frozen DLI portions. This product was transferred at a dose of 1.0 Mio CD3<sup>+</sup> T cells/kg body weight on day 105 post-allo-SCT. As shown in Fig 3A, CD8<sup>+</sup> T cells expanded after adoptive transfer for 8 days (day 105 to 113), followed by a decline over 13 days until day 126 and stable maintenance thereafter.

When the TCR $\beta$  repertoire within the donor's PBMC fraction used as DLI (Fig 3B, day 0) was analyzed, we obtained 2375 clonotypes within the CD4<sup>+</sup> compartment and 1957 clonotypes within the CD8<sup>+</sup> compartment, which is a typical degree of TCR diversity observed in healthy donors with the assay used here [46]. Consistent with an expected narrowing of the TCR repertoire following allo-SCT [48], our patient's TCR $\beta$  repertoire was strongly reduced in

Table 2. Expansion of distinct clonotypes after EBV-derived peptide stimulation.

CD8 <sup>+</sup> T cells day 0		CD8 <sup>+</sup> T cells day 9		HLA multimer-sorted T cell product		
reads (%)	CDR3	reads (%)	CDR3	reads (%)	CDR3	peptide
1.426	CASSTPGGRNEKLF	14.464	CASGTEAFF	13.732	CASRDRVGEAFF	EPL
1.426	CATSRARGSGANVLT	10.491	CASSSRQGRTYEQYF	5.709	CASSDSGTFNEQFF	
1.271	CSAKGSLETEAFF	7.862	CASSTRGAGNTIYF	3.672	CASSDSGIHNSPLHF	
1.044	CASSYPGQLNEKLF	7.020	CASGTEAFF	3.487	CASDTSALNTEAFF	
0.975	CASSQDPGNTEAFF	2.700	CASGTEAFF	3.425	CAISTGDSNPQPHF	
0.757	CASSEGYSNQPQHF	2.407	CASSTRGGGNTIYF	3.132	CASRGGQGQETQYF	
0.629	CASDGTGISGANVLT	2.359	CASGNEQYF	2.604	CASRTGEVNEQFF	
0.605	CASGTEAFF	2.028	CASSQASYVQGDGYTF	2.081	CASSTGDSNPQPHF	
0.572	CASSQDYAGHPQPHF	1.959	CASRDRVGEAFF	1.817	CASGTFDSNPQPHF	
0.454	CSAKGGYDTEAFF	1.929	CASGSEAFF	1.730	CASSDSGMTTEAFF	
0.440	CASLNNGEGTYEQYF	1.339	CAISTGDSNPQPHF	38.810	CASGTEAFF	HPV
0.436	CSVRGRENPLHF	1.170	CASSPGGGTEAFF	17.472	CASGTEAFF	
0.356	CASSMALTATNEKLF	1.144	CASSLNTEAFF P2	9.966	CASGTEAFF	
0.354	CASSPTGNTEAFF	0.984	CSARDRGTIYEQYF	7.303	CASGSEAFF	
0.347	CASSTRGAGNTIYF	0.940	CASRTGEVNEQFF	3.890	CASRPTGFDGYTF	
0.326	CASSQESDYGTYF	0.925	CSAGQGEQYEQYF	1.998	CASGNEQFF	
0.319	CASSQADSFSGNTIYF	0.863	CASRPPGPFYEQYF	1.383	CSAALRPVPRTYGTYF	
0.273	CASSQESGHLNTEAFF	0.862	CASSTGDVNPQPHF	1.130	CASSRSGLFFF	
0.246	CASSAETGGGKKAFF	0.853	CASSQGLPLNTEAFF	1.019	CASIPRTKTEAFF	
0.242	CASRDRVGEAFF	0.827	CASSYPYEQYF	0.636	CASGNEQFF	
0.226	CASSQGPNYEQYF	0.746	CASSDSGIHNSPLHF	18.947	CASSTRGAGNTIYF	RAK
0.217	CASSIGQAYEQYF	0.729	CASRGGQGQETQYF	9.985	CASSSRQGRTYEQYF	
0.216	CASSEPAGEQYF	0.672	CASSDSGTFNEQFF	5.449	CASSQGLPLNTEAFF	
0.203	CSARDPGSSYEQYF	0.583	CASSLNTEAFF P2	5.294	CASSTRGGGNTIYF	
0.202	CASSLAPGYLYEQYF	0.479	CSARGASPQANYGYTF	2.834	CSAGQGEQYEQYF	
0.195	CSARGGETEAF	0.432	CASDTSALNTEAFF	2.810	CASSLNTEAFF P2	
0.192	CASSEAGTGRSEQYF	0.427	CASSYSSFRGGNSPLHF	2.442	CASSLNTEAFF P2	
0.189	CASSKTMGMGTDQYF	0.414	CASGNEQFF	2.330	CASSLIASGGYNEQFF	
0.186	CASGTEAFF	0.403	CASSLNTEAFF	2.025	CASSQGVTDYWNEQFF	
0.175	CASSLSYEQYF	0.394	CASSQPGGLEQYF	1.946	CASSQGTGFNYGYTF	

Ranking of the top 30 TCR $\beta$  clonotypes in donor-derived CD8<sup>+</sup> T cells before peptide stimulation (day 0, left column), after peptide stimulation (day 9, middle column), and after peptide stimulation with HLA multimer FACS sorting on day 9 (right column, top 10 clonotypes for each specificity). Clonotypes with identical CDR3 peptide sequence are presented separately in case of a different underlying CDR3 DNA sequence and marked in red. The most dominant clonotype per multimer-sorted T cells are color-coded regarding the peptide used for sorting. P2: public clonotypes previously published. [47]

<https://doi.org/10.1371/journal.ppat.1010206.t002>

both compartments (CD4<sup>+</sup>: 236, CD8<sup>+</sup>: 108 clonotypes) on day 60 after allo-SCT (before DLI and adoptive transfer of EBV peptide-stimulated T cells). In line with hematologic relapse, one clone was predominant in the CD4<sup>+</sup> fraction of peripheral blood (CSARDRTGSEKLF). This clone represented the CD4<sup>+</sup> AITL, which was confirmed by analysis of DNA retrieved from a lymph node biopsy at the time of initial diagnosis (S1 Fig). On day 120 (fifteen days after adoptive transfer of peptide-stimulated T cells), we observed an increase in T cell diversity, which was higher in CD8<sup>+</sup> T cells (645 clonotypes) than in CD4<sup>+</sup> T cells (402 clonotypes). This suggested that adoptive transfer on day 105 contributed to diversification of the patient's TCR repertoire, in particular through transfer of EBV-specific CD8<sup>+</sup> T cells.

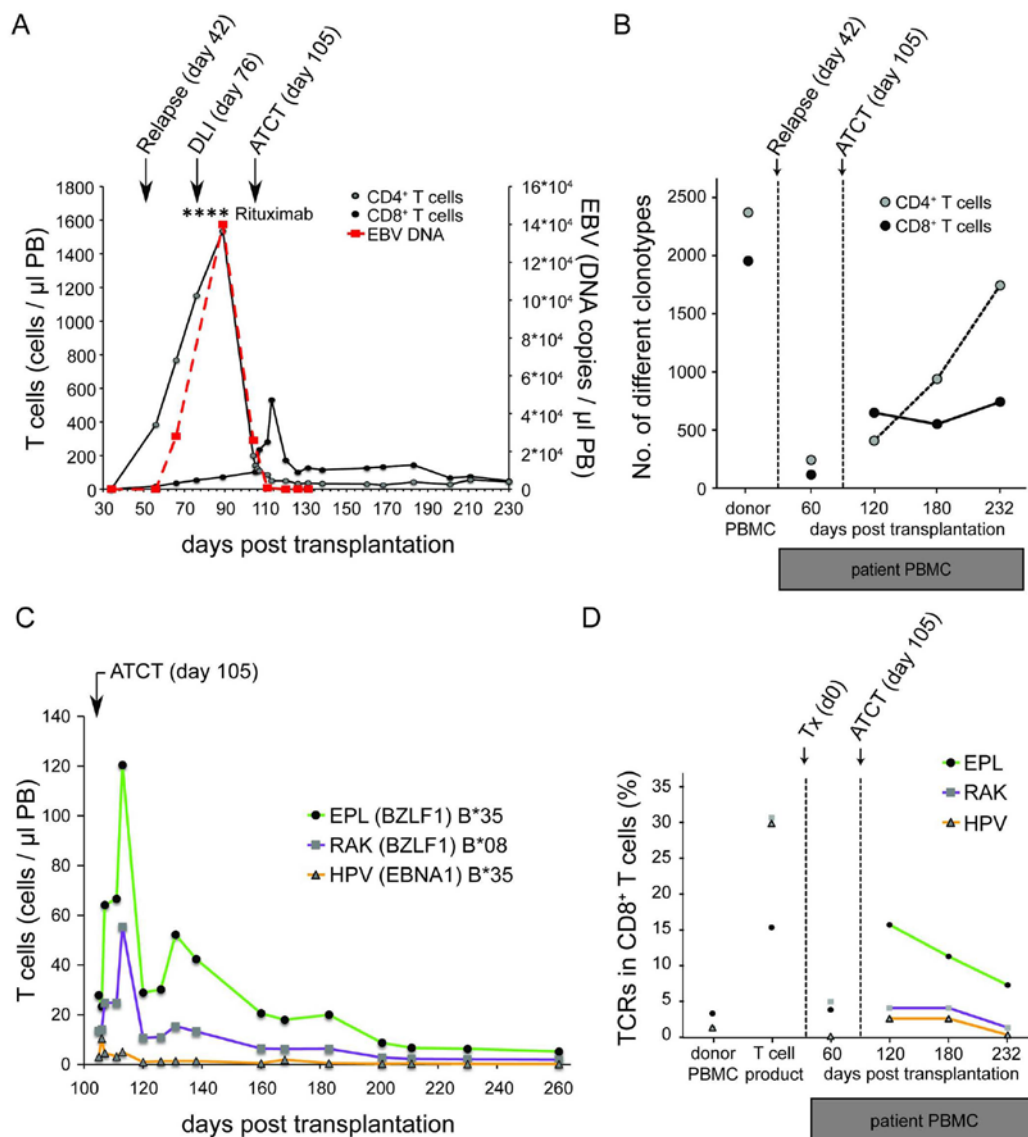


**Fig 3. T cell and clonotype expansion after allogeneic stem cell transplantation and adoptive transfer of EBV-specific T cells.** (A) Flow cytometric monitoring of absolute numbers of CD4<sup>+</sup> and CD8<sup>+</sup> T cells and EBV DNA copy number in peripheral blood. Relapse of the CD4<sup>+</sup> T cell lymphoma was detected on day 56 in peripheral blood. Time points of Rituximab application are marked with an asterisk (\*). ATCT = adoptive T cell transfer. (B) TCR clonotype diversity in CD4<sup>+</sup> and CD8<sup>+</sup> T cells in peripheral blood of the patient. For comparison, the diversity in donor's PBMC is shown. (C) Flow cytometric monitoring of peripheral blood CD8<sup>+</sup> T cells using HLA peptide-MHC multimers (EPL, RAK, HPV) on the day of ATCT (day 105) and thereafter. (D) Cumulative frequency of TCR clonotypes specific for each of the epitopes EPL, RAK, and HPV in CD8<sup>+</sup> T cell populations. Data points for donor's PBMC, T cell product after peptide stimulation, and peripheral blood of the patient before (day 60) and after ATCT (day 120, day 180, and day 230) are shown.

<https://doi.org/10.1371/journal.ppat.1010206.g003>



Multimer staining was used to track EBV-specific T cells until day 232 after allo-SCT (Fig 3C). We observed a strong expansion of EPL- and RAK-specific CD8<sup>+</sup> T cells, which were two of the three dominant EBV specificities in the T cell product. On day 105, immediately before adoptive transfer, a small fraction of HLA multimer-binding CD8<sup>+</sup> T cells had been detectable in peripheral blood. Over the course of 8 days after transfer, RAK- and EPL-multimer-binding CD8<sup>+</sup> T cells strongly expanded *in vivo* (from 14/ $\mu$ l to 55/ $\mu$ l and from 28/ $\mu$ l to 120/ $\mu$ l, respectively). Analysis of the TCR $\beta$  repertoire (Fig 3D) before adoptive T cell transfer (ATCT) on day 60 revealed that the patient had not mounted a significant T cell response against EPL, RAK, and HPV epitopes: Only 6 of 77 epitope-specific clonotypes were detectable. This situation had changed 15 days after adoptive transfer of peptide-stimulated T cells (day 120), when the total number of different multimer-binding clonotypes present had increased to 61. In comparison to day 60, by day 120 EPL- and HPV-specific T cell read frequencies increased significantly (EPL: from 3.67% to 15.43%, HPV: 0.00% to 2.37%), while RAK was relatively stable (RAK: 4.78% to 5.06%). Thereafter, clonotype diversity in CD8<sup>+</sup> T cells remained rather constant (Fig 3B), while epitope-specific clonotypes gradually declined until day 232 but were detectable throughout the observation period (follow-up of epitope-specific TCRs in S5 Table).

A complete frequency analysis of the 77 EBV epitope-specific clonotypes is shown in Fig 4A as a heat map (comparison in the T cell product before and after multimer sort in S8 Fig). At the beginning of the EBV peptide-stimulated T cell product manufacture (which at this point represents the donor's natural T cell repertoire on day 0), we found 55 EBV-specific clonotypes to be present in the patient at this time. These clonotypes represent 5.43% of the CD8<sup>+</sup> TCR $\beta$  repertoire before peptide-stimulation on day 0 (S5 Table). 15 days after adoptive transfer (day 120), the 77 EBV epitope-specific clonotypes accounted for 22.86% of all TCR gene reads found in the patient. On our last measurement (day 232), 45 EBV-specific clonotypes remained detectable, representing 8.49% of all TCR reads. Thus, by adoptive transfer of peptide-stimulated T cells, we reinstalled a large part of the donor's specific T cell repertoire targeting three EBV epitopes, which is especially reflected by the dominant clonotypes for each epitope (Fig 4B upper panel and Table 2). EBV-specific T cell reconstitution in the patient included two previously described (and thus public) clonotypes specific for EPL and RAK (Fig 4B, lower panel, and Table 2), but one of these became undetectable on day 232 [31,33]. It is noteworthy that neither dominant nor proven public clonotypes were found among the 6 EBV-specific clonotypes on day 60 in the patient, when EBV began to reactivate in the period before ATCT.

## Discussion

Adoptive transfer of EBV-specific T cells for the treatment of EBV-associated lymphoma in the immunocompromised host has been shown to effectively mediate virus control [50]. Furthermore, it has been demonstrated that adoptively transferred EBV-specific T cells contribute to long-term immunity [20]. However, although several dominant EBV-derived T cell epitopes and their HLA restriction were identified over the past decades [30–43], it remains unclear which and how many TCRs recognize those epitopes and are being expanded *in vivo*. Follow-up in patients after primary infection with EBV suggests few clonotypes with high frequencies dominate epitope-specific responses long-term [51]. Similar observations were made after adoptive transfer of EBV-specific T cells [52,53], thus pointing towards TCR clonotypes of potential clinical interest. Beyond single clonotypes, EBV-specific T cell frequencies, repertoire diversity, and long-term survival of TCR clonotypes contribute to control active EBV infection [54], latency [55], and EBV-associated malignancies [56–58].

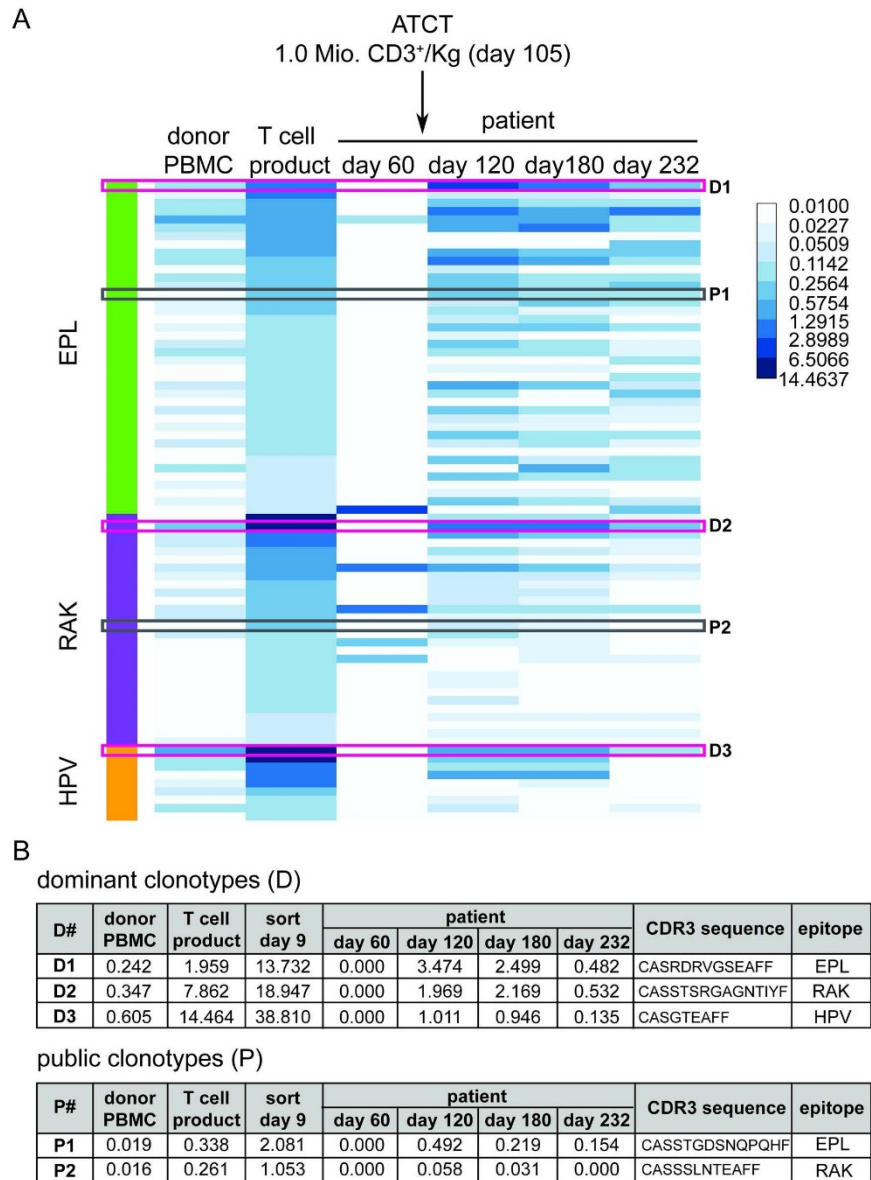


**Fig 4. Frequencies of specific TCRβ clonotypes before and after adoptive T cell transfer.** (A) Frequency heatmap of individual epitope-specific TCR clonotypes in donor PBMC, T cell product, and four time points after transplantation in the patient (day 60, day 120, day 180, and day 232). Clonotype frequency is displayed as a percentage from 0.01% (limit of detection) to 14.4637 by increasing colour depth. Each row represents one specific TCR clonotype. Identified public TCR sequences (P1 and P2) previously published [47,49] are shown in grey boxes. The most dominant clones (D1-3) within each specificity are shown in pink boxes. ATCT: adoptive T cell transfer. (B) Frequencies of public clonotypes (P) and dominant clonotypes (D) in different samples.

<https://doi.org/10.1371/journal.ppat.1010206.g004>

In this study, we manufactured and extensively analyzed at a molecular level the fate of adoptively transferred T cells enriched for specificity against multiple EBV-derived epitopes. *In vitro* stimulation with defined EBV latent and lytic epitopes resulted in a strong expansion of three EBV epitope-specific CD8<sup>+</sup> T cell populations (two lytic antigen epitopes and one latent antigen epitope). Each of the three specificities were reconstituted *in vivo* and T cells were maintained in the patient for at least five months. Furthermore, we comprehensively characterized the T cell clonotype repertoire for each of the epitope specificities by combining flow cytometry and high-throughput sequencing of TCR $\beta$  rearrangements.

This study was carried out in an EBV-seropositive patient who, after chemotherapy and allo-SCT for a CD4<sup>+</sup> AITL, suffered from relapse and simultaneous increase of peripheral blood EBV load, most likely associated with the leukemic relapse of the lymphoma. EBV-encoded RNA (EBER) *in situ* hybridization (ISH) analysis of AITL in the lymph node at diagnosis revealed the AITL tumor to be EBV negative (S2 Fig). This suggests that high EBV titers derived from an active infection site other than the AITL. However, simultaneous high EBV viremia and AITL relapse suggests a strong association between AITL and EBV infection, including a possible role in its pathogenesis [2] and increased aggressiveness [4].

Despite DLJ and Rituximab treatment, adoptive transfer of T cells enriched for EBV epitopes was provided due to persistence of severe B-symptoms and increasing levels of EBV viral DNA in the peripheral blood. In addition, on day 60 post allo-SCT, we observed a complete lack of EBV peptide-MHC multimer-binding T cells for the six known HLA-relevant epitopes. Owing to the risk of recurrent EBV reactivation [59] and its concomitant occurrence with AITL relapse, we believe adoptive transfer of EBV-specific T cell products hold promise to support the treatment of AITL by controlling EBV infection [60,61].

We cannot exclude at this point that the conventional DLJ may indeed have contributed to the surviving EBV memory T cell pool; nonetheless, we were able to track EBV-specific T cell clonotypes coming from the adoptive transfer that persisted long-term in the patient. In contrast to the conventional DLJ, EBV-specific T cells immediately expanded after adoptive transfer, resulting in a profound cytokine release syndrome (S4 Fig).

Variance between *ex vivo* and *in vivo* expansion of epitope-specific cells, especially against antigens of latency and lytic phases, may arise from differences in differentiation phenotype and epitope availability at both stages. Although T cells in the cellular product mostly lacked CCR7 expression (CCR7<sup>+</sup>CD45RA<sup>-</sup>), both lytic BZLF-1 EPL- and RAK-specific T cells had stronger CD62L expression than latent EBNA1 HPV-specific T cells (S5 Fig). CD62L expression facilitates homing into lymph nodes through adhesion to high endothelial venules (HEV) [62], with a closer association to central memory phenotype (CD62L<sup>+</sup>CD45RA<sup>-</sup>) [63]. This difference may indicate a higher proliferative strength, a stronger expansion (as seen in Fig 3C), less exhaustion, and better homing ability of the lytic antigen-specific T cells. An alternative hypothesis to the difference in expansion between lytic and latent antigen-specific T cells is the availability of their target epitope: The strong expansion of EPL- and RAK-specific T cells in peripheral blood and cytokine release (S4 Fig) happened directly after transfer, when ongoing EBV viremia (suggestive for lytic cycle) may have provided profound lytic epitope presentation. EBV viremia decrease over time and lesser epitope availability would explain why few clonotypes remained and survived long-term, which is expected as a natural modulation of the immune T cell response. On the other hand, HPV-specific T cells (latent antigen EBNA1) strongly expanded *ex vivo* but not in peripheral blood *in vivo*, either due to its homing to an active infection site, such as a lymph node, or the unavailability of their target antigen. In either case, we demonstrated that *in vitro* T cell stimulation with a defined set of peptides results in broad spectrum TCR $\beta$  repertoire expansion of various dominant clonotypes for relevant latent and lytic epitope specificities, which then get further selected *in vivo* based on need during the

course of viral reactivation. They might therefore contribute to reinstallation of a natural occurring immunity similar to the one observed in the donor.

Approximately 10 days after adoptive transfer of EBV-specific T cells and approximately 40 days after conventional DLI, the patient developed a skin rash, high bilirubin and liver enzyme elevation in the sense of acute GvHD (see [S9 Fig](#)). We cannot clearly attribute this to either DLI or the T cell product. The conventional DLI contained approximately 53.6% naïve T cells (equivalent to day 0 analysis for the manufacturing, see [Fig 1D](#)). In total 201 Mio. naïve T cells were infused with the conventional DLI (5.0 Mio. CD3<sup>+</sup> T cells/kg). In contrast, a total of only 11.55 Mio. naïve T cells were infused along with the EBV-specific T cell product (1 Mio. CD3<sup>+</sup> T cells/kg). We would speculate retrospectively that GvHD was mainly due to the conventional DLI, and that the cytokine release syndrome induced by the EBV-specific T cell product augmented the naïve T cell response. The patient received 1mg/kg Prednisone and responded very quickly to this treatment, which is also reflected in the rapid decline of CD8<sup>+</sup> T cells in the peripheral blood. However, despite the high dose of steroids, the patient did not reactivate EBV again and EBV-specific T cells persisted at a lower level demonstrating steroid resistance.

Our TCR high-throughput sequencing approach is based on samples of 100 ng cellular DNA and therefore has a limited resolution of 14,500 T cells, with a frequency cut-off of 0.01% (approximately 100 reads per T cell). This is suitable to obtain insights into clonotype diversity but will not detect every virus-specific TCR clonotype in patient samples or T cell products. High-throughput sequencing was able to reveal multiple EBV-specific clonotypes even in the complex T cell repertoire of the healthy donor, whose cells were used to manufacture EBV-specific T cells for adoptive transfer.

Expansion of EPL-, RAK-, and HPV-MHC multimer-binding T cells after peptide stimulation correlated with the expansion of distinct clonotypes, as shown by flow cytometry and TCR $\beta$  high throughput sequencing. However, we found TCRs in the MHC multimer-sorted CD8<sup>+</sup> population that were not enriched (as compared with unsorted populations) but were still detectable, presumably due to unspecific MHC multimer-binding. Nonetheless, this fraction represented the purest pool of T cells for a defined specificity (sorting purity above 98%) and was used to for multimer ternary exclusion.

Of note, the use of peptide-MHC multimer binding introduces a bias for TCRs with higher affinities because the affinity threshold required for multimer binding is higher than the one for T cell activation [64]. Therefore, we would conclude both BZLF1- and EBNA1-specific clonotypes identified in this study to have relatively higher affinity levels.

We mapped TCR sequences from peptide-MHC multimer-binding T cells back to the unsorted T cell pools before (d0) and after (d9) peptide stimulation. Using this strategy, we were able to identify previously described TCR $\beta$  sequences [31,32] and numerous new and naturally occurring clonotypes with relatively high frequencies in the normal donor. For example, three sequences with three distinct specificities found in the donor ([Table 2](#), highlighted) accounted for 1.1% of the donor's repertoire. These were among the donor's 30 clonotypes with the highest frequencies and persisted long term after adoptive transfer in the patient. The presence of dominant clonotypes for single peptide specificities is reinforced by the fact that three different DNA sequences coded for HPV-specific TCR $\beta$  clonotype CASGTEAFF.

TCR clonotypes complying with both inclusion criteria (frequency above 0.1% before and after multimer sort in T cell product and multimer ternary analysis) were identified as EBV epitope-specific. The frequency cutoff of 0.1% was selected to reduce noise, while ternary analysis allows us to exclude unspecific multimer-binding clonotypes. Using both criteria combined, we were able to identify EBV epitope-specific T cells which clearly dominate the T cell

product (77 of 471 clonotypes account for 74.8% of reads) and persist long-term after adoptive transfer.

It is relevant that such few EBV-specific clonotypes were detectable on day 60, while the patient's EBV viral load in peripheral blood was increasing. In contrast, EBV epitope-specific clonotypes from the unsorted and MHC multimer-sorted CD8<sup>+</sup> populations on day 9 were found 15 days after adoptive transfer (day 120) with a significant increase in frequencies and diversity of TCR clonotypes (Fig 4A). Therefore, we could see an association between the presence of several EBV epitope-specific clonotypes on day 120 and the absence of EBV DNA in the peripheral blood thereafter. Due to the association of EBV infection and AITL relapse, EBV control could have positively influenced AITL regression, as has been observed in PTLD [65].

Success of ATCT after allo-SCT depends on restoring immunity against viruses without viral reactivation, in the absence of Graft versus Host Disease (GvHD) [66]. Several indicators of restored EBV-specific T cell immunity are: (i) the persistence of adoptively transferred, functional virus-specific T cells [20,67–69], (ii) absence and regression of EBV-associated lymphomas [65,70–72], and (iii) control of virus reactivation and viremia *in vivo* [69,73–76]. We would therefore argue that the presence of EBV epitope-specific, expanded clonotypes in the T cell product, their long-term persistence in the patient, and lack of further EBV reactivation or relapse point to an important role of these clonotypes in controlling EBV, AITL, and other EBV-associated malignancies.

In conclusion, we were able to confirm the long-term presence of expanded, EBV epitope-specific CD8<sup>+</sup> T cell clonotypes following adoptive transfer in the patient, thereby restoring anti-EBV T cell immunity. To further validate these findings, a recently closed multicenter phase I/IIa clinical study (NCT02227641, EudraCT: 2012-004240-30) used this manufacture technique to generate T cell products with double specificity against CMV and EBV for patients after allo-SCT. The results of this study will further increase our knowledge on potentially protective virus-specific TCR repertoires after allo-SCT.

## Material and methods

### Ethics statement

The patient gave written informed consent prior to transplantation for extended immunomonitoring using standard flow cytometry, multimer analysis, and TCR HTS. The ethics committee of Friedrich-Alexander-University Erlangen-Nürnberg gave approval for this study (approval No.: 4388). In addition, the patient gave written consent for the attempt to cure using donor-derived EBV-specific T cells.

### EBV viral load analysis

EBV viral load measurement was carried out with whole blood EDTA as part of regular follow-up in the hospital for all allo-SCT patients. The QiaSymphony DSP Virus/Pathogen Mini Kit (QIAGEN, Hilden, Germany) was used for viral nucleic acid purification, while real-time PCR was established in-house and adapted from literature [77].

### *in situ* hybridization

EBER *in situ* hybridization was carried out on an AITL lymph node sample at time of diagnosis.

### Generation of EBV-specific T cells

EBV-specific peptides were generated in a GMP-conform fashion as described previously [68]. Peptides used for stimulation are shown in Table 1. In brief: frozen donor lymphocytes were obtained and thawed for Ficoll density centrifugation, yielding  $826 \times 10^6$  PBMC. PBMC were frozen until use. 600 million PBMC were incubated with peptide mix for 2h. After subsequent washing steps, cells were incubated in a closed bag system for 9 days. Medium was added according to the manufacturing protocol on day 5. Quality assessment of the product included bacterial culture and eubacterial PCR, flow cytometric analysis, and trypan blue method for viability.

### Flow cytometry analysis of cultivated cells and peripheral blood

To quantify cell types, peripheral blood (50  $\mu$ l per sample) was stained in TruCount tubes containing fluorescent beads (BD Biosciences) with the following antibodies: anti-CD8 FITC (clone SK1), anti-CD25 PE (clone 2A3), anti-CD14 PerCP (clone M $\phi$ P9), anti-CD56 APC (clone B159), anti-CD19 PE-Cy7 (clone SJ25C1), anti-CD4 APC-Cy7 (clone RPA-T4), anti-CD3 V450 (clone UCHT1), and anti-CD45 V500 (clone HI30, all clones from BD Bioscience). After incubation at room temperature for 15 min, 450  $\mu$ l of red cell lysis buffer (BD Biosciences) was added and samples were incubated for further 20 min. Cells were analyzed subsequently after staining using a FACS Canto II flow cytometer (Becton Dickinson). Leukocytes were gated as CD45<sup>+</sup> and lymphocytes as CD45<sup>high</sup>CD14<sup>-</sup> cells. Within the lymphocyte population, T cells were determined as CD3<sup>+</sup>, B cells as CD19<sup>+</sup>, NK cells as CD56<sup>+</sup> cell populations. T cell subpopulations were analyzed for CD4 and CD8 expression. Cell counts/ $\mu$ l were calculated based on bead count and sample volume in TruCount tubes (BD Bioscience). Cultivated cells were stained with the same panel but without cell quantification by TruCount tubes.

For analysis of T cells with multimer staining,  $1 \times 10^6$  cells either PBMC isolated from peripheral blood by Ficoll density centrifugation or taken from cultivated cells on day 0 and day 9, were stained with HLA-matched peptide-MHC pentamers (ProImmune, Oxford, UK), and subsequently counterstained with PE-fluorotag (ProImmune), anti-CCR7 FITC (clone 150503, R&D Systems, Minneapolis, MN, USA), anti-CD8 PerCP (clone SK1), anti-CD62L APC (clone DREG-56), anti-CD45RA PE-Cy7 (clone HI100), anti-CD4 APC-Cy7 (clone RPA-T4), and anti-CD3 V450 (clone UCHT1, all clones BD Biosciences). Cells were analyzed using a FACS Canto II flow cytometry analyzer (Becton Dickinson). Vital lymphocytes were gated in FSC vs. SSC. T cells were identified by their CD3 expression. T cell subpopulations were identified by CD4 and CD8 expression. T cells binding an EBV peptide-MHC multimer were analyzed within the CD8<sup>+</sup> T cell population.

Cultivated cells after harvest were further analyzed for IFN- $\gamma$  production upon antigen-specific restimulation. Therefore, day 9 cells were restimulated with the epitopes RLR, RAK, QAK, EPL, HPV, or YPL (each peptide 0.5 $\mu$ g/ml), or PMA-ionomycin for positive control. To inhibit IFN- $\gamma$  secretion, GolgiStop (BD Biosciences) was added for the time of restimulation (5 hours). Afterwards, cells were harvested and stained with the following surface markers: anti-CD3 PerCP (clone SK7), anti-CD8 PE-Cy7 (SK1), and anti-CD4 APC-Cy7 (clone RPA-T4). Then, cells were washed and treated with 250 $\mu$ l CellFix /Perm buffer (BD Biosciences) for 20 minutes, 4°C. Cells were then washed with Perm-/Wash buffer (BD Biosciences) and subsequently intracellularly stained with anti-IFN- $\gamma$ -FITC (clone B27) for 30 minutes at 4°C. Afterwards, cells were once washed with Perm-/Wash-buffer and once with PBS. After cell fixation, samples could be analyzed by flow cytometry.

### Cell sorting

Whole blood samples (EDTA) were processed by density gradient centrifugation (Ficoll) to obtain mononuclear blood cells (PBMC). For flow cytometry sorting, PBMC were stained with anti-CD4 FITC (clone SK3), anti-CD8 PE (clone SK1), anti-CD14 PerCP (clone MφP9, all clones BD Biosciences, Franklin Lakes, NJ, USA), and anti-TCR $\alpha\beta$  (clone BW242/412, Miltenyi Biotec, Bergisch Gladbach, Germany). Cells were gated on (i) vital lymphocytes in forward/side scatter, (ii) exclusion of doublets, and (iii) TCR $\alpha\beta$ <sup>+</sup> CD14<sup>-</sup> T cells. Within the T cell population, CD4<sup>+</sup> and CD8<sup>+</sup> T cells were sorted into separate tubes (MoFlow, Beckman Coulter, Brea, CA, USA). A purity of > 98.0% was achieved as monitored by reanalysis of the sorted samples.

Multimer cell sorting was performed using HLA-matched peptide-MHC pentamers obtained from ProImmune. Of the EBV-specific expanded T cells (day 9), 40x10<sup>6</sup> cells were incubated with RAK-HLA-B\*08:01-, 40x10<sup>6</sup> cells with HPV-HLA\*B35:01-, and 18x10<sup>6</sup> cells with EPL-HLA\*B35:01-multimers, according to manufacturer's recommendation. Afterwards cells were washed and stained with PE-fluorotag (ProImmune) binding to the peptide loaded HLA multimers, anti-CD8 FITC (clone SK1, BD Biosciences), anti-CD14 PerCP (clone MφP9, BD Biosciences), and anti-TCR $\alpha\beta$  (clone BW242/412, Miltenyi Biotec, Bergisch Gladbach, Germany). Cells were gated on (i) vital lymphocytes in forward/side scatter, (ii) exclusion of doublets, and (iii) TCR $\alpha\beta$ <sup>+</sup> CD14<sup>-</sup> T cells. Then, the CD8<sup>+</sup> multimer-binding population was sorted out and used for further analysis by TCR $\beta$  sequencing.

### DNA isolation

DNA was extracted from flow cytometry-sorted T cells using the Qiagen AllPrep DNA/RNA Mini Kit (Qiagen) according to the manufacturer's instructions. Quantification of the extracted DNA was done employing a Qubit 1.0 Fluorometer (Invitrogen, Carlsbad, CA, USA).

### Capillary electrophoresis

CDR3 length repertoires of TCR $\beta$  sequences were generated by using the BIOMED-2 primer sets for PCR-based clonality analysis [78]. The fluorescence-labeled amplicons were size-separated and detected via automated laser scanning by a 3130 Genetic Analyzer (Applied Biosystems; Darmstadt, Germany).

### High-throughput sequencing of TCR $\beta$ gene clonotypes

Amplification of TCR $\beta$  from 100 ng of cellular DNA (approximately 14,500 T cells) with multiplex PCR, sequencing of amplified TCR $\beta$  gene libraries (HiSeq2000), and data processing were performed as previously described [46]. Employing a two-step PCR strategy, the TCR $\beta$  amplicons were tagged with universal Illumina adapter sequences, including an additional barcode during a second amplification step, allowing parallel sequencing of several samples on Illumina HiSeq2000 (Illumina, San Diego, CA). Our amplicon sequences covered the entire CDR3 length and V $\beta$  and J $\beta$  segments in parts and using the Illumina paired-end technology (2x 100 bp) provided a high sequence accuracy.

The multiplex primers used contain a universal adapter sequence as a tail at the 5' end complementary to the 3' ends of second amplification adaptor primers. The adaptor PCR primers contained universal sequences that permitted solid-phase PCR on the Illumina Genome Analyzer (HiSeq 2000 Sequencing System). Primary amplification (final volume: 50  $\mu$ L) was processed, including 100 ng DNA, 1.0  $\mu$ M equimolar V $\beta$  and J $\beta$  primer pools, PCR buffer, 3mM

MgCl<sub>2</sub>, 0.2mM of each dNTP and 1U AmpliTaq Gold DNA Polymerase (Applied Biosystems, Foster City, CA). The amplification was performed on a DNA thermal cycler (GeneAmp1 PCR System 9700, Applied Biosystems) for 34 cycles at 62°C annealing temperature. All PCR products were purified using the QIAquick PCR Purification Kit (Qiagen) and diluted (final amount: 500 pg) for further amplifications. Adapter PCRs were set up with Phusion HF Buffer, 1.0 μM forward and reverse adapter primers, 0.05mM of each dNTP and 1U Phusion High-Fidelity DNA Polymerase (Finnzymes, Espoo, Finland). Secondary amplification was performed for 12 cycles at 58°C annealing temperature. Products were isolated from a 2% agarose gel using the Wizard1 SV Gel and PCR Clean-Up System (Promega, Mannheim, Germany). DNA concentration was determined via the Qubit1 1.0 Fluorometer (Invitrogen) [46]. Clonotypes were defined as TCRβ clonotypes with a percentage of reads equal to or above a 0.01% cut-off. Reads with frameshift or stop codon were considered as non-functional TCRβ rearrangements and excluded from analysis.

### Peptides

The manufacturing process involved stimulation of peripheral mononuclear cells by a fixed pool of peptides derived from various EBV proteins. The sequence of selected peptides, their HLA restriction, and reference is shown in Table 1. Peptides were synthesized by JPT Peptides Berlin (Germany) at a purity of 95%. All raw materials used for peptide synthesis were CE certified and all materials were fully synthetic. 5% contamination of the peptide product is considered to be smaller oligomers of the original design, due to inefficient elongation.

### Identification of EBV epitope-specific TCR clonotypes

We applied two criteria to TCR clonotypes found in the T cell product, either before or after multimer sort, to consider them as epitope-specific: First, we used a cutoff of 0.1%, representing approximately 10 T cells, to reduce noise. Then, we applied a ternary exclusion criterion based on the multimer enrichment ratio, defined as frequency after multimer sort / frequency before multimer sort. The enrichment factor for a given multimer must be at least ten times bigger than for the other two multimers to be considered epitope-specific.

### Supporting information

**S1 Fig. Lymphoma diagnosis and relapse.** (A) GeneScan analysis of T cell receptor gamma (TRG) and beta (TRB) demonstrated clonal T cell populations in the lymph node biopsy (day 166 before transplant). (B) HTS of TCRβ rearrangements of the lymph node permit identification of the lymphoma-specific TCRβ sequence (in bold). (C) The lymphoma-specific TCRβ sequence could be identified again in the recipient on day 60 after transplantation in peripheral blood.  
(TIF)

**S2 Fig. No presence of EBV in the AITL.** (A) EBER *in situ* hybridization (IsH) of the lymph node at diagnosis. An infectious mononucleosis sample was used as positive control. (B) Staining of the lymph node at diagnosis. H&E: Hematoxylin and eosin.  
(TIF)

**S3 Fig. Timeline of patient clinical history.** dpt: days post transplantation; ECOG: Eastern Cooperative Oncology Group; R-ICE: Rituximab, Ifosfamide, Carboplatin, and Etoposide Phosphate; GvHD: Graft-versus-Host Disease.  
(TIF)



**S4 Fig. Serum cytokine levels after adoptive transfer of EBV-specific T cells (ATCT)**  
(TIF)

**S5 Fig. T cell differentiation markers in the cellular product.** Multimer binding T cells were gated on CD8<sup>+</sup> T cells. Plots were gated on multimer-binding T cells. Numbers indicate percentages.  
(TIF)

**S6 Fig. Sorting of peptide-MHC multimer-binding T cells.** (A) Flow cytometric analysis gating for peptide-MHC multimer sorting. (B) Re-analysis of peptide-MHC multimer-sorted cells. Numbers indicate percentages.  
(TIF)

**S7 Fig. Identification of epitope-specific T cells.** Scatter plots show frequency before and after multimer sort of the T cell product on day 9 of T cell clonotypes with a frequency above 0.1% in both populations. Each dot represents a single TCR clonotype. Red dots symbolize TCR clonotypes that pass a ternary exclusion criterion of at least ten times the multimer enrichment ratio for one multimer as compared with the other two and were, therefore, identified as epitope-specific.  
(TIF)

**S8 Fig. Enrichment of epitope-specific clonotypes after sorting on day 9.** Frequencies of epitope-specific clonotypes (77 TCRs) is shown in unsorted CD8<sup>+</sup> T cell product and MHC multimer-sorted sample. Clonotype frequency is displayed as a percentage from 0.01 (limit of detection) to 14.4637 by increasing colour depth. Each row represents one specific TCR rearrangement. Identified public TCR sequences (P1 and P2) published [28,30] are highlighted in grey boxes. The most dominant clones (D 1–3) within each specificity are highlighted in pink boxes.  
(TIF)

**S9 Fig. GvHD monitoring.** (A) Enzyme levels in blood and (B) biomarker levels in plasma were used to monitor GvHD progress. GOT: glutamic oxaloacetic transaminase, AST: aspartate transaminase, GLDH: glutamate dehydrogenase, LDH: Lactate dehydrogenase, gGT: gamma-glutamyltransferase, CRP: C-reactive protein.  
(TIF)

**S1 Table. Patient characteristics and treatment.** AITL: angioimmunoblastic T cell lymphoma; IgG: Immunoglobulin G; IgM: Immunoglobulin M; pos.: positive; neg.: negative; R-CHOP: Rituximab, Cyclophosphamide, Hydroxydaunomycin, Oncovin, and Prednisone; R-ICE: Rituximab, Ifosfamide, Carboplatin, and Etoposide; Fc: fragment crystallizable region; PD: progressive disease; SD: stable disease; allo-SCT: allogeneic stem cell transplantation; ATG: antithymocyte globulin; HLA: human leukocyte antigen; CMV: Cytomegalovirus; EBV: Epstein-Barr Virus; DLI: donor lymphocyte infusion; ATCT: adoptive T cell transfer; GvHD: Graft-versus-Host Disease; CsA: cyclosporin; HSV-1: Herpes-Simplex Virus-1.  
(PDF)

**S2 Table. EPL-specific T cells.** TCR $\beta$  VJ ID: identification number for TCR $\beta$  variable-joining rearrangement, AA: amino acid.  
(PDF)

**S3 Table. RAK-specific T cells.** TCR $\beta$  VJ ID: identification number for TCR $\beta$  variable-joining rearrangement, AA: amino acid.  
(PDF)

**S4 Table. HPV-specific T cells.** TCR $\beta$  VJ ID: identification number for TCR $\beta$  variable-joining rearrangement, AA: amino acid.  
(PDF)

**S5 Table. Presence of EPL-, RAK-, and HPV-specific T cells in different samples.**  
(PDF)

### Acknowledgments

We would like to thank the staff of the department for transfusion medicine for their kind support of this study. Many thanks go to the staff of the Erlangen Bone Marrow Transplantation (BMT) unit and BMT outpatient clinic for excellent care taking of the patient.

### Author Contributions

**Conceptualization:** Volkhard Seitz, Andreas Mackensen, Armin Gerbitz.

**Data curation:** María Fernanda Lammoglia Cobo, Julia Ritter, Regina Gary, Volkhard Seitz, Josef Mautner, Michael Aigner, Simon Völkl, Stefanie Schaffer, Stephanie Moi, Anke Seegebarth, Kerstin Amann, Andreas Moosmann.

**Formal analysis:** María Fernanda Lammoglia Cobo, Julia Ritter, Regina Gary, Stefanie Schaffer, Stephanie Moi, Anke Seegebarth, Heiko Bruns, Kerstin Amann, Maike Büttner-Herold, Michael Hummel, Andreas Moosmann, Armin Gerbitz.

**Funding acquisition:** Volkhard Seitz, Andreas Mackensen, Armin Gerbitz.

**Investigation:** Anke Seegebarth, Heiko Bruns, Steffen Hennig, Armin Gerbitz.

**Methodology:** Steffen Hennig, Michael Hummel, Andreas Moosmann, Armin Gerbitz.

**Project administration:** Andreas Mackensen.

**Resources:** Heiko Bruns, Steffen Hennig.

**Software:** María Fernanda Lammoglia Cobo, Andreas Moosmann.

**Supervision:** Josef Mautner, Anke Seegebarth, Maike Büttner-Herold, Michael Hummel, Andreas Moosmann, Armin Gerbitz.

**Validation:** Josef Mautner.

**Visualization:** María Fernanda Lammoglia Cobo.

**Writing – original draft:** María Fernanda Lammoglia Cobo, Julia Ritter, Volkhard Seitz, Michael Aigner, Simon Völkl, Wolf Rösler, Maike Büttner-Herold, Michael Hummel, Andreas Moosmann, Armin Gerbitz.

**Writing – review & editing:** María Fernanda Lammoglia Cobo, Volkhard Seitz, Josef Mautner, Kerstin Amann, Maike Büttner-Herold, Steffen Hennig, Andreas Mackensen, Andreas Moosmann, Armin Gerbitz.

### References

1. Ru Y, Zhang X, Song T, et al. Epstein-Barr virus reactivation after allogeneic hematopoietic stem cell transplantation: multifactorial impact on transplant outcomes. *Bone Marrow Transplant* 2020; 55(9): 1754–62. <https://doi.org/10.1038/s41409-020-0831-7> PMID: 32066862

2. Zhou Y, Attygalle AD, Chuang S-S, et al. Angioimmunoblastic T-cell lymphoma: histological progression associates with EBV and HHV6B viral load. *Br J Haematol* 2007; 138(1): 44–53. <https://doi.org/10.1111/j.1365-2141.2007.06620.x> PMID: 17555446
3. Wang C, Gong Y, Liang X, Chen R. Epstein–Barr Virus Positive Diffuse Large B-Cell Lymphoma Transformed into Angioimmunoblastic T-Cell Lymphoma After Treatment: A Case Report and Literature Review 2021
4. Facchinelli D, Polino A, Dima F, Parisi A, Ambrosetti A, Veneri D. Two cases of angioimmunoblastic T-cell lymphoma with concomitant positive serology for acute Epstein-Barr virus infection. *Hematol Rep* 2017; 9(3): 7088. <https://doi.org/10.4081/hr.2017.7088> PMID: 29071053
5. Weiss LM, Jaffe ES, Liu XF, Chen YY, Shibata D, Medeiros LJ. Detection and localization of Epstein-Barr viral genomes in angioimmunoblastic lymphadenopathy and angioimmunoblastic lymphadenopathy-like lymphoma. *Blood* 1992; 79(7): 1789–95. PMID: 1373088
6. Kishimoto W, Takiuchi Y, Nakae Y, et al. A case of AITL complicated by EBV-positive B cell and monoclonal plasma cell proliferation and effectively treated with lenalidomide. *Int J Hematol* 2019; 109(4): 499–504. <https://doi.org/10.1007/s12185-018-02587-6> PMID: 30604313
7. Takahashi T, Maruyama R, Mishima S, et al. Small bowel perforation caused by Epstein-Barr virus-associated B cell lymphoma in a patient with angioimmunoblastic T-cell lymphoma. *J Clin Exp Hematop* 2010; 50(1): 59–63. <https://doi.org/10.3960/jslrt.50.59> PMID: 20505277
8. Anagnostopoulos I, Hummel M, Finn T, et al. Heterogeneous Epstein-Barr virus infection patterns in peripheral T-cell lymphoma of angioimmunoblastic lymphadenopathy type. *Blood* 1992; 80(7): 1804–12. <https://doi.org/10.1182/blood.V80.7.1804.1804> PMID: 1327284
9. Lee WJ, Won KH, Choi JW, et al. Cutaneous angioimmunoblastic T-cell lymphoma: Epstein-Barr virus positivity and its effects on clinicopathologic features. *J Am Acad Dermatol* 2019; 81(4): 989–97. <https://doi.org/10.1016/j.jaad.2018.06.053> PMID: 30240776
10. Battagay M, Berger C, Rochlitz C, et al. Epstein-Barr virus load correlating with clinical manifestation and treatment response in a patient with angioimmunoblastic T-cell lymphoma. *Antivir Ther* 2004; 9(3): 453–9. PMID: 15259909
11. Eladl AE, Shimada K, Suzuki Y, et al. EBV status has prognostic implication among young patients with angioimmunoblastic T-cell lymphoma. *Cancer Med* 2020; 9(2): 678–88. <https://doi.org/10.1002/cam4.2742> PMID: 31793218
12. Styczynski J, van der Velden W, Fox CP, et al. Management of Epstein-Barr Virus infections and post-transplant lymphoproliferative disorders in patients after allogeneic hematopoietic stem cell transplantation: Sixth European Conference on Infections in Leukemia (ECIL-6) guidelines. *Haematologica* 2016; 101(7): 803–11. <https://doi.org/10.3324/haematol.2016.144428> PMID: 27365460
13. Sanz J, Andreu R. Epstein-Barr virus-associated posttransplant lymphoproliferative disorder after allogeneic stem cell transplantation. *Curr Opin Oncol* 2014; 26(6): 677–83. <https://doi.org/10.1097/CCO.000000000000119> PMID: 25162331
14. Liu L, Liu Q, Feng S. Management of Epstein-Barr virus-related post-transplant lymphoproliferative disorder after allogeneic hematopoietic stem cell transplantation. *Ther Adv Hematol* 2020; 11: 2040620720910964. <https://doi.org/10.1177/2040620720910964> PMID: 32523657
15. Al Hamed R, Bazarbachi AH, Mohty M. Epstein-Barr virus-related post-transplant lymphoproliferative disease (EBV-PTLD) in the setting of allogeneic stem cell transplantation: a comprehensive review from pathogenesis to forthcoming treatment modalities. *Bone Marrow Transplant* 2020; 55(1): 25–39. <https://doi.org/10.1038/s41409-019-0548-7> PMID: 31089285
16. Andrei G, Trompet E, Snoeck R. Novel Therapeutics for Epstein-Barr Virus. *Molecules* 2019; 24(5). <https://doi.org/10.3390/molecules24050997> PMID: 30871092
17. van der Velden WJFM, Mori T, Stevens WBC, et al. Reduced PTLD-related mortality in patients experiencing EBV infection following allo-SCT after the introduction of a protocol incorporating pre-emptive rituximab. *Bone Marrow Transplant* 2013; 48(11): 1465–71. <https://doi.org/10.1038/bmt.2013.84> PMID: 23749107
18. Abdel-Azim H, Elshoury A, Mahadeo KM, Parkman R, Kapoor N. Humoral Immune Reconstitution Kinetics after Allogeneic Hematopoietic Stem Cell Transplantation in Children: A Maturation Block of IgM Memory B Cells May Lead to Impaired Antibody Immune Reconstitution. *Biol Blood Marrow Transplant* 2017; 23(9): 1437–46. <https://doi.org/10.1016/j.bbmt.2017.05.005> PMID: 28495643
19. D'Orsogna LJ, Wright MP, Krueger RG, et al. Allogeneic hematopoietic stem cell transplantation recipients have defects of both switched and igh memory B cells. *Biol Blood Marrow Transplant* 2009; 15(7): 795–803. <https://doi.org/10.1016/j.bbmt.2008.11.024> PMID: 19539210
20. Heslop HE, Slobod KS, Pule MA, et al. Long-term outcome of EBV-specific T-cell infusions to prevent or treat EBV-related lymphoproliferative disease in transplant recipients. *Blood* 2010; 115(5): 925–35. <https://doi.org/10.1182/blood-2009-08-239186> PMID: 19880495

21. Prockop S, Doubrovina E, Suser S, et al. Off-the-shelf EBV-specific T cell immunotherapy for rituximab-refractory EBV-associated lymphoma following transplantation. *J Clin Invest* 2020; 130(2): 733–47. <https://doi.org/10.1172/JCI121127> PMID: 31689242
22. Ricciardelli I, Blundell MP, Brewin J, Thrasher A, Pule M, Amrolia PJ. Towards gene therapy for EBV-associated posttransplant lymphoma with genetically modified EBV-specific cytotoxic T cells. *Blood* 2014; 124(16): 2514–22. <https://doi.org/10.1182/blood-2014-01-553362> PMID: 25185261
23. Bollard CM, Rooney CM, Heslop HE. T-cell therapy in the treatment of post-transplant lymphoproliferative disease. *Nat Rev Clin Oncol* 2012; 9(9): 510–9. <https://doi.org/10.1038/nrclinonc.2012.111> PMID: 22801669
24. Gary R, Aigner M, Moi S, et al. Clinical-grade generation of peptide-stimulated CMV/EBV-specific T cells from G-CSF mobilized stem cell grafts. *J Transl Med* 2018; 16(1): 124. <https://doi.org/10.1186/s12967-018-1498-3> PMID: 29743075
25. Schaff N, Lankiewicz B, Drexhage J, et al. T cell re-targeting to EBV antigens following TCR gene transfer: CD28-containing receptors mediate enhanced antigen-specific IFN $\gamma$  production. *Int Immunol* 2006; 18(4): 591–601. <https://doi.org/10.1093/intimm/dxh401> PMID: 16507598
26. Cho H-I, Kim U-H, Shin A-R, et al. A novel Epstein-Barr virus-latent membrane protein-1-specific T-cell receptor for TCR gene therapy. *Br J Cancer* 2018; 118(4): 534–45. <https://doi.org/10.1038/bjc.2017.475> PMID: 29360818
27. Zhang C, Tan Q, Li S, et al. Induction of EBV latent membrane protein-2A (LMP2A)-specific T cells and construction of individualized TCR-engineered T cells for EBV-associated malignancies. *J Immunother Cancer* 2021; 9(7). <https://doi.org/10.1136/jitc-2021-002516> PMID: 34210819
28. Dudanec K, Westendorf K, Nössner E, Uckert W. Generation of Epstein-Barr Virus Antigen-Specific T Cell Receptors Recognizing Immunodominant Epitopes of LMP1, LMP2A, and EBNA3C for Immunotherapy. *Hum Gene Ther* 2021; 32(17–18): 919–35. <https://doi.org/10.1089/hum.2020.283> PMID: 33798008
29. Chen L, Dong L, Ma Y, et al. An efficient method to identify virus-specific TCRs for TCR-T cell immunotherapy against virus-associated malignancies. *BMC Immunol* 2021; 22(1): 65. <https://doi.org/10.1186/s12865-021-00455-3> PMID: 34583647
30. Lee SP, Thomas WA, Murray RJ, et al. HLA A2.1-restricted cytotoxic T cells recognizing a range of Epstein-Barr virus isolates through a defined epitope in latent membrane protein LMP2. *J Virol* 1993; 67(12): 7428–35. <https://doi.org/10.1128/JVI.67.12.7428-7435.1993> PMID: 7693972
31. Steven NM, Annels NE, Kumar A, Leese AM, Kurilla MG, Rickinson AB. Immediate early and early lytic cycle proteins are frequent targets of the Epstein-Barr virus-induced cytotoxic T cell response. *J Exp Med* 1997; 185(9): 1605–17. <https://doi.org/10.1084/jem.185.9.1605> PMID: 9151898
32. Scotet E, David-Ameline J, Peyrat MA, et al. T cell response to Epstein-Barr virus transactivators in chronic rheumatoid arthritis. *J Exp Med* 1996; 184(5): 1791–800. <https://doi.org/10.1084/jem.184.5.1791> PMID: 8920887
33. Saulquin X, Ibsch C, Peyrat M-A, et al. A global appraisal of immunodominant CD8<sup>+</sup> T cell responses to Epstein-Barr virus and cytomegalovirus by bulk screening. *Eur. J. Immunol.* 2000; 30(9): 2531–9. [https://doi.org/10.1002/1521-4141\(200009\)30:9<2531::AID-IMMU2531>3.0.CO;2-O](https://doi.org/10.1002/1521-4141(200009)30:9<2531::AID-IMMU2531>3.0.CO;2-O) PMID: 11009086
34. Meij P, Leen A, Rickinson AB, et al. Identification and prevalence of CD8<sup>+</sup> T-cell responses directed against Epstein-Barr virus-encoded latent membrane protein 1 and latent membrane protein 2. *Int J Cancer* 2002; 99(1): 93–9. <https://doi.org/10.1002/ijc.10309> PMID: 11948498
35. Hill AB, Lee SP, Haurum JS, et al. Class I major histocompatibility complex-restricted cytotoxic T lymphocytes specific for Epstein-Barr virus (EBV)-transformed B lymphoblastoid cell lines against which they were raised. *J Exp Med* 1995; 181(6): 2221–8. <https://doi.org/10.1084/jem.181.6.2221> PMID: 7539044
36. Burrows SR, Gardner J, Khanna R, et al. Five new cytotoxic T cell epitopes identified within Epstein-Barr virus nuclear antigen 3. *J Gen Virol* 1994; 75 (Pt 9): 2489–93. <https://doi.org/10.1099/0022-1317-75-9-2489> PMID: 7521394
37. Bogedain C, Wolf H, Modrow S, Stuber G, Jilg W. Specific cytotoxic T lymphocytes recognize the immediate-early transactivator Zta of Epstein-Barr virus. *J Virol* 1995; 69(8): 4872–9. <https://doi.org/10.1128/JVI.69.8.4872-4879.1995> PMID: 7609055
38. Rickinson AB, Moss DJ. Human cytotoxic T lymphocyte responses to Epstein-Barr virus infection. *Annu Rev Immunol* 1997; 15: 405–31. <https://doi.org/10.1146/annurev.immunol.15.1.405> PMID: 9143694
39. Landais E, Saulquin X, Scotet E, et al. Direct killing of Epstein-Barr virus (EBV)-infected B cells by CD4 T cells directed against the EBV lytic protein BHRF1. *Blood* 2004; 103(4): 1408–16. <https://doi.org/10.1182/blood-2003-03-0930> PMID: 14563644

40. Leen A, Meij P, Redchenko I, et al. Differential immunogenicity of Epstein-Barr virus latent-cycle proteins for human CD4(+) T-helper 1 responses. *J Virol* 2001; 75(18): 8649–59. <https://doi.org/10.1128/JVI.75.18.8649-8659.2001> PMID: 11507210
41. Adhikary D, Behrends U, Moosmann A, Witter K, Bornkamm GW, Mautner J. Control of Epstein-Barr virus infection in vitro by T helper cells specific for virion glycoproteins. *J Exp Med* 2008; 203(4): 995–1006. <https://doi.org/10.1084/jem.20051287> PMID: 16549597
42. Mautner J, Pich D, Nimmerjahn F, et al. Epstein-Barr virus nuclear antigen 1 evades direct immune recognition by CD4+ T helper cells. *Eur J Immunol* 2004; 34(9): 2500–9. <https://doi.org/10.1002/eji.200324794> PMID: 15307182
43. Milosevic S, Behrends U, Adhikary D, Mautner J. Identification of major histocompatibility complex class II-restricted antigens and epitopes of the Epstein-Barr virus by a novel bacterial expression cloning approach. *J Virol* 2006; 80(21): 10357–64. <https://doi.org/10.1128/JVI.01193-06> PMID: 17041216
44. Tan LC, Gudgeon N, Annels NE, et al. A re-evaluation of the frequency of CD8+ T cells specific for EBV in healthy virus carriers. *J Immunol* 1999; 162(3): 1827–35. PMID: 9973448
45. Omiya R, Buteau C, Kobayashi H, Paya CV, Celis E. Inhibition of EBV-induced lymphoproliferation by CD4(+) T cells specific for an MHC class II promiscuous epitope. *J Immunol* 2002; 169(4): 2172–9. <https://doi.org/10.4049/jimmunol.169.4.2172> PMID: 12165547
46. Ritter J, Seitz V, Balzer H, et al. Donor CD4 T Cell Diversity Determines Virus Reactivation in Patients After HLA-Matched Allogeneic Stem Cell Transplantation. *Am J Transplant* 2015; 15(8): 2170–9. <https://doi.org/10.1111/ajt.13241> PMID: 25873100
47. Miconnet I, Marrau A, Farina A, et al. Large TCR diversity of virus-specific CD8 T cells provides the mechanistic basis for massive TCR renewal after antigen exposure. *J Immunol* 2011; 186(12): 7039–49. <https://doi.org/10.4049/jimmunol.1003309> PMID: 21555537
48. van Heijst JWW, Ceberio I, Lipuma LB, et al. Quantitative assessment of T cell repertoire recovery after hematopoietic stem cell transplantation. *Nat Med* 2013; 19(3): 372–7. <https://doi.org/10.1038/nm.3100> PMID: 23435170
49. Miles JJ, Elhassen D, Borg NA, et al. CTL recognition of a bulged viral peptide involves biased TCR selection. *J Immunol* 2005; 175(6): 3826–34. <https://doi.org/10.4049/jimmunol.175.6.3826> PMID: 16148129
50. Rooney CM, Aguilar LK, Huls MH, Brenner MK, Heslop HE. Adoptive immunotherapy of EBV-associated malignancies with EBV-specific cytotoxic T-cell lines. *Curr Top Microbiol Immunol* 2001; 258: 221–9. [https://doi.org/10.1007/978-3-642-56515-1\\_14](https://doi.org/10.1007/978-3-642-56515-1_14) PMID: 11443864
51. Klarenbeek PL, Remmerswaal EBM, Berge IJM ten, et al. Deep sequencing of antiviral T-cell responses to HCMV and EBV in humans reveals a stable repertoire that is maintained for many years. *PLoS Pathog* 2012; 8(9): e1002869. <https://doi.org/10.1371/journal.ppat.1002869> PMID: 23028307
52. Keller MD, Darko S, Lang H, et al. T-cell receptor sequencing demonstrates persistence of virus-specific T cells after antiviral immunotherapy. *Br J Haematol* 2019; 187(2): 206–18. <https://doi.org/10.1111/bjh.16053> PMID: 31219185
53. Annels NE, Callan MF, Tan L, Rickinson AB. Changing patterns of dominant TCR usage with maturation of an EBV-specific cytotoxic T cell response. *J Immunol* 2000; 165(9): 4831–41. <https://doi.org/10.4049/jimmunol.165.9.4831> PMID: 11046006
54. Iancu EM, Gannon PO, Laurent J, et al. Persistence of EBV antigen-specific CD8 T cell clonotypes during homeostatic immune reconstitution in cancer patients. *PLoS One* 2013; 8(10): e78686. <https://doi.org/10.1371/journal.pone.0078686> PMID: 24205294
55. Hislop AD, Kuo M, Drake-Lee AB, et al. Tonsillar homing of Epstein-Barr virus-specific CD8+ T cells and the virus-host balance. *J Clin Invest* 2005; 115(9): 2546–55. <https://doi.org/10.1172/JCI24810> PMID: 16110323
56. Wang G, Mudgal P, Wang L, et al. TCR repertoire characteristics predict clinical response to adoptive CTL therapy against nasopharyngeal carcinoma. *Oncoimmunology* 2021; 10(1): 1955545. <https://doi.org/10.1080/2162402X.2021.1955545> PMID: 34377592
57. Hernández DM, Valderrama S, Gualtero S, et al. Loss of T-Cell Multifunctionality and TCR-Vβ Repertoire Against Epstein-Barr Virus Is Associated With Worse Prognosis and Clinical Parameters in HIV+ Patients. *Front Immunol* 2018; 9: 2291. <https://doi.org/10.3389/fimmu.2018.02291> PMID: 30337929
58. Annels NE, Kalpoe JS, Bredius RGM, et al. Management of Epstein-Barr virus (EBV) reactivation after allogeneic stem cell transplantation by simultaneous analysis of EBV DNA load and EBV-specific T cell reconstitution. *Clin Infect Dis* 2006; 42(12): 1743–8. <https://doi.org/10.1086/503838> PMID: 16705581
59. van Esser JW, van der Holt B, Meijer E, et al. Epstein-Barr virus (EBV) reactivation is a frequent event after allogeneic stem cell transplantation (SCT) and quantitatively predicts EBV-lymphoproliferative

- disease following T-cell—depleted SCT. *Blood* 2001; 98(4): 972–8. <https://doi.org/10.1182/blood.v98.4.972> PMID: 11493441
60. Toner K, Bollard CM, Dave H. T-cell therapies for T-cell lymphoma. *Cytotherapy* 2019; 21(9): 935–42. <https://doi.org/10.1016/j.jcyt.2019.04.058> PMID: 31320195
  61. Bingjie W, Lihong W, Yongjin S, Huihui L, Jinping O, Xi'nan C. The efficacy and safety of Epstein-Barr virus-specific antigen peptide-activated cytotoxic T-cells treatment for refractory or recurrent angioimmunoblastic T-cell lymphoma: A prospective clinical observational study. *Hematol Oncol* 2020; 38(3): 272–6. <https://doi.org/10.1002/hon.2726> PMID: 32083758
  62. Berg EL, Robinson MK, Warnock RA, Butcher EC. The human peripheral lymph node vascular addressin is a ligand for LECAM-1, the peripheral lymph node homing receptor. *J Cell Biol* 1991; 114(2): 343–9. <https://doi.org/10.1083/jcb.114.2.343> PMID: 1712790
  63. Sallusto F, Lenig D, Förster R, Lipp M, Lanzavecchia A. Two subsets of memory T lymphocytes with distinct homing potentials and effector functions. *Nature* 1999; 401(6754): 708–12. <https://doi.org/10.1038/44385> PMID: 10537110
  64. Laugel B, van den Berg HA, Gostick E, et al. Different T cell receptor affinity thresholds and CD8 receptor dependence govern cytotoxic T lymphocyte activation and tetramer binding properties. *J Biol Chem* 2007; 282(33): 23799–810. <https://doi.org/10.1074/jbc.M700976200> PMID: 17540778
  65. Khanna R, Bell S, Sherritt M, et al. Activation and adoptive transfer of Epstein-Barr virus-specific cytotoxic T cells in solid organ transplant patients with posttransplant lymphoproliferative disease. *Proc Natl Acad Sci U S A* 1999; 96(18): 10391–6. <https://doi.org/10.1073/pnas.96.18.10391> PMID: 10468618
  66. Barrett AJ, Bollard CM. The coming of age of adoptive T-cell therapy for viral infection after stem cell transplantation. *Ann Transl Med* 2015; 3(5): 62. <https://doi.org/10.3978/j.issn.2305-5839.2015.01.18> PMID: 25992361
  67. Riddell SR, Watanabe KS, Goodrich JM, Li CR, Agha ME, Greenberg PD. Restoration of viral immunity in immunodeficient humans by the adoptive transfer of T cell clones. *Science* 1992; 257(5067): 238–41. <https://doi.org/10.1126/science.1352912> PMID: 1352912
  68. Moosmann A, Bigalke I, Tischer J, et al. Effective and long-term control of EBV PTLD after transfer of peptide-selected T cells. *Blood* 2010; 115(14): 2960–70. <https://doi.org/10.1182/blood-2009-08-236356> PMID: 20103780
  69. Icheva V, Kayser S, Wolff D, et al. Adoptive transfer of Epstein-Barr virus (EBV) nuclear antigen 1-specific T cells as treatment for EBV reactivation and lymphoproliferative disorders after allogeneic stem-cell transplantation. *J Clin Oncol* 2013; 31(1): 39–48. <https://doi.org/10.1200/JCO.2011.39.8495> PMID: 23169501
  70. Xiang Z, Liu Y, Zheng J, et al. Targeted activation of human Vγ9Vδ2-T cells controls Epstein-Barr virus-induced B cell lymphoproliferative disease. *Cancer Cell* 2014; 26(4): 565–76. <https://doi.org/10.1016/j.ccr.2014.07.026> PMID: 25220446
  71. Linnerbauer S, Behrends U, Adhikary D, Witter K, Bornkamm GW, Mautner J. Virus and autoantigen-specific CD4+ T cells are key effectors in a SCID mouse model of EBV-associated post-transplant lymphoproliferative disorders. *PLoS Pathog* 2014; 10(5): e1004068. <https://doi.org/10.1371/journal.ppat.1004068> PMID: 24853673
  72. Smith C, Tsang J, Beagley L, et al. Effective treatment of metastatic forms of Epstein-Barr virus-associated nasopharyngeal carcinoma with a novel adenovirus-based adoptive immunotherapy. *Cancer Res* 2012; 72(5): 1116–25. <https://doi.org/10.1158/0008-5472.CAN-11-3399> PMID: 22282657
  73. Meij P, van Esser JWJ, Niesters HGM, et al. Impaired recovery of Epstein-Barr virus (EBV)—specific CD8+ T lymphocytes after partially T-depleted allogeneic stem cell transplantation may identify patients at very high risk for progressive EBV reactivation and lymphoproliferative disease. *Blood* 2003; 101(11): 4290–7. <https://doi.org/10.1182/blood-2002-10-3001> PMID: 12576337
  74. Antsiferova O, Müller A, Rämmer PC, et al. Adoptive transfer of EBV specific CD8+ T cell clones can transiently control EBV infection in humanized mice. *PLoS Pathog* 2014; 10(8): e1004333. <https://doi.org/10.1371/journal.ppat.1004333> PMID: 25165855
  75. Savoldo B, Huls MH, Liu Z, et al. Autologous Epstein-Barr virus (EBV)-specific cytotoxic T cells for the treatment of persistent active EBV infection. *Blood* 2002; 100(12): 4059–66. <https://doi.org/10.1182/blood-2002-01-0039> PMID: 12393655
  76. Bollard CM, Kuehnlé I, Leen A, Rooney CM, Heslop HE. Adoptive immunotherapy for posttransplantation viral infections. *Biol Blood Marrow Transplant* 2004; 10(3): 143–55. <https://doi.org/10.1016/j.bbmt.2003.09.017> PMID: 14993880
  77. Plentz A, Jilg W, Kochanowski B, Ibach B, Knöll A. Detection of herpesvirus DNA in cerebrospinal fluid and correlation with clinical symptoms. *Infection* 2008; 36(2): 158–62. <https://doi.org/10.1007/s15010-007-6354-y> PMID: 18379728

78. van Dongen JJM, Langerak AW, Brüggemann M, et al. Design and standardization of PCR primers and protocols for detection of clonal immunoglobulin and T-cell receptor gene recombinations in suspect lymphoproliferations: report of the BIOMED-2 Concerted Action BMH4-CT98-3936. *Leukemia* 2003; 17(12): 2257–317. <https://doi.org/10.1038/sj.leu.2403202> PMID: [14671650](https://pubmed.ncbi.nlm.nih.gov/14671650/)

## **Curriculum Vitae**

"My curriculum vitae does not appear in the electronic version of my paper for reasons of data protection."



## Publication list

**Lammoglia Cobo MF**, Welters C, Rosenberger L, Leisegang M, Dietze K, Pircher C, Penter L, Gary R, Bullinger L, Takvorian A, Moosmann A, Dornmair K, Blankenstein T, Kammertöns T, Gerbitz A, Hansmann L. Rapid single-cell identification of Epstein-Barr virus-specific T-cell receptors for cellular therapy. *Cytotherapy* 2022; 1(Pt 9): 156.

*Cytotherapy* Impact Factor 2020: 5.414

**Lammoglia Cobo MF**, Ritter J, Gary R, Seitz V, Mautner J, Aigner M, Völkl S, Schaffer S, Moi S, Seegebarth A, Bruns H, Rösler W, Amann K, Büttner-Herold M, Hennig S, Mackensen A, Hummel M, Moosmann A, Gerbitz A. Reconstitution of EBV-directed T cell immunity by adoptive transfer of peptide-stimulated T cells in a patient after allogeneic stem cell transplantation for AITL. *PLoS Pathog* 2022; 18(4): e1010206.

*PLoS Pathogens* Impact Factor 2020: 6.823

Penter L, Dietze K, Ritter J, **Lammoglia Cobo MF**, Garmshausen J, Aigner F, Bullinger L, Hackstein H, Wienzek-Lischka S, Blankenstein T, Hummel M, Dornmair K, Hansmann L. Localization-associated immune phenotypes of clonally expanded tumor-infiltrating T cells and distribution of their target antigens in rectal cancer. *Oncoimmunology* 2019; 8(6): e1586409.

*Oncoimmunology* Impact Factor 2020: 8.110

Varela JN, **Lammoglia Cobo MF**, Pawar SV, Yadav VG. Cheminformatic Analysis of Antimalarial Chemical Space Illuminates Therapeutic Mechanisms and Offers Strategies for Therapy Development. *J Chem Inf Model* 2017; 57 (9): 2119–2131.

*Journal of Chemical Information and Modeling* Impact Factor 2020: 4.956

**Lammoglia Cobo MF**, Lozano Reyes R, García Sandoval C, Avilez Bahena C, Trejo Reveles V, Muñoz Soto R, López Camacho C. La revolución en ingeniería genética: sistema CRISPR/Cas. *Investigación en Discapacidad* 2016; 5 (2): 116-128.

*Investigación en Discapacidad* Impact Factor: N.A.

## Acknowledgments

I would like to thank my advisor, Armin Gerbitz, for his trust, his teachings, and being a humane example of a scientist and clinician driving his efforts towards the patient's well-being. I am especially grateful to Leo Hansmann for his academic and scientific guidance to develop and successfully complete this project. I would also deeply thank Thomas Kammertöns for his counsel and openness to discussion.

I would like to express my gratitude to the colleagues I worked with at the lab: Carlotta Welters, Livius Penter, Kerstin Dietze, Serena Stadler, Josefin Garmshausen, Alexej Ballhausen, Maurizio Raso, Christian Stein, Marthe-Lina Welters, and Amin Ben Hamza. I would also like to thank our collaborators Thomas Blankenstein, Matthias Leisegang, Leonie Rosenberger, Christian Pircher, and Meng-Tung Hsu for their insights and contribution to the development of the final therapeutic product; Katy Hausmann and Anna Takvorian for welcoming me at Charité; Andreas Moosmann and Josef Mautner for their insightful suggestions and passion for science; and Regina Gary for her friendly guidance on the establishment of a manufacturing process.

I am thankful to the Berlin School of Integrative Oncology (BSIO), the Mexican National Council of Science and Technology (CONACYT), and German Cancer Consortium (DKTK) for funding my doctoral research and position.

To my brother Luis, my parents Margarita and Luis Martín, and grandmother Margarita I have the utmost gratitude: Without your constant encouragement, example, and unconditional love this would not have been possible. You are my anchor and I deeply admire your perseverance, kindness, and noble hearts. To Arya and Nera, for their love and company. Muchas gracias por todo, familia. Los quiero.

My biggest thanks to Helia Pimentel, Karsten Lutzke, Maddalena Grimaldi, Holger Kratzat, Michael Pflanz, Gaby Pflanz, and Mohamed Elmissiry for being my family in Berlin and Justė Steponavičiūtė, Ieva Vasiliūnė, Saulius Padegimas, and Paulius Vasiliunas in Lithuania. I am also thankful to César Contreras, María José Martínez, Efrén A. Pérez, María José Gómez, Luis Vélez, José Pablo Domínguez, Gerd Borho, and Jorge Luis Rivera for their words of wisdom to help me through challenging times.